SURFACE MODIFICATION OF MODEL SILICONE HYDROGEL CONTACT LENSES WITH DENSELY GRAFTED PHOSPHORYLCHOLINE POLYMERS

SURFACE MODIFICATION OF MODEL SILICONE HYDROGEL CONTACT LENSES WITH DENSELY GRAFTED PHOSPHORYLCHOLINE POLYMERS

By

ALYSHA SPADAFORA, H.BSc.

A Thesis

Submitted to the School of Graduate Studies

In Partial Fulfillment of the Requirements

For the Degree of Master of Applied Science

McMaster University

MASTER OF APPLIED SCIENCE (2017) McMaster University

(Biomedical Engineering) Hamilton, Ontario

TITLE: Surface Modification of Model Silicone Hydrogel Contact Lenses with Densely Grafted Phosphorylcholine Polymers

AUTHOR: Alysha Spadafora, H.BSc. (University of Windsor)

SUPERVISOR: Professor Heather Sheardown

NUMBER OF PAGES: xv, 88

ABSTRACT

When a biomaterial is inserted into the body, the interaction of the surface with the surrounding biological environment is crucial. Given the importance of the surface, the ability to alter the surface properties to support a compatible environment is therefore desirable. Silicone hydrogel contact lenses (CL) allow for improved oxygen permeability through the incorporation of siloxane functional groups. These groups however are extremely surface active and upon rotation, can impart hydrophobicity to the lens surface, decreasing lens wettability and increasing protein and lipid deposition. Lens biofouling may be problematic and therefore surface modification of these materials to increase compatibility is exceedingly recognized for importance in both industry and research.

The current work focuses on the creation of a novel anti-fouling polymer surface by the incorporation of 2-methacryloyloxyethyl phosphorylcholine (MPC), well known for its biomimetic and anti-fouling properties. A controlled polymerization method was used to generate a unique double-grafted architecture to explore the effect of increasing surface density of polyMPC chains on corresponding anti-fouling properties. The novel free polymer was synthesized by a 3-step atom transfer radical polymerization (ATRP). First, poly(2-hydroxyethyl methacrylate) (polyHEMA) was polymerized by ATRP, where the hydroxyl (OH) groups of the polymer then underwent an esterification to create macroinitiating sites. From these sites, a second ATRP of poly(MPC) varying in length occurred, yielding the double-grafted polymer poly(2(2-bromoisobutyryloxy-ethyl methacrylate)-graft-poly(2-methacryloyloxyethyl phosphorylcholine (pBIBEM-g-pMPC). The polymer was designed for resistance to protein adsorption through a possible synergistic effect between the surface induced hydration layer by surrounding PC groups coupled with steric repulsion of the densely grafted chains.

To test its potential as a surface modifier, the polymer was grafted from model silicone hydrogel CL through a 4-step surface initiated ATRP (SI-ATRP) in a similar manner to the free polymer. First, the ATRP initiator was immobilized from the HEMA OH groups of the unmodified CL, generating Intermedate-1. A polyHEMA brush was grafted from the initiating sites yielding pHEMA-50, followed by the generation of a second initiator layer (Intermediate-2). A sequential ATRP of poly(MPC) then generated the target pMPC-50/pMPC-100 surfaces.

For the free pBIBEM-g-pMPC polymer analysis, ^{1}H-NMR and GPC determined polymers formed with a predictable MW and low polydispersity (PDI). For surface grafting, using a sacrificial initiator, ^{1}H-NMR and GPC indicated that the pHEMA-50 and pMPC-50/pMPC-100 polymers were well-controlled, with a MW close to the theoretical and a low PDI. For surface chemical composition, ATR-FTIR showed the presence of the ATRP initiator (Intermediate-1 and 2) by the appearance of a C-Br peak and disappearance of the OH peak. XPS confirmed the chemical composition of the 4-step synthesis by a change in the fraction of expected surface elements. Both the surface wettability and EWC of the materials increased upon pMPC modification, further improving upon increasing pMPC chain length. The contact angle was as low as 16.04 ± 2.37^{o} for pMPC-50 surfaces and complete wetting for pMPC-100. Finally, the single protein adsorption using lysozyme and bovine serum albumin (BSA) showed significantly decreased protein levels for pMPC-50/100 lenses, as much as 83% ($p<0.00036$) for lysozyme and 73% ($p<0.0076$) for BSA, with no significant difference upon chain length variation. The aforementioned data demonstrates that the novel polymer has potential in providing an anti-fouling and extremely wettable surface, specifically regarding silicone hydrogel CL surfaces.

ACKNOWLEDGEMENTS

First and foremost, I would like to thank my supervisor, Dr.Heather Sheardown for the incredible opportunity to be apart of such an inspiring research group. Heather, despite your incredibly busy schedule, you always make time for all of your grad students and that never will never go unnoticed. Your words of encouragement have given me the confidence to complete this Master's degree and I will forever miss being your chemist.

Next I would like to thank all of my fellow lab members within the Sheardown research group. Firstly, to Lina, you are always a phone call away and willing to help anyone and I truly want to thank you for all of your support. Cheryl, you contributed so much to my Master's degree. Thank you for always being my constant support system and the fire to keep me going. The late lab nights running columns, lunch breaks at random rooms that you have access to, and times in my apartment will never be forgotten. Myrto, the "greek goddess/contact lens guru", thank you so much for everything you have done for me, especially help with the radiolabelling work. Your knowledge and experience within your field is amazing and I will be eternally grateful for your words of wisdom and obviously our Starbucks writing days. Fran, you have been such an amazing role model and were always there for me with anything I needed, for that I am truly thankful. I also want to thank my summer students Andrea and Patrick- you both have a very incredible future awaiting you. Finally, to everyone else in the Sheardown lab (Nicole, Ben, Jeff, Ryan, Nadine, Moiz, Talena, Marion, Vida, Ivana, Fei, Musa, Aakash, Megan, and Lindsay), you have all contributed to this work in some form or another- thank you!

I also want to thank Lukas from Dr.Hoare's lab for helping me begin the process of conducting an ATRP synthesis. Thank you as well to Sam and Nick from Dr.Stöver's lab for

their help with GPC analysis. Finally, I would like to thank Danielle for her help with XPS as well as contact angle measurements.

To my Windsor family, you are a huge reason to my success within this journey. To my best friend Mel, thank you for always being my constant reminder of home. To Matt's family (Mr/Mrs. John, Natalie, little Abby, Celso, and Jessica), thank you for always being there for me, from watching my crazy Gizmo to providing so many words of encouragement- I appreciate all of you so much. Tasha, John-Eric, and my little Emmie, thank you for all of the rides to and from home and for being my constant support system- you guys helped more than you will ever know. Searra, my baby sister, thank you for providing me with countless laughs and so many words of encouragement. Josh, first of all, I guess we can officially agree that you lost the bet that I would do my PhD! Nonetheless, you have always believed in me more than anyone I know- thank you. To my mom and dad, my cheerleaders. Dad, thank you for always checking up on me and reminding me that I was capable of doing this. Mom, my best friend, if it wasn't for you being my voice of reason and shoulder to cry on, I don't know what I would have done- thank you.

Finally, to my boyfriend and my best friend Matthew. It goes without saying that I would not be where I am without your support. Thank you for driving three hours to see me at least every three weeks. You have been crutch, my sanity, my laugher, and the voice in my head telling me to keep on going. I cannot wait to see where this next step takes us, and our crazy, ridiculous, semi-dog, string/electrical cord eating, and ever so entertaining kitty Gizmo.

TABLE OF CONTENTS

LIST OF FIGURES

LIST OF TABLES

LIST OF SCHEMES

LIST OF ABBREVIATIONS

ATR-FTIR	Attenuated total reflectance- fourier transform infrared spectroscopy
ATRP	Atom transfer radical polymerization
BBIB	Benzyl-bromoisobutyrate
BIBB	α-Bromoisobutyryl bromide
BPY	2,2-Bipyridyl
BSA	Bovine serum albumin
CL	Contact lens
CLRP	Controlled living radical polymerization
CW	Continuous wear
DCM	Dichloromethane
DMAP	4-Dimethylaminopyridine
DMF	N,N-Dimethylformamide
DMSO	Dimethyl sulfoxide
DW	Daily wear
EGDMA	Ethylene glycol dimethacrylate
EtOH	Ethanol
EWC	Equilibrium water content
FDA	Federal drug and administration
GPC	Giant papillary conjunctivitis
GPC	Gel permeation chromatography
HCl	Hydrochloric acid
HEMA	2-Hydroxyethyl methacrylate

H_2O	Water
HPLC	High performance liquid chromatography
IMC	In-mould coating
IPN	Interpenetrating network
MA	Methacrylic acid
MeOH	Methanol
MMA	Methyl methacrylate
MMEQ	Monomethyl ether hydroquinone
Mn	Number average molecular weight
MPC	2-Methacryloyloxyethyl phosphorylcholine
MW	Molecular weight
Na_2CO_3	Sodium carbonate
Na_2SO_4	Sodium sulfate
NMR	Nuclear magnetic resonance
NVP	N-Vinyl pyrrolidone
PBIBEM	Poly(2-(2-bromoisobutryloxy)ethyl methacrylate
PBS	Phosphate buffer saline
PC	Phosphorylcholine
PDI	Polydispersity index
PDMS	Polydimethylsiloxane
PEG	Polyethylene glycol
PBIBEM-g-pMPC	Poly(2-(2-bromoisobutryloxyl)ethyl methacrylate)-graft-poly(2-methacryloyloxyethyl phosphorylcholine)

PMMA	Poly(methyl methacrylate)
PolyHEMA/pHEMA	Poly(2-hydroxyethyl methacrylate)
PolyMPC/pMPC	Poly(2-methacryloyloxyethyl phosphorylcholine)
P(SiMA)	Polybis(trimethylsilyoxy)methylsilylropyl glycerol methacrylate
PrLTF	Pre-lens tear film
PoLTF	Post-lens tear film
PVP	Polyvinylpyrrolidone
RGP	Rigid gas permeable
SAMs	Self-assembled monolayers
SI-ATRP	Surface initiated-atom transfer radical polymerization
TEA	Triethylamine
THF	Tetrahydrofuran
TRIS	3[Tris(trimethylsiloxy)silyl]propyl methacrylate
UPC	Upper palpebral conjunctiva
XPS	X-ray photoelectron spectroscopy

1. INTRODUCTION

1.1. Surface Modification of Silicone Hydrogel Contact Lenses

One of the most pertinent requirements of a biomaterial upon insertion into the body is compatibility with the surrounding environment without inducing an adverse reaction (ASM International, 2003). One exceedingly popular biomaterial-host interaction is that of contact lenses and the surrounding biological environment, specifically the tear film. Silicone hydrogel CL have become exceedingly popular, making up 68 percent of the amount of CL fitted per year in the United States in 2014 (Heiting, 2016). Their increased oxygen permeability by the incorporation of bulky siloxane functional groups permits extended wear beyond that of the conventional type lenses and promotes better ocular health overall (Goda & Ishihara, 2006; Sweeney, 2000). In fact, silicone hydrogel lenses enable up to five times more oxygen to permeate through the bulk material to reach the cornea compared to conventional lenses (Heiting, 2016).

Nevertheless, there is an associated downfall with these commonly used biomaterials, which centers around their incorporation of this highly hydrophobic silicone component (Tighe, 2004). These siloxane functional groups are known to demonstrate excellent mobility and are therefore extremely surface active (Stapleton, Stretton, Papas, Skotnitsky, & Sweeney, 2006). They can easily rotate to the surface of the lens imparting their hydrophobicity, resulting in a surface that is less wettable and more prone to deposition from the tear film (Nicolson, 2003). One common group of biomolecules deposited to a silicone hydrogel lens surface is lipids from the tear film. As well, despite enabling lower protein adsorption than seen with conventional lenses, the protein adsorbed to the surface of silicone hydrogel CL has been proven to be more

prone to denaturation (Jones et al., 2003; Senchyna et al., 2004; Subbaraman, Glasier, Senchyna, & Jones, 2005; Suwala, Glasier, Subbaraman, & Jones, 2007). The denaturation of proteins on the surface can stimulate CL material biofouling, which is the accumulation of unwanted biological organisms on the surface of a material (Lorentz & Jones, 2007). Such reactions can lead to corresponding immunological responses (Lorentz & Jones, 2007; Thissen et al., 2010).

The need for modification of these lenses to increase patient compliance and comfort has therefore been increasingly recognized. The typical modifications that exist for commercially available silicone hydrogel CL incorporate wetting agents or CL surface treatment (Keir & Jones, 2013). There clearly have been significant advances in the use of silicone hydrogel CL, granting them the most primary mode of CL choice for the wearer. However, the problem of end-of-day discomfort and dryness coupled with associated immunological disorders has driven a decrease in patience compliance and discontinuation of wear (Sankaridurg, de la Jara, & Holden, 2013). Consequently, the research in this field is highly regarded due to various unresolved challenges and untapped opportunity.

Over recent years, one type of surface modification technique that has gained pronounced attention is surface-initiated atom transfer radical polymerization (SI-ATRP). Compared with other surface modification techniques, SI-ATRP is versatile, granting the ability to graft polymer brushes of various controllable molecular architectures (Khabibullin, Mastan, Matyjaszewski, & Zhu, 2016). The sole requirement for SI-ATRP is the immobilization of the ATRP initiator on the surface, from which a polymer chain of controllable and tuneable MW and chain length can then be grafted (Khabibullin, Mastan, Matyjaszewski, & Zhu, 2016). Above all, SI-ATRP is highly regarded due to its permanent nature; the polymers are covalently grafted from the

substrate, minimizing the risk of exfoliation off of the surface (Khabibullin, Mastan, Matyjaszewski, & Zhu, 2016; Rossner & Vana, 2016).

Of the common techniques used to surface modify commercially available silicone hydrogels, surface plasma treatment is one of the most frequently used methods. Over time however, this method is known to become a temporary means to modification, with a high probability of recovering the underlying hydrophobic material (Hillborg et al., 2004; Oláh, Hillborg, & Vancso, 2005; Roth et al., 2008; Xia & Whitesides, 1998). SI-ATRP therefore has potential as an improvement over other surface modification techniques used in the CL field, despite the limited research and work with respect to CL applications.

SI-ATRP has also been used widely in the creation of bio-inert and anti-fouling surfaces by grafting various anti-fouling polymers from the substrate of interest (Tsujii, Ohno, Yamamoto, Goto, & Fukuda, 2006). Due to the controllability of molecular architecture by SI-ATRP, it has also been applied to create surfaces modified with densely grafted polymer brushes that act as a means to resist non-specific protein adsorption (De Vos, Leermakers, Lindhoud, & Prescott, 2011). One of the materials commonly used to prepare anti-fouling surfaces is 2-methacryloyloxyethyl phosphorylcholine (MPC). MPC is a hydrophilic, zwitterionic monomer that when polymerized, is known to reduce fouling (Goda, Ishihara, & Miyahara, 2015). Its unique structure allows it to act as a biomimetic agent, as it mimics that of the phospholipid layer of the cell membrane. MPC has been applied frequently to increase the anti-fouling character of various substrates by the SI-ATRP grafting of linear polyMPC chains (Feng, Zhu, Ishihara, & Brash, 2005; Feng, Brash, & Zhu, 2006, 2004; Feng, Zhu, Ishihara, & Brash, 2006; Iwata et al., 2004; Jin, Feng, Zhu, Sheardown, & Brash, 2010a; Seo, Matsuno, Konno, Takai, & Ishihara, 2008; Yan & Ishihara, 2008). However, to our knowledge, there has been minimal work

executed on varying the molecular architecture of polyMPC chains to evaluate the corresponding anti-fouling effects, especially in the application of CL.

1.2. Overall Objectives

The overall objective of this research is to synthesize a novel anti-fouling polymer to be utilized for surface modification applications, specifically with respect to the surface modification of silicone hydrogel contact lenses. The polymer should be able to be synthesized via a controlled polymerization technique (ATRP) in order to generate a tunable polymer chain length and molecular weight. The polymer should be densely grafted with anti-fouling polyMPC chains to evaluate a possible synergistic effect between the steric hindrance of the densely grafted molecular architecture coupled with the use of anti-fouling phosphorylcholine groups.

When applied to a biomaterial surface such as a model silicone hydrogel contact lens, the polymer should be able to be grafted from the material surface by a controllable and covalently bound surface modification alternative (SI-ATRP). The surface grafting should act as a low maintenance modification substitute that decreases the risk of exfoliation from the biomaterial. The surface grafted polymer should be characterizable and quantifiable with respect to the chain length, molecular weight, and chemical composition deposited on the surface. As well, the polymer should greatly improve surface characteristics of the silicone hydrogel CL by increasing surface wettability, water content, and acting as a means of decreasing lens protein adsorption that can initiate biofouling and impending immunological responses.

1.3. Thesis Outline

The information in this thesis is organized into six chapters. The first chapter (Chapter 1) introduces the topic of the research and project idea as well as the objectives of the thesis and outline. Chapter 2 is the literature review which introduces the main topics of the work including

aspects of silicone hydrogel contact lenses and how they correlate to protein deposition, the properties of 2-methacryloyloxyethyl phosphorylcholine (MPC) and its ophthalmic applications, as well as surface-initiated atom transfer radical polymerization (SI-ATRP) and its mechanism to achieve controlled architectures of surface polymer brushes. Chapter 3 (Materials and Methods) as well as Chapter 4 (Results and Discussion) are both presented in two sections. Part A includes the details of the novel anti-fouling polymer as a free polymer in solution and Part B includes the details of the novel polymer grafted from the surface of a model silicone hydrogel lens. Chapter 5 includes the concluding and future remarks, and Chapter 6 contains all the literature references used in the thesis.

2. LITERATURE REVIEW

2.1. The Exterior Eye

The human eye, depicted in Figure 1, is one of the most complex organs of the body and is separated into two main parts: the interior and exterior eye. The exterior eye (also referred to as the ocular coat) is most pertinent to contact lens wear and is made up of the cornea and the sclera, which are in junction by the limbus (Kiel, 2010). The cornea is avascular and optically transparent and acts as the primary refractive element of the eye (McCaa, 1982). Due to the absence of vascularization within the cornea, nutrients are driven by diffusion of either the aqueous humor or the tear film and oxygen is received directly from the surrounding air (Wolff, 1951). The sclera is a white and fibrous layer that is completely opaque in order to prevent light from entering anywhere within the eye except the cornea. Lining the sclera and eyelids is a part of the exterior eye known as the conjunctiva, which is a thin mucous membrane that offers protection and lubrication of the exterior layer of the eye (Holland, Mannis, & Lee, 2013). Finally, the border between the cornea and the sclera is formed by the limbus which comprises the pathways of the aqueous humor outflow (Van Buskirk, 1989).

Within a healthy eye, the tear film forms a layer over the cornea; interacting specifically with the outermost epithelial layer of the cornea. When a CL is inserted into the eye, it resides within the structure of the tear film and therefore the tear film and its function is of significance in CL applications.

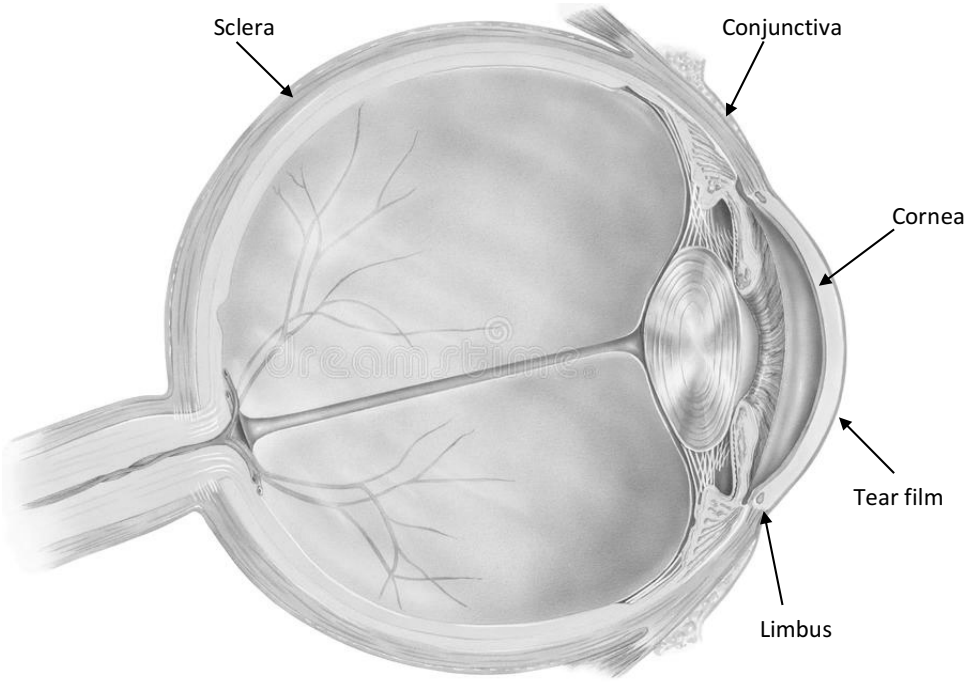

Figure 1. Cross sectional image of the eye, highlighting parts of the exterior eye based on the above descriptions. Image adapted from: https://www.dreamstime.com/stock-photo-eye-cross-section-human-eyeball-showing-following-structures-iris-anterior-limiting-membrane-posterior-limiting-membrane-image60390195.

2.1.1. The Tear Film

The tear film and its unique structure serve a very important role with respect to the function and homeostasis of eye. The thickness of the tear film ranges from 4-7 μm and is comprised of a variety of components including enzymes, proteins, lipids, glycoproteins, small molecules and metabolites (Omali, Subbaraman, Coles-Brennan, Fadli, & Jones, 2015; Tomlinson, 1992). Some of main roles of the tear film include but are not limited to: lubrication of the eyelids, conjunctiva, and cornea (Prydal, Artal, Woon, & Campbell, 1992), maintenance of a smooth surface to allow for light refraction (Lemp & Blackman, 1981), transportation of metabolic by-products to corneal surface and supplying cornea with nutrients (Prydal & Campbell, 1992),

removal or foreign matter from conjunctiva and cornea (King-Smith et al., 2000), protecting the ocular surface from pathogens (Lamberts, 1994), and providing the white blood cells with access to the conjunctiva and cornea (King-Smith et al., 2000). Overall, the mean pH value of the tear film ranges from 7.4-7.5, which is similar to the pH of plasma (Yamada, Mochizuki, Kawai, Yoshino, & Mashima, 1997).

2.1.1.1. Layers of the Tear Film

The tear film consists of a unique three-layered structure composed of the outermost lipid layer, an aqueous middle layer, and the inner mucous layer as illustrated in Figure 2 (Wolff, 1951). The outermost lipid layer, commonly referred to as the oily layer, is produced by the meibomian glands of the eyelids (Driver & Lemp, 1996). The role of this layer is primarily to reduce the evaporation of the tear film, while also providing a smooth ocular surface that prevents debris and other containments from entering the tear film (Driver & Lemp, 1996). The middle aqueous layer is composed of water, nutrients, oxygen, proteins, and antibacterial factors such as immunoglobulins (Davidson & Kuonen, 2004; Iwata, 1983). The aqueous layer is secreted by the lacrimal glands that are located above the eye. Soluble mucin present within this layer allows for an increase in the coherence and spreading of the tear film by decreasing the surface tension, contributing to an overall increase in viscosity (Davidson & Kuonen, 2004). Finally, the mucus layer of the tear film is comprised of multiple components including mucin, urea, glucose, salts, immunoglobulins, enzymes, leukocytes, water, and even cellular debris (Nichols, Chiappino, & Dawson, 1985). The mucus layer is secreted mainly by the conjunctival goblet cells, however, the conjunctival epithelium and corneal epithelium also contribute (Davidson & Kuonen, 2004). The main role of the mucin layer is to provide lubrication, protecting the cornea. The corneal epithelium is inherently hydrophobic, however, a hydrophilic

layer created by the mucus permits an even spreading of the aqueous layer over the ocular surface. This action protects the corneal epithelium from desiccation, bacterial contamination, and the effects of shear forces (Zhao, Jumblatt, Wood, & Jumblatt, 2001).

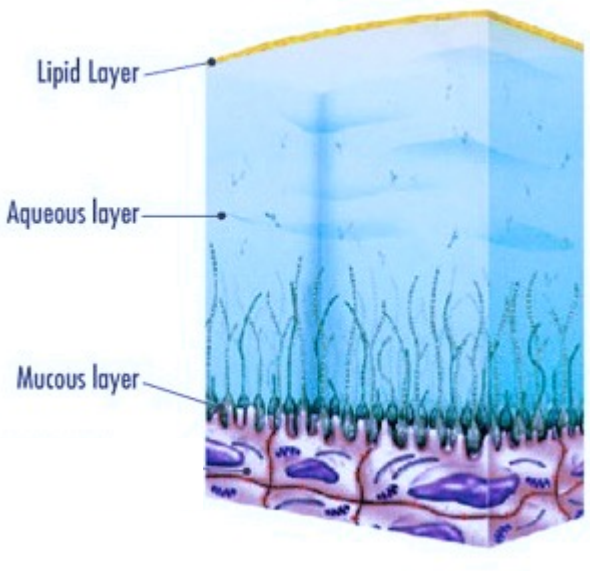

Figure 2. Structure of the tear film composed of outer lipid layer, middle aqueous layer, and inner mucous layer. Image adapted from: http://www.collinsoptometrists.com.au/dry-eye-clinic/understanding-the-tear-film-and-dry-eye/).

2.2. Contact Lens Biomaterials

With an estimated 140 million users worldwide, contact lenses have become one of the most successful and useful biomaterials (Hui, Sheardown, & Jones, 2012). The type of contact lens materials that exist on the market today can be mainly broken down into two different categories based on their constituent components: rigid gas permeable (RGP) lenses and soft lenses. Rigid gas permeable lenses were originally formulated as hard lenses made solely from polymethyl methacrylate (PMMA) (Fonn & Holden, 1988). These lenses were quickly replaced to incorporate materials such as silicon (siloxymethacrylates) or fluorine (fluorocarbon methacrylates) within their matrix to increase oxygen permeability and comfort (Fonn & Holden,

1988). Despite this, 90 percent of contact lens wearers still prefer the soft lens type to RGP lenses due to the initial increase of comfort, compliance, and resistance to dryness.

Soft lenses, more commonly referred to as "hydrogel lenses", are composed of hydrophilic monomers cross-linked together to create a three-dimensional network that absorbs significant amounts of water (López-Alemany, Compañ, & Refojo, 2002). Common types of hydrophilic monomers used in the synthesis of soft lenses include 2-hydroxyethyl methacrylate (HEMA), N-Vinylpyrrolidone (NVP), methyl methacrylate (MMA), and methacrylic acid (MA) polymerized in various combinations to create lenses known as conventional soft lenses (Hu et al., 2011).

These hydrophilic domains allow the lenses to absorb large amounts of water and by diffusion, oxygen can then be delivered to the cornea through this aqueous phase (Alvord et al., 1998; López-Alemany et al., 2002). However, for overnight extended lens wear, a minimum oxygen transmissibility of 87 barrer/mm is required to avoid overnight corneal swelling that can lead to ocular infection (Holden & Mertz, 1984). Consequently, the limit of oxygen permeability in water imposes a restriction to the amount of oxygen that can actually reach the cornea using a conventional hydrogel lens (Benjamin, 1993). As a result to this, the use of conventional hydrogel lenses has been confined solely to daily wear (DW), as they commonly lead to hypoxic responses when worn on an overnight basis (Alvord et al., 1998; Nicolson & Vogt, 2001).

2.2.1. Silicone Hydrogel Contact Lenses

To be a candidate for extended wear, lenses should employ softness, on-eye comfort, surface wettability, hydrated mechanical strength, optical transparency, and adequate oxygen transmissibility to reach the cornea (Nicolson & Vogt, 2001). Silicone hydrogel contact lenses were created to satisfy all of the above, with the emphasis on improved oxygen permeability

compared to their conventional counterparts (Sweeney, 2000). Silicone polymers contain a backbone composed entirely of silicon-oxygen bonds, also known as siloxanes and due to the bulkiness and chain mobility of the siloxane group, silicone polymers are known to facilitate significant oxygen permeability (Goda & Ishihara, 2006).

Silicone hydrogels, developed to overcome the oxygen delivery limitations of conventional hydrogel materials, are therefore composed of the highly oxygen permeable siloxane groups of polydimethylsiloxane (PDMS)-based macromers/monomers within the hydrophilic hydrogel network (Goda & Ishihara, 2006). These hybrid lenses incorporate the comfort of conventional hydrogel lenses, while simultaneously gaining an extremely high oxygen permeability that can be greater than 150 barrer/mm (Efron, Morgan, Cameron, Brennan, & Goodwin, 2007).

2.2.1.1. Silicone Hydrogels in Contact with the Tear Film

The interaction of contact lenses with the tear film is very important for the maintenance of ocular health. When a contact lens that is approximately ten times thicker than the tear film is inserted into the eye, it divides the structure into two layers: the outermost layer referred to as the pre-lens tear film (PrLTF), and innermost layer that lies between the back of the CL and the cornea referred to as the post-lens tear film (PoLTF), as shown in Figure 3 (Keir & Jones, 2013; Nichols, Mitchell, & King-Smith, 2005). This thus results in a surface chemistry of the CL that is quite different than that of the natural ocular surface. Studies have shown that CL wear disrupts the normal tear physiology and balance through thinning of tear film (Holly, 1981; Nichols, Mitchell, & King-Smith, 2005; Nichols & King-Smith, 2004) coupled with evaporation (Guillon, Optom, & Maissa, 2008), which ultimately can lead to dry spot formation and CL deposition (Bruce, Golding, Au, & Rowhani, 1995).

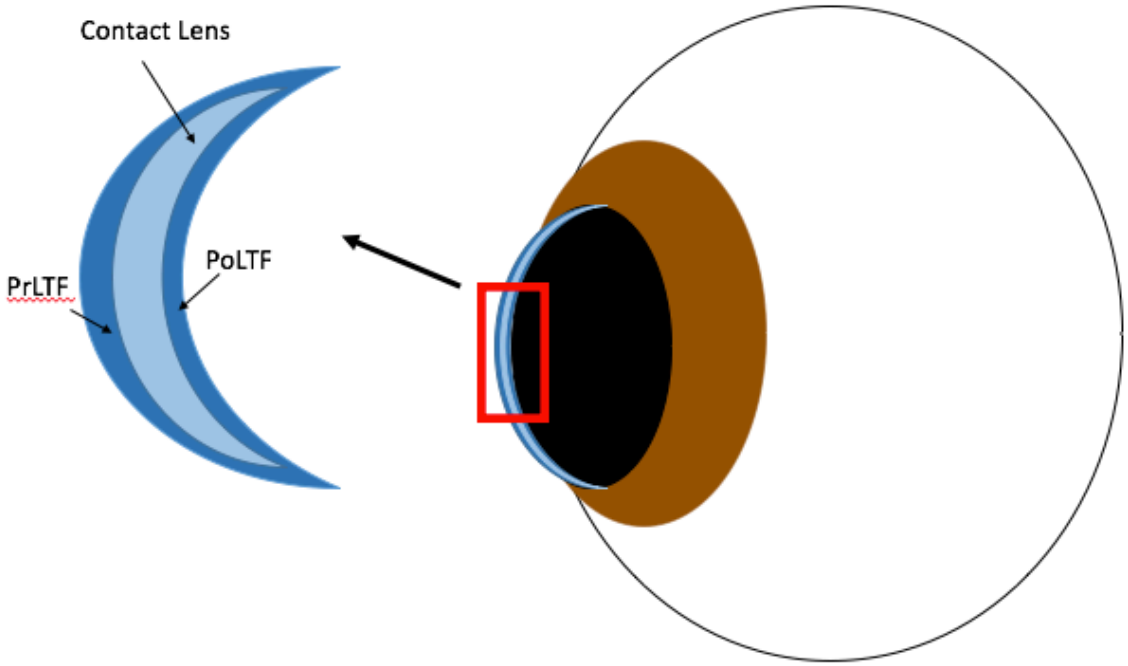

Figure 3. Illustration representing the insertion of a contact lens within the tear film. The arrows locate the position of the pre-lens tear film (PrLTF) and the post-lens tear film (PoLTF) upon insertion.

Hydrogels, specifically silicone hydrogels, are considered to have exceedingly dynamic surfaces, where the highly hydrophobic siloxane group is known to be extremely surface active (Stapleton, Stretton, Papas, Skotnitsky, & Sweeney, 2006). Nicolson related this phenomena to the concept of "like attracts like" in terms of the surrounding hydrophobic air and native hydrophobicity of the siloxane functional group (Nicolson, 2003). This interaction is believed to be the result of the ease of rotation and concentration of the hydrophobic silicone on the surface of the CL, demonstrated in Figure 4 (Nicolson, 2003). This contributes to overall surface hydrophobicity of the CL, causing these lenses to be prone to deposition of lipids and the adsorption of protein (Nicolson, 2003). Therefore, the inherit hydrophobic surfaces of these CL

prompted the need for surface modification for continuous wear (CW) applications.

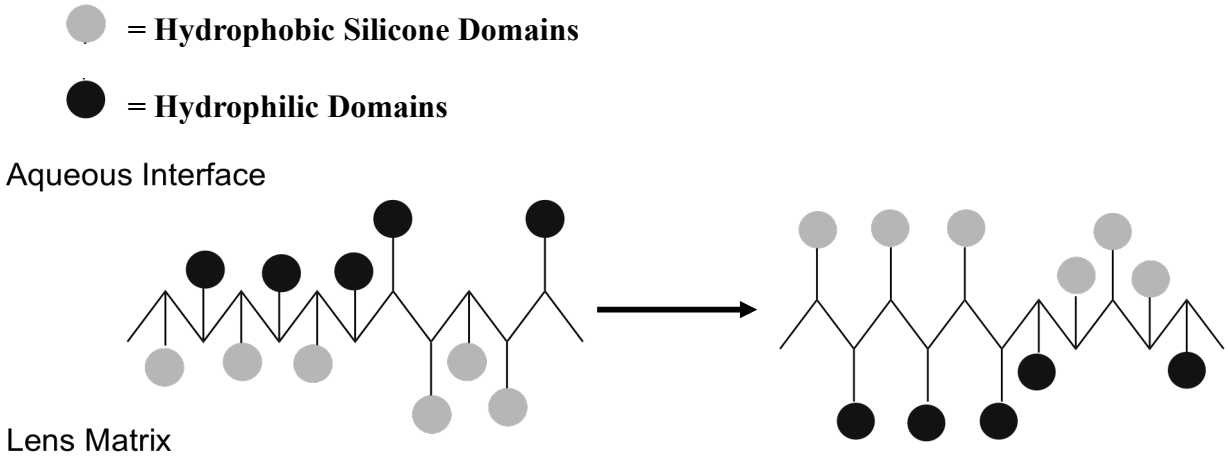

Figure 4. Silicone hydrogel bond rotation upon aerial exposure. The surface active silicon-oxygen (Si-O) bond rotates freely upon exposure to air, inducing a hydrophobic surface. Image adapted from: http://www.visioncareprofessional.com/emails/alcon/33/WettingArticle.pdf

2.2.1.2. Surface Pre-Treatment and Modification of Silicone Hydrogels

Emphasis has been placed on surface treatment for the improvement of these CW silicone hydrogel lenses to increase surface wettability, hydrophilicity, and decrease corresponding protein adsorption and lipid deposition. The first generation of silicone hydrogels used gas plasma treatment by two different methods (Nicolson, 2003; Tighe, 2004). CIBA Vision used plasma coating to launch Focus Night & Day® and O_2 Optix™ (lotrafilcon A, lotrafilcon B) materials (Nicolson, 2003; Tighe, 2004). These materials use surface gas plasma treatment to create a 25 nm coating of a proprietary polymer that forms a covalently bound homogenous layer more wettable that the underlying lens surface (González-Méijome et al., 2006; Nicolson, 2003). Bausch & Lomb created Purevision®, that used plasma oxidation on the core polymer to convert hydrophobic silicone to silicate (Tighe, 2004). This has been described as creating fissures that have "islands of glass", opening down on the substrate polymer, bridging water over the fissures to create a more wettable surface (Tighe, 2004).

The second generation of silicone hydrogels do not use plasma modification to create a more hydrophilic surface; rather they incorporate the use of a high molecular weight internal wetting agent into the hydrogel network (Tighe, 2004). Johnson & Johnson Vision incorporated high molecular weight polyvinylpyrrolidone (PVP) into the polymer structure to create Acuvue® Advance® (galyfilcon A) and Acuvue® Oasys™ (senofilcon A). These materials incorporate various macromers and monomers together alongside a hydrophilic PVP material that, while entrapped, can migrate to the surface of the lens to increase lens wettability, while maintaining high oxygen permeability (Jones, 2007).

Finally, the third generation materials were developed by CooperVision. Biofinity® (comfilcon A) and AVAIRA™ (enfilcon A) do not use surface treatment or wetting agents. Rather these materials have sufficiently high oxygen permeability through the use of silicone-based macromers and achieve high surface wettability using common hydrophilic monomers (Jones, 2007).

2.3. Protein Adsorption and Deposition

2.3.1. Tear Film Proteins Interacting with Contact Lenses

There are a variety of proteins that are present within the human tear film that can interact with contact lens biomaterials. Over 100 proteins have been identified within the proteomic profile deposited on contact lenses (de Souza, Godoy, & Mann, 2006). Specific to silicone hydrogels, some of the main deposited proteins include lipocalin, lactoferrin, albumin, and lysozyme (Green-Church & Nichols, 2008; Zhou et al., 2006).

One well studied protein in terms of contact lens deposition is lysozyme. Lysozyme constitutes a high concentration within the human tear film at 1.9 mg/mL and acts as an antimicrobial agent. Therefore it is often used as a “model protein” for in vitro contact lens

deposition studies (Fullard & Tucker, 1991; Sack, Tan, & Tan, 1992). Lysozyme consists of a single polypeptide chain of 129 amino acid residues, resulting in a molecular weight of around 14.3 kDa (Canfield, 1963). Lysozyme has an isoelectric point of 11.1 and is positively charged at physiological pH, inducing its interaction with negatively charged (anionic) contact lens materials (Fullard & Tucker, 1991; Sack, Tan, & Tan, 1992).

Another well studied protein in terms of contact lens deposition is albumin. Albumin constitutes the highest fraction of any other protein found within the blood serum and is therefore involved in the initial response to host biomaterial implantation (Tang, Thevenot, & Hu, 2008). The concentration of albumin in the tear film varies; making up 0.02-0.04 mg/mL during the day (Fullard & Snyder, 1990; Ng, Cho, Wong, & Chan, 2001) reaching as high as 0.5 mg/mL after sleeping (Choy, Cho, Benzie, & Ng, 2004; Sack, Tan, & Tan, 1992; Tan, Sack, Holden, & Swarbrick, 1993). It has a higher molecular weight than that of lysozyme (66 kDa) and is composed of 585 amino acids. Albumin has an isoelectric point of 4.9 and is negatively charged at physiological pH, which, contrary to lysozyme, tends to attract positively (cationic) charged lens materials (Fullard & Snyder, 1990; Ng, Cho, Wong, & Chan, 2001). Due to their opposite charges, prevalence within the tear film, and significant roles, these two proteins were chosen for the focus of the protein adsorption work within this study.

2.3.2. Principles of Protein Adsorption

A protein is a three-dimensional structure composed of long chains of amino acids, which are hydrophilic or hydrophobic in nature. Hydrophobic (non-polar) amino acids are typically protected within the three-dimensional protein network, while the hydrophilic (polar) amino acids with or without charged groups can interact with a surrounding surface (Luensmann & Jones, 2012). The protein is folded into this three-dimensional structure held together by forces

such as hydrogen bonds, Van der Waals forces, and hydrophobic forces (Voet, & Voet, 2004).

There are several factors that can influence protein adsorption to biomaterial surfaces, including properties of the protein influencing their surface interaction and properties of the surfaces influencing their interaction with proteins (Dee, Puleo, & Bizios, 2002). Some of these common interactions are summarized in Table 1 and Table 2.

Table 1. Properties of proteins influencing their interaction with material surfaces. Table adapted from (Dee, Puleo, & Bizios, 2002).

Property	Effect
Size	The larger the molecule, the more sites of contact with the surface.
Stability	If the protein is unstable and has points of intramolecular cross-linking, it has the ability to unfold to a greater extent and form more contact with the surface.
Charge	Molecules that are closer to their isoelectric point have the tendency to adsorb to a surface more readily.
Unfolding Rate	If a protein can unfold rapidly, it can have the ability to form contacts with the surface very quickly.

Table 2. Properties of material surfaces influencing their interaction with corresponding proteins. Table adapted from (Dee, Puleo, & Bizios, 2002).

Property	Effect
Potential	Surface potential can influence the interaction with oppositely charged proteins and cause ions to distribute within solutions.
Hydrophobicity	More protein tends to bind to hydrophobic surfaces.
Topography	The amount of surface area for protein to bind to will increase when the amount of surface texture increases.
Composition	The types of intermolecular forces to interact with proteins are governed by the chemical makeup of the surface.
Heterogeneity	If a surface is not uniform, the domains of uniformity on the surface material will interact differently with proteins

Of the aforementioned interactions, contact of proteins with a hydrophobic surface is an aspect that is well studied. Once protein adsorption occurs to a biomaterial surface, a monolayer of protein can form on the surface of the biomaterial (Latour, 2005). Upon adsorption, a protein within the monolayer can have the tendency to alter its structure to conform to the surrounding environment, making the structure of the protein a metastable one (Luensmann & Jones, 2012).

When a protein is exposed to a water-based solution, the interaction with this solution is energetically unfavourable as it tends to increase the Gibbs free energy, making an aqueous environment unfavourable for surface adsorption (Norde, 1992). Upon exposure to a hydrophobic surface, proteins can easily rearrange their structure in a way to favour the adsorption to the surface (Norde, 1992). The act of hydrophobic surface adsorption is therefore energetically favored, as the overall process tends to lower the associated Gibbs free energy (Roach, Farrar, & Perry, 2005).

A conformational change and unfolding in a protein structure is termed "denaturation" and causes an alteration in the protein's typical function (Norde, 1986). It is therefore very well known that proteins exposed to a hydrophobic surface are much more likely to denature than when interacting with hydrophilic surfaces (Castillo, Koenig, Anderson, & Lo, 1985; Garrett, Garrett, & Milthorpe, 1999; Lee, Li, & Park, 2001). Other than the hydrophobicity of the surface, protein denaturation can also be greatly influenced by contact time with the surface, surrounding pH, temperature, and chemical make up of the interacting surface (Norde & Lyklema, 1991; Norde, 1986; Norde & Anusiem, 1992).

Following denaturation, proteins are altered in a way such that they are no longer able to perform their typical function and can be disruptive by interacting with other proteins and cells. Living cells (particularly inflammatory cells) arriving at the biomaterial surface interact with the molecular structure of the adsorbed protein monolayer instead of the biomaterial surface itself (Latour, 2005; Norde, 1986). If the monolayer is composed of proteins that are denatured, this may cause aggregation and lead to the triggering of an immune response (Allansmith et al., 1977; Lindgren, Sörgjerd, & Hammarström, 2005).

2.3.2.1. Protein Adsorption and Deposition to Silicone Hydrogels

As mentioned previously, the introduction of silicone into conventional hydrogels allows for increased oxygen permeability through the lens matrix. However, the introduction of the silicone also results in a decrease in the overall surface wettability and an increase in the deposition of lipids from the tear film (Jones et al., 2003; Lorentz & Jones, 2007; Nicolson & Vogt, 2001).

The deposition of proteins specific to contact lens surfaces, however, can be influenced by a variety of factors including surface charge, water content, wear time, tear-film composition, and degree of hydrophilicity (Garrett & Milthorpe, 1996; Jones, Mann, Evans, Franklin, & Tighe, 2000; Lee, Li, & Park, 2001; Tighe, Jones, Evans, & Franklin, 1998). Studies have demonstrated that compared to conventional lenses, silicone hydrogels do deposit lower levels of protein, however the protein that is deposited does experience a different outcome with respect to denaturation after exposure (Jones et al., 2003; Senchyna et al., 2004; Subbaraman, Glasier, Senchyna, & Jones, 2005; Suwala, Glasier, Subbaraman, & Jones, 2007). Jones and colleagues evaluated the activity of lysozyme adsorbed to group IV ionic hydrogel materials (etafilcon A) and silicone hydrogel lenses (Jones et al., 2003). They discovered that while etafilcon adsorbed the greatest amount of lysozyme compared to other lenses, the majority of the lysozyme retained its activity, with only 5-10% actually denatured (Jones et al., 2003). More notably, they found that even though silicone hydrogels adsorbed lower amounts of lysozyme than conventional materials, the amount of lysozyme denatured was significantly higher, a trend also reported by other researchers (Ng, Cho, Wong, & Chan, 2001; Senchyna et al., 2004; Suwala, Glasier, Subbaraman, & Jones 2007).

This discovery was of great importance because numerous works have suggested a

correlation between denatured proteins on the surface of a contact lens and the initiation of a variety of responses including end-of-day discomfort and more significantly, an immunological response (Allansmith, 1985; Allansmith et al., 1977; Trocme, Kephart, Allansmith, Bourne, & Gleich, 1989).

One common associated immunological response to contact lens wear is giant papillary conjunctivitis (GPC) (Allansmith et al., 1977). GPC is often times a reversible condition associated with an inflammatory reaction of a part of the anterior eye called the upper palpebral conjunctiva (UPC) (Spring, 1974). GPC causes an enlarged papillae, increased mucus secretion, and palpebral hyperemia with typical symptoms of ocular discomfort and itching, leading to CL intolerance (Allansmith et al., 1977; Korb et al., 1980). There has been a linked association of increased GPC for patients wearing silicone hydrogels, even compared to the conventional counterparts (Dumbleton, 2003).

GPC, while a very common response to EW lenses, is one of the many associated immunological responses to silicone hydrogels. Another common problem regarding CL wear is microbial keratitis, a condition resulting in an infection of the cornea due to the colonization of bacteria on the CL (Eltis, 2011). Microbial keratitis in its severe form can lead to corneal ulceration; a condition that when left untreated can result in the loss of vision (Eltis, 2011).

The quantity and deposition profile of proteins on silicone hydrogel CL materials is perhaps of greater importance than conventional lenses due to their intended lengthy wear period of 30 days without removal (Jones et al., 2003). It goes without saying that the need for increased knowledge and research concerning the in vivo deposition of proteins to silicone hydrogel contact lenses is crucial.

2.4. 2-Methacryloyloxyethyl Phosphorylcholine (MPC)

Biomimetic and bio-inspired materials have been known to improve corresponding fouling reactions upon insertion of the biomaterial within the body. One approach focuses on modelling the natural cell membrane with the use of phospholipids, the most fundamental unit in the construction of the cell membrane (Goda & Ishihara, 2006). In particular, in 1990, Ishihara and colleagues successfully synthesized the 2-methacryloylethyl phosphorylcholine (MPC) monomer, specifically designed to mimic the phosphorlycholine (PC) group, one of the most fundamental polar phospholipids of the cell membrane (Figure 5) (Goda, Ishihara, & Miyahara, 2015).

MPC contains a reactive methacrylate group that allows it to easily polymerize under a variety of polymerization techniques (Ishihara & Takai, 2009; Iwasaki & Ishihara, 2005, 2012; Lewis, 2000). The inherent anti-fouling capabilities of the monomer extend from its zwitterionic PC side chain, decreasing electrostatic interactions and creating a thick hydration shell with mobile water molecules, further described in 2.4.1 (Goda, Ishihara, & Miyahara, 2015).

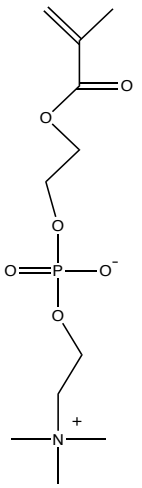

Figure 5. Structure of commercially available 2-methacryloyloxyethyl phosphorylcholine (MPC) monomer.

2.4.1. Proposed Mechanism of Anti-Fouling

MPC is a zwitterionic monomer that, upon polymerization, is referred to as a polyzwitterionic material. PolyMPC can be classified in literature as a polybetaine, referring to a molecule carrying both a negative and positive charge on a single monomeric unit (Chen, Li, Zhao, & Zheng, 2010). The mechanism of anti-fouling associated with these molecules has been widely studied, however still not fully definitive. It is hypothesized that the anti-fouling nature of these materials is correlated with the presence of a surface hydration layer that interacts with the material (Chen, Li, Boozer, & Jiang, 2000; Herrwerth, Eck, Reinhardt, & Grunze, 2003; Zheng et al., 2005). This hydration layer is also thought to be a similar mechanism of anti-fouling for polyethylene glycol (PEG) materials, well known for their ability to resist non-specific protein adsorption (Chen, Li, Zhao, & Zheng, 2010).

Kitano et al., discovered a difference in surface hydration induced by ionic hydration and hydrogen bonding, observing more surface bound water around zwitterionic materials as opposed to other hydrophilic and hydrophobic materials (Kitano et al., 2005). This discovery lead to the hypothesis that the positive and negative charges on polyMPC can electrostatically bind water molecules to create a tightly bound electrostatic-induced hydration layer (Chen, Li, Zhao, & Zheng, 2010). This tightly bound surface hydration layer is thought to form an energetic and physical barrier, which then acts to resist non-specific protein adsorption at the surface (Chen, Li, Zhao, & Zheng, 2010). This described anti-fouling mechanism is illustrated below in Figure 6.

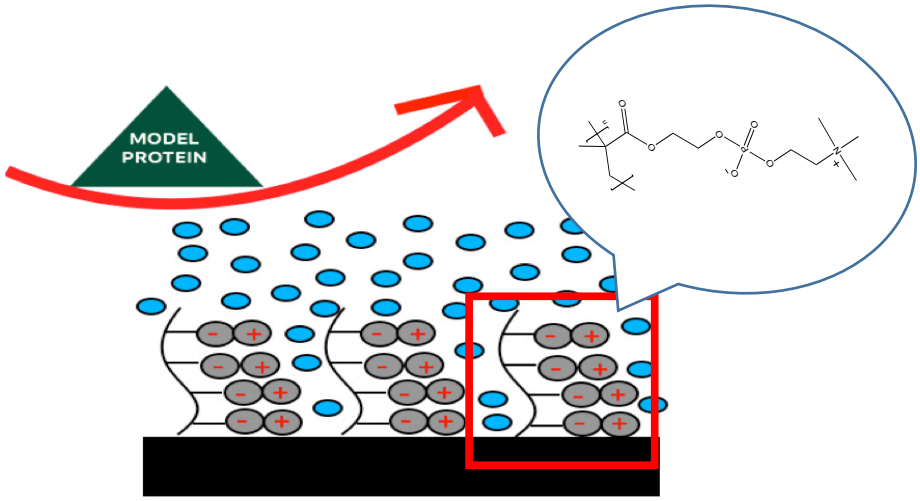

Figure 6. Proposed mechanism of anti-fouling for surfaces modified by polyMPC. Non-specific protein adsorption is reduced by water molecules that are bound tightly to the surface by an electrostatic-induced hydration layer.

2.4.2. Contact Lens Applications

Since the discovery of MPC, the material has been implemented into the design of contact lens biomaterials. Currently there exists a commercially available phospholipid-based conventional soft contact lens made by Biocompatibles Co. Ltd (UK) named Proclear® (omafilcon A), designed to mimic the ocular surface. These CL are composed of HEMA and MPC monomers crosslinked with an ethyleneglycol dimethacrylate (EGDMA) crosslinker and are FDA approved to "provide improved comfort for contact lens wearers who experience mild discomfort or symptoms relating to dryness during lens wear" (Harrington, 2011).

Biocompatibles Co. Ltd (UK) has since also developed a novel PC-coated extended wear silicone hydrogel incorporating a hydrophilic silicone-based macromer (Willis et al., 2001). An in-mould coating (IMC) technique was used to fabricate the uniform PC-coated lenses, while still maintaining mechanical strength as well as oxygen and solute permeability suitable for extended wear (Goda & Ishihara, 2006; Willis et al., 2001).

There has also been a large contribution within this field from Ishihara and colleagues (Shimizu, Goda, Minoura, Takai, & Ishihara, 2010). They constructed a superhydrophilic silicone hydrogel CL through the creation of an interpenetrating network (IPN) by cross-linked p(MPC) and polybis(trimethylsilyoxy)methylsilylropyl glycerol methacrylate (p(SiMA)) chains, yielding PSiMA-*ipn*-PMPC (Shimizu, Goda, Minoura, Takai, & Ishihara, 2010). The PSiMA-*ipn*-PMPC material proved to demonstrate optical and mechanical properties suitable for CL wear, along with increased surface wettability and reduced protein adsorption.

2.5. Polymer Surface Modification for Enhanced Material Compatibility

The interaction between a biomaterial and the surrounding biological environment is governed by the surface properties of the material and thus, the ability to alter these properties to support a compatible environment is crucial. One way to modify such surface properties as friction, wettability, lubrication, and the corresponding fouling reactions is through the deposition of a polymer brush layer with end-group functionalization (Zdyrko & Luzinov, 2011). These methods are known to enhance surface characteristics, with the advantage of achieving minimal impact on the overall bulk material properties (Zdyrko & Luzinov, 2011).

Polymer brushes are not only mechanically robust, but also have the capability to introduce a wide variety of functional groups to the surface of a material, granting vast synthetic capabilities (Xu, Neoh, & Kang, 2009). The brushes can be prepared in one of two ways: physisorption or covalent modification. In the former, polymer chains contain ‘sticky’ functional groups and adsorb to a substrate non-covalently. However, this has been noted to be unstable and easily exfoliated off of the surface (Xu, Neoh, & Kang, 2009). In the latter, the ability to tether polymer brushes to biomaterial surfaces covalently to govern anti-fouling and biologically compatible attributes has gained significant attention (Edmondson, Osborne, & Huck, 2004;

Goddard & Hotchkiss, 2007; Pyun, Kowalewski, & Matyjaszewski, 2003; Senaratne, Andruzzi, & Ober, 2005; Zhao & Brittain, 2000). Covalent tethering to the surface is a much more stable method due to the fact that the target component is covalently bound to the surface of interest, decreasing the risk of exfoliation (Zhao & Brittain, 2000). The process to achieve covalent surface grafting can occur by one of two ways: grafting "to" or grafting "from" the surface, as depicted in Figure 7.

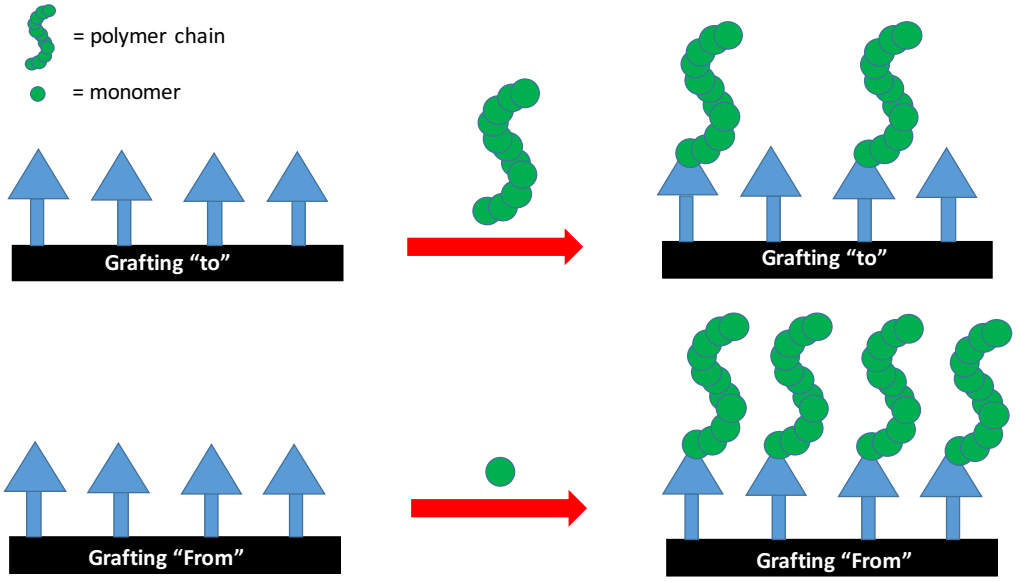

Figure 7. Illustration of "grafting to" and "grafting from" procedure for surface modification applications. Illustration adapted from (Banerjee, Paira, & Mandal, 2014).

2.5.1. "Grafting to" Approach

In the process of "grafting to", the polymers used to surface modify are end-group functionalized initially, and undergo a reaction (or series of reactions) to become end-tethered to the surface of interest, through covalent linkages (Zhao & Brittain, 2000). The end-group functionalized polymer brushes can be synthesized using either cationic, anionic, conventional free radical, controlled living radical, or ring opening metathesis polymerization techniques (Zdyrko & Luzinov, 2011).

Despite the benefits, there are challenges and major drawbacks with the "grafting to" procedure. Only a small amount of polymer can actually become immobilized on the surface, and this amount is limited to a low grafting density and thickness (Zhao & Brittain, 2000). This is a self-limiting method because the polymer chains must be able to diffuse through the polymer film to reach the reactive sites for attachment. However, this barrier increases as the thickness of the polymers that are tethered to the surface increases, limiting the amount of polymer that can be immobilized on the surface (Jones, Lehnert, Schonherr, & Vancso, 1999). Due to these shortcomings, another approach to surface modify to generate greater grafting density and thickness termed "grafting from" was developed.

2.5.2. "Grafting from" Approach

In terms of polymeric surface modifications, the "grafting from" approach, commonly referred to as surface-initiated polymerization, has gained substantial attention. In this process, the surface of the material is chemically modified with an initiator monolayer, and the polymer chains grow directly "from" the reactive sites on the surface (Edmondson, Osborne, & Huck, 2004; Stamm, 2008; Zhao & Brittain, 2000). The diffusion and steric limitation encountered in the "grafting to" method is less substantial because, instead of large polymer chains diffusing to the surface, the small monomer molecules will move to the initiator immobilized surfaces (Zhao & Brittain, 2000). Furthermore, the functional group for covalent tethering remains at the surface, limiting the diffusion barrier encountered by the reactive monomers. Consequently, much thicker polymer brush surface layers with higher grafting densities and longer chain lengths are achievable (Xu, Neoh, & Kang, 2009).

The chemical nature of the initiators covalently bound to the surface to be "grafted from" will vary based on the type of polymerization mechanism chosen. Several polymerization

methods for the "grafting-from" approach have been developed such as surface-initiated anionic polymerization (Jordan, Ulman, Kang, Rafailovich, & Sokolov, 1999), cationic polymerization (Jordan & Ulman, 1998), ring-opening polymerization (Carrot et al., 2002), conventional free-radical, and controlled living radical polymerization (CLRP) (Edmondson, Osborne, & Huck, 2004; Pyun, Kowalewski, & Matyjaszewski, 2003; Senaratne, Andruzzi, & Ober, 2005). In order to achieve well-defined brushes with controlled structure, thickness, composition, and low polydispersity, much emphasis has been placed CLRP. Of these controlled surface-initiated techniques, one that has gained pronounced attention and has proven to be most versatile and well studied is Atom Transfer Radical Polymerization (ATRP) for surface functionalization (Edmondson, Osborne, & Huck, 2004; Pyun, Kowalewski, & Matyjaszewski, 2003).

2.6. Atom Transfer Radical Polymerization (ATRP)

As one of the most robust and well studied CLRP techniques to achieve polymers with a controlled molecular architecture and MW, ATRP has gained significant attention in recent years. This technique is attractive due to its compatibility with a wide range of commercially available monomers (Kamigaito, Ando, & Sawamoto, 2001; Matyjaszewski & Xia, 2001; Wang & Matyjaszewski, 1995), solvents, commercially available initiators, and broad reaction conditions (Matyjaszewski & Tsarevsky, 2009; Rossner & Vana, 2016).

The mechanism of ATRP is depicted in Scheme 1. This polymerization technique employs a nitrogen based ligand, a transition metal halide catalyst, a monomer of choice, and an ATRP solvent (Patten, Xia, Abernathy, & Matyjaszewski, 1996; Wang & Matyjaszewski, 1995). The process is governed by the equilibrium that exists between the propagating radicals (R•) and the dormant species (R-X, which X= Br or Cl, and R is the polymer chain), which is typically a macromolecular species or an initiating alkyl halide (Matyjaszewski, 2012). This dormant

species will react with what is called an activator or deactivator sporadically. The activator (Mt^m/L_n, where Mt is the transition metal catalyst, m is the oxidation state, and L_n is the ligand) in the lower oxidation state, will react with this dormant species to form active radicals (R•) with a rate constant of activation (k_{act}). The deactivator ($X\text{-}Mt^{m+1}/L_n$) is the higher oxidation state transition metal catalyst, coordinated with the transferred halide ligand. The deactivator will react in reverse with the propagating radical with a rate constant of k_{deact} to re-form for dormant species. This dormant species will then go on to regenerate the activator (Matyjaszewski, 2012; Rossner & Vana, 2016).

The polymer chain grows by continuing the addition of monomer (M) to the propagating radicals at a rate of k_p. Termination occurs at a rate of k_t through the mechanism of disproportionation or recombination. However, due to the fact that the concentration of propagating radicals is sufficiently lower than that of the dormant species, the fraction of chains undergoing termination can be suppressed to roughly <5%, producing well-defined polymer chains (Matyjaszewski, 2012). In a successful ATRP, the initiation process should occur quickly to ensure the constant concentration of growing polymer chains. As well, due to the dynamic equilibrium that exists between the dormant and propagating radicals, the dormant chains should also retain the ability to grow (Matyjaszewski, 2012).

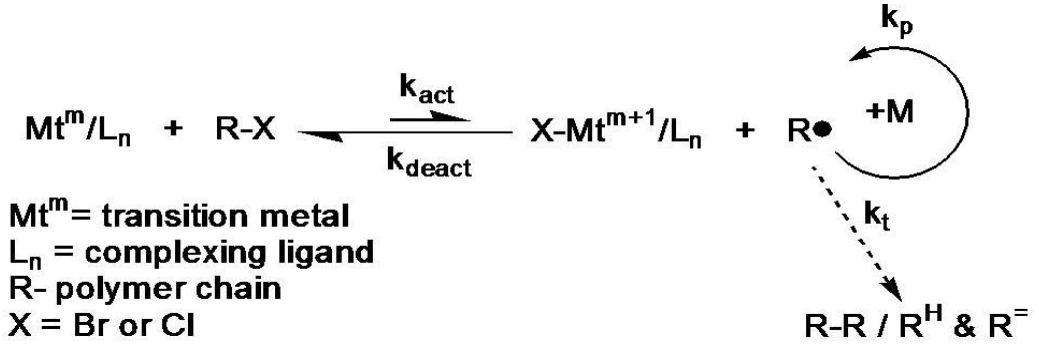

Scheme 1. Overall mechanism of Atom Transfer Radical Polymerization (ATRP). Image adapted from: http://www.cmu.edu/maty/chem/fundamentals-atrp/atrp.html.

2.6.1. Surface-Initiated ATRP (SI-ATRP)

Surface-initiated ATRP has been applied to a wide variety of surfaces, with well defined polymer brushes extending from particles, flat surfaces, porous materials, and various other commonly used biomaterial substrates (Tsujii, Ohno, Yamamoto, Goto, & Fukuda, 2006). The mechanism of action remains unchanged with surface-initiated ATRP (SI-ATRP). There is, however, a particularly low initiator concentration on the surface, and therefore a very low concentration of deactivating (Cu^{II}) species, which can lead to an uncontrollable chain growth (Pyun, Kowalewski, & Matyjaszewski, 2003).

The first attempt to overcome this was Ejaz et al., during the preparation of poly(methyl methacrylate) (PMMA) brushes from self-assembled monolayers (SAMs) (Ejaz, Yamamoto, Ohno, Tsujii, & Fukuda, 1998). They added the additional free (sacrificial) initiator of *p*-toluenesulfonyl chloride to regain control over the polymerization (Ejaz, Yamamoto, Ohno, Tsujii, & Fukuda, 1998). Another method was discovered by Matyjaszewski et al., in the synthesis of polystyrene brushes from silicone wafers functionalized by bromoisobutyrate (Matyjaszewski et al., 1999). They discovered that, in order to overcome the lack of deactivator, the deactivating Cu^{II} species could be added directly to the solution to control the polymerization. Nevertheless, the benefit of using the sacrificial initiator approach is that the MW characteristics of the free polymers formed by the sacrificial initiator in solution can be used to correlate with the MW characteristics of those on the surface, which are difficult to otherwise measure and characterize (Pyun, Kowalewski, & Matyjaszewski, 2003; Xu, Neoh, & Kang, 2009).

2.6.1.1. SI-ATRP of 2-Methacryloxyethyl Phosphorylcholine (MPC)

SI-ATRP has been used extensively in the application and creation of anti-fouling substrates and surfaces. One class of materials that have gained pronounced attention in terms of anti-fouling reactions are zwitterionic polymers, specifically those of poly(MPC) brushes (Xu, Neoh, & Kang, 2009). The mechanism of anti-fouling is thought to be associated with the hydration layer bound to the PC-group, further described in 2.4.1.

Another group of materials that are well studied and often compared to zwitterions are PEG-based materials and brushes. However, it has been discovered that PEG can oxidize to produce aldehyde side products that are reactive when in the presence of transition metal ions or oxygen, giving zwitterionic materials an advantage (Li, Chen, Zheng, Ratner, & Jiang, 2005; Ostuni, Chapman, Holmlin, Takayama, & Whitesides, 2001).

There has been a lot of focus on the SI-ATRP of various substrates with pMPC brushes and evaluation of the surfaces corresponding anti-fouling properties (Feng, Zhu, Ishihara, & Brash, 2005; Feng, Brash, & Zhu, 2006, 2004; Feng, Zhu, Ishihara, & Brash, 2006; Iwata et al., 2004; Jin, Feng, Zhu, Sheardown, & Brash, 2010a; Seo, Matsuno, Konno, Takai, & Ishihara, 2008; Yan & Ishihara, 2008). These studies have demonstrated surfaces that, as expected, show significantly decreased fouling reactions, with in some cases even up to >99% overall decrease compared to control materials (Feng, Zhu, Ishihara, & Brash, 2005). There also has been a direct correlation between the increase in anti-fouling properties and surface wettability with increasing chain length and grafting density of corresponding pMPC surfaces brushes (Feng, Zhu, Ishihara, & Brash, 2005; Feng, Brash, & Zhu, 2006; Feng, Brash, & Zhu, 2004; Jin et al., 2009; Yan & Ishihara, 2008).

Despite these findings, there has been minimal work towards the effect of altering the molecular architecture and surface density of these polyMPC brushes to evaluate the corresponding interactions with the phospholipid moieties.

2.6.2. Effect of Molecular Architecture on Fouling Reactions

One of the other benefits of SI-ATRP is that in addition to linear brushes, SI-ATRP also has the ability to synthesize much more complex brush architectures in a controlled manner (Barbey et al., 2009). The dormant polymer chains can maintain their ability to grow by the reversibility of the catalyst-initiator system, generating well defined polymers with controllable architecture (Barbey et al., 2009). Some of the main molecular brush architectures that have been successfully achieved by SI-ATRP, shown in Figure 8, include linear, block, random, hyper branched/highly branched, and various gradient brushes (Barbey et al., 2009).

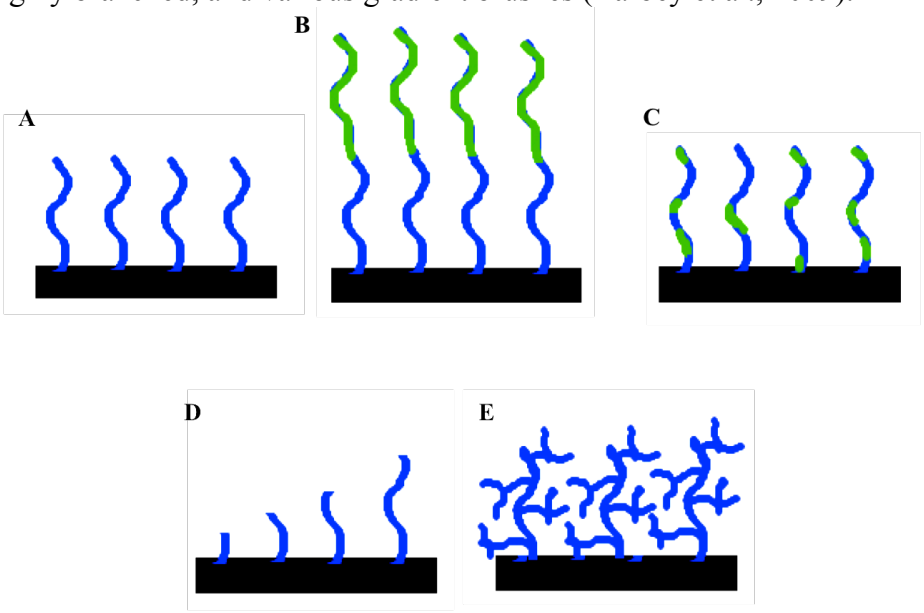

Figure 8. Examples of achievable molecular architectures of polymer brushes by SI-ATRP: A= linear, B= block, C= random, D= gradient, and E= hyper-branched/highly branched. Picture adapted from (Barbey et al., 2009).

It was discovered that the architecture of the polymer brush alone may actually work as a mechanism of anti-fouling (Currie, Norde, & Cohen Stuart, 2003; De Vos, Leermakers,

Lindhoud, & Prescott, 2011; Gunkel, Weinhart, Becherer, Haag, & Huck, 2011; Halperin & Leckband, 2000; Zheng et al., 2005). In the case of densely grafted polymers, the density of the polymer brush alone can act as a physical barrier to fouling particles trying to reach the surface (De Vos, Leermakers, Lindhoud, & Prescott, 2011). If a fouling protein is attempting to reach the surface and instead comes into contact with a polymer brush, it must penetrate and deform the equilibrium established by the brush structure. The brush can use a restoring force and push the molecule out of the brush and away from the surface (De Vos, Leermakers, Lindhoud, & Prescott, 2011).

This trend was further evaluated in the work of Gunkel and colleagues who assessed the dependence of polymer brush architecture on biofouling using sterically demanding polyoligoglycerol-based linear and dendronized brushes synthesized by SI-ATRP (Gunkel, Weinhart, Becherer, Haag, & Huck, 2011). They found a direct correlation between biofouling reactions and brush architecture, with the bulky and flexible dendronized brushes exhibiting an ideal anti-fouling/protein repelling behavior compared to their linear counterparts (Gunkel, Weinhart, Becherer, Haag, & Huck, 2011).

All in all, as highlighted within 2.6.1.1, there is a significant body of work on the use of polyMPC brushes to yield anti-fouling surfaces. It may, however, be vital to study the effect of increasing the surface density and altering the molecular architecture of these polyMPC brushes to evaluate the corresponding effect on existing anti-fouling properties.

2.4 Scope of Work

Therefore, the objective of this thesis is to synthesize a novel polymer that can be applied to a biomaterial surface to increase compatibility with the surrounding biological environment. Specifically, in this work, model silicone hydrogels were used as the material of interest due to

the need to enhance their surface characteristics to increase overall comfort.

MPC, well known based on its biomimetic and anti-fouling nature, was chosen as the principal feature of this novel polymer surface modification. Based on the downfalls of silicone hydrogel CL, the polymer was constructed to greatly enhance surface wettability and invoke superior resistance to protein adsorption. By use of a controlled polymerization technique, the target polymer was designed in a graft-on-graft architecture to provide an increased surface density of MPC chains, tunable in length. Based on nature of the polymer, the hypothesis is that the surface induced hydration layer by the PC groups coupled with the steric repulsion of the densely grafted surface polymer brushes can synergistically work together to create a surface that is not only more wettable, but also less fouling, leading to a more comfortable material.

3. MATERIALS AND METHODS

3.1. Materials

2-Hydroxyethyl Methacrylate (HEMA) (99%, Sigma-Aldrich), 3[Tris(trimethylsiloxy)silyl]propyl methacrylate (TRIS) (98%, Sigma-Aldrich), Ethylene Glycol Dimethacrylate (EGDMA) (98%, Sigma-Aldrich) were all passed through a column of inhibitor remover for hydroquinone and monomethyl ether hydroquinone (MMEQ) (Sigma-Aldrich) prior to use. 2-Methacryloyloxyethyl phosphorylcholine (MPC) (97%, Sigma-Aldrich) was diluted with methanol and passed through a column of inhibitor remover for hydroquinone and monomethyl ether hydroquinone (MMEQ) immediately prior to use. 2,2-Bipyridyl (bpy) (99%), α-bromoisobutyryl bromide (BIBB) (98%), triethylamine (TEA) ≥ 99%, 4-(dimethylamino) pyridine (DMAP) ≥ 99%, anhydrous dichloromethane (DCM) ≥ 99.8%, anhydrous toluene ≥ 99.8%, and anhydrous pyridine ≥ 99.8% were purchased from Sigma-Aldrich and used as received. N,N-Dimethylformamide (DMF) (reagent grade, Caledon Laboratories), methanol (MeOH) (HPLC grade, Caledon Laboratories), toluene (reagent grade, Caledon Laboratories), tetrahydrofuran (THF) (reagent grade, Caledon Laboratories), anhydrous diethyl ether (reagent grade, Caledon Laboratories), and anhydrous ethanol (EtOH) (Commercial Alcohols) were used as received. Cu(I)Br ≥ 97 % was purchased from Sigma-Aldrich, stirred in glacial acetic acid overnight, rinsed with ethanol and diethyl ether, and stored under nitrogen to prevent oxidation (Keller & Wycoff, 1946). For radiolabelling studies, bovine serum albumin (BSA, 97%, Sigma-Aldrich) and lysozyme from chicken egg white (14.7 kDa, 53000 units/mg, Sigma-Aldrich) were used as received.

3.2. Synthesis of Benzyl-Bromo Isobutyrate (BBIB) Initiator

A 250 mL round bottom flask equipped with a magnetic stir bar was charged with dry DCM (50 mL), triethylamine (26.4 mmol), benzyl alcohol (24 mmol), and dimethyl amino pyridine (0.32 mmol) and bubbled under nitrogen for 30 minutes. The flask was cooled to 0°C and then α-bromoisobutyryl bromide (26.4 mmol) was added dropwise while stirring. The flask was allowed to warm to room temperature while reacting for a period of 24 hours. At this time, the solvent was removed by rotary evaporation to yield a yellow oil. Diethyl ether (100 mL) was added to the oil and washed with a 0.1 M HCl solution (4x100 mL), followed by further washing with a 0.1 M Na_2CO_3 solution (4x75 mL). The remaining diethyl ether layer was dried over Na_2SO_4 and then concentrated by rotary evaporation to yield a pale yellow oil (Scheme 2). The compound was then purified by column chromatography using a 9:1 hexanes: ethyl acetate solvent system, giving a final yield of 86%.

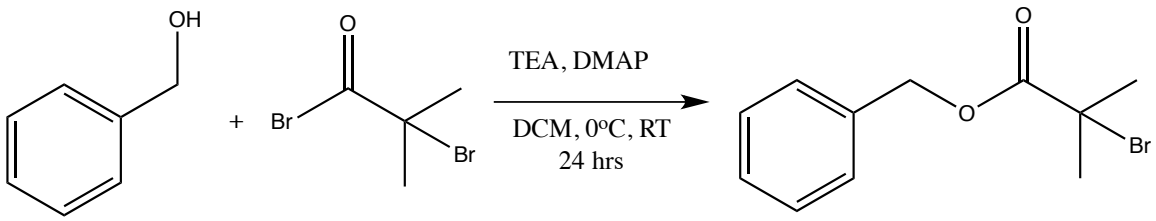

Scheme 2. Synthesis of benzyl-bromo isobutyrate (BBIB) Initiator.

3.3. Part A: Synthesis of Anti-fouling pBIBEM-g-pMPC Polymer

3.3.1. ATRP synthesis of polyHEMA (pHEMA)

To a 25 mL round bottom flask, 3.77 g (29 mmol) of HEMA, 5 mL of MeOH, as well as 0.15 g (0.58 mmol) of BBIB initiator were added. In ATRP, the chain lengths are controlled by variation of the molar ratio of monomer: ATRP initiator. Therefore, the molar ratio was chosen to be 50:1 to yield a 50 chain length polymer respectively. The flask was sealed with parafilm

and degassed by bubbling with nitrogen on an ice bath for a period of 45 minutes. A 25 mL schlenk flask equipped with a magnetic stir bar was charged with 0.181 g (1.16 mmol) of bpy ligand, 0.083 g (0.58 mmol) of CuBr catalyst, as well as 0.0065 g (0.029 mmol) of $CuBr_2$. The flask was degassed under vacuum and backfilled with nitrogen a total of three times. A 10 mL nitrogen purged syringe was then used to transfer the liquid contents from the 25 mL round bottom flask into the 25 mL schlenk flask and the mixture stirred upon addition. The reaction was allowed to proceed for 4 hours at room temperature and was stopped by exposure to air, where the dark brown solution turned blue to indicate the atmospheric oxidation of Cu(I) to Cu(II). The reaction mixture was diluted with 15 mL of methanol, passed through a silica column to remove oxidized Cu(II), followed by concentration by rotary evaporation. The colourless solution was further purified by precipitation in cold (~0°C) diethyl ether to remove residual HEMA monomer and other associated impurities. The polymer was dried in a vacuum oven at 40 °C for 48 hours to yield the resulting solid white polyHEMA polymer of > 99% conversion (Scheme 3).

3.3.2. Synthesis of poly(2-(2-bromoisobutryloxy)ethyl methacrylate) Macroinitiator (pBIBEM Macroinitiator)

In a 50 mL round bottom flask equipped with a magnetic stir bar, 1 g of polyHEMA (7.68 mmol –OH initiating groups) was dissolved in 12.5 mL of anhydrous pyridine. The reaction flask was cooled to -15 °C by an NaCl ice bath and 3.575 g (15.56 mmol) of α-bromoisobutyryl bromide was added to the reaction mixture dropwise over a period of 30 minutes. The solution was reacted at 0 °C for 5 hrs and then at room temperature for an additional 24 hrs. The pyridinium salts were filtered off and the product was concentrated via rotary evaporation, dissolved in toluene, and subsequently purified by passing through a neutral

aluminum oxide column. The resulting product was precipitated in cold methanol (~0 °C) and dried in the vacuum oven for a period of 24 hrs to give a final yield of 60% (Scheme 3).

3.3.3. ATRP Synthesis of polyBIBEM-graft-polyMPC (pBIBEM-g-pMPC)

In a 25 mL round bottom flask, 31.31 mg of pBIBEM-g-pMPC macroinitiator (0.111 mmol of initiating bromine groups) was dissolved in 5 mL of DMSO. To this flask, 1.64 g of MPC (5.55 mmol) (for a 50 chain length polymer) dissolved in 6 mL of MeOH was added. These molar ratios between the monomer: ATRP initiator were adjusted to be either 25:1, 50:1, or 100:1 to give either a 25, 50, or 100 chain length polymer respectively. The flask was stirred for 5 minutes to ensure complete dissolution, sealed with parafilm, and degassed by bubbling with nitrogen on an ice bath for a period of 45 minutes. A 25 mL schlenk flask equipped with a magnetic stir bar was charged with 34.67 mg (0.222 mmol) of bpy ligand, and 16 mg (0.111 mmol) of CuBr. The flask was degassed under vacuum and backfilled with nitrogen three times. A 25 mL nitrogen purged syringe was then used to transfer the liquid contents from the 25 mL round bottom flask into the 25 mL schlenk flask and the mixture stirred upon addition. The polymerization took place for 24 hours at room temperature. The reaction was stopped by exposure to air, where the dark red/brown solution turned blue to indicate the oxidation of Cu(I) to Cu(II). The reaction mixture was diluted with 25 mL of methanol, passed through a silica column to remove oxidized Cu(II), and concentrated by rotary evaporation. The colourless solution was then further purified by precipitation in cold (~0 ºC) THF to remove residual MPC monomer and other associated impurities. The polymer was dried in a vacuum oven for 48 hours to give the resulting off-white coloured polymer (Scheme 3).

Step 1- ATRP Synthesis of pHEMA

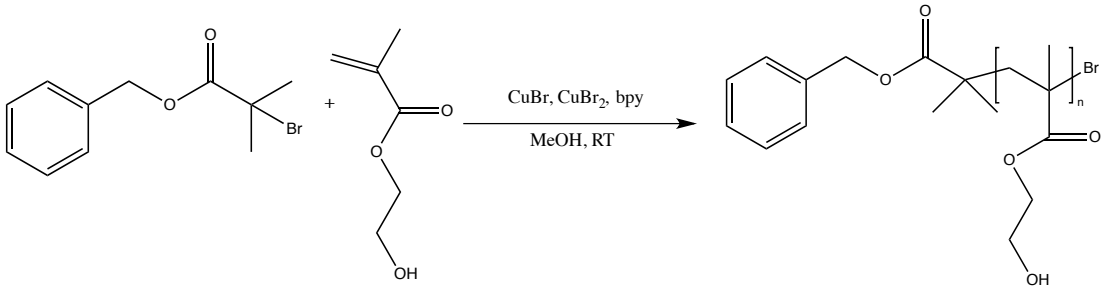

Step 2- Synthesis of pBIBEM Macroinitiator

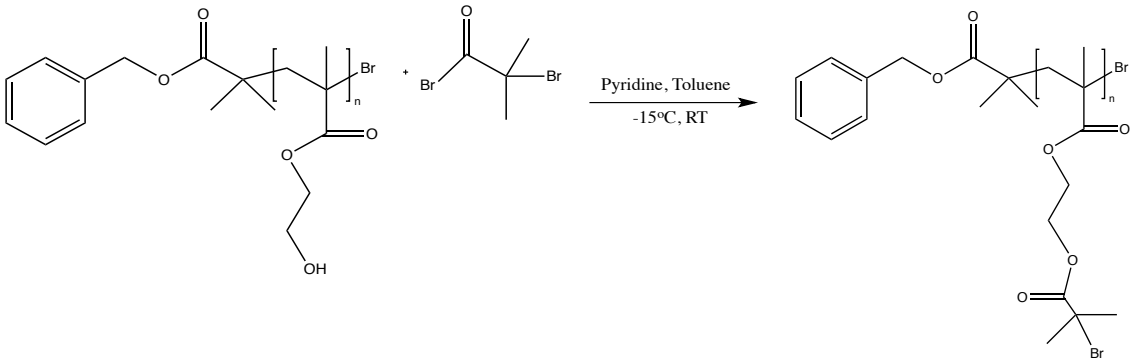

Step 3- ATRP Synthesis of pBIBEM-g-pMPC

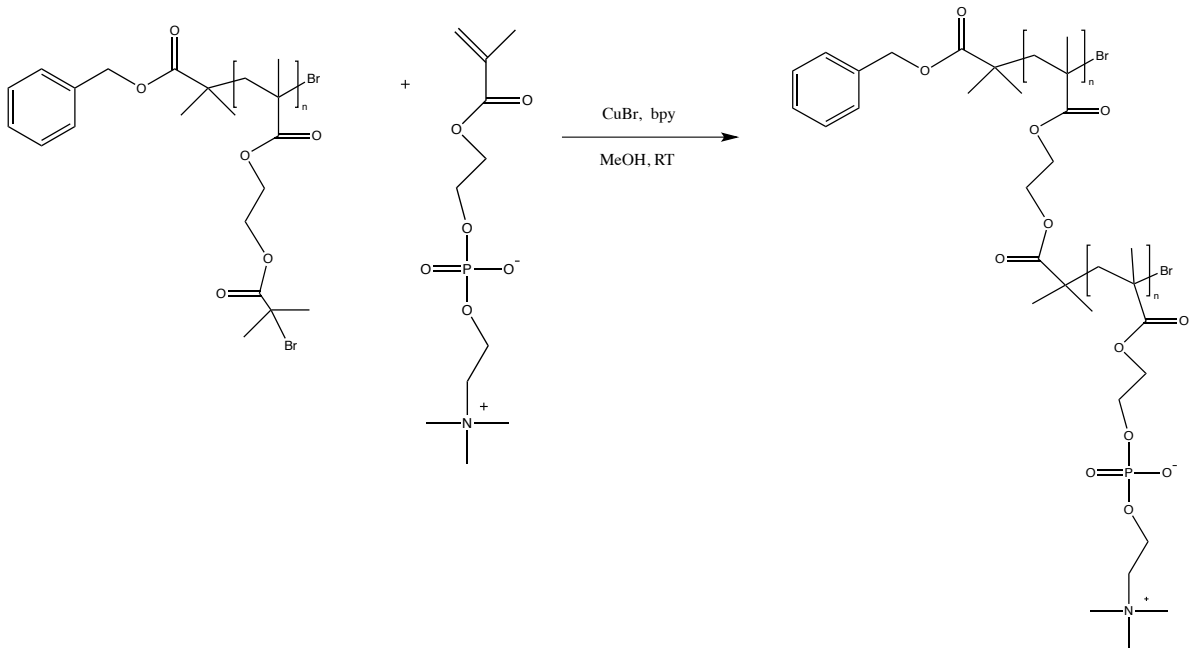

Scheme 3. Overall 3-step synthesis of graft-on-graft pBIBEM-g-pMPC polymer via ATRP.

3.4. Polymer Characterization

3.4.1. Nuclear Magnetic Resonance (NMR)

Polymer conversion and theoretical MW (Mn) was measured by ^{1}H-NMR spectroscopy (Bruker AV 600). ATRP synthesized polymers of pHEMA and pBIBEM-g-pMPC were recorded in methanol-d_4 and pBIBEM macroinitiaor in DMSO-d_6. For the pHEMA and pBIBEM polymers, terminal benzyl protons of the polymer were used for end-group Mn determination. For the pBIBEM-g-pMPC polymer, ^{1}H-NMR was no longer reliable for Mn determination due to decreased sensitivity and loss of end-group analysis at > 30,000 g/mol (Ghosh, 2006).

3.4.2. Gel Permeation Chromatography (GPC)

Gel Permeation Chromatography (GPC) was used to measure the MW and polydispersity index (PDI) of grafted pHEMA and pBIBEM-g-pMPC polymers. For the pHEMA polymers, a Waters GPC consisting of a 590 HPLC pump and 441 absorbance detector was used. The mobile phase consisted of DMF as a solvent containing 50 mM lithium bromine with a flow rate of 0.5 mL/min at 30°C. For the pBIBEM-g-pMPC polymers, a Waters GPC with a 717plus autosampler was used, with a 515 HPLC pump and 2414 refractive index detector. The mobile phase consisted of 0.5 sodium nitrate buffer (pH 10.04) with 10 ppm sodium azide and 25 mM N-cyclohexyl-2-aminoethanesulfonic acid with a flow rate of 0.8 mL/min at 30°C. Both systems were calibrated using poly(ethylene glycol) (PEG) standards (Waters Inc.) with a range of molecular weight extending from 106 Da to 881 kDa.

3.5. Synthesis of Model Silicone Hydrogel Lenses (Unmodified)

The p(HEMA-co -TRIS) (90:10 wt%) hydrogels were synthesized to model the properties of commercially available silicone hydrogel contact lenses as previously described (Korogiannaki, Guidi, Jones, & Sheardown, 2015). In a glass vial, 2700 mg of the hydrophilic HEMA monomer

(90 wt%), 300 mg of the hydrophobic TRIS monomer (10 wt%), and 150 mg of an EDGMA crosslinker (5 wt%), were added and mixed for a period of 30 minutes. 16 mg of the photoinitiatior Irgacure® 184 (0.028 wt%) was then added to the mixture and stirred until complete dissolution. This monomer solution was then injected into a mold for polymerization. Briefly, the mold was created with two acrylic plates separated by a 0.5 mm thick Teflon spacer. The plates were lined with sheets of polyester to prevent polymer adhesion and the entire mold was bolted together. Once the pre-polymer solution was injected, it was placed into a 400 W UV chamber (Cure Zone 2 Control-cure, Chicago, IL, USA), at wavelength of 365 nm for a polymerization time of 12 minutes. After polymerization, the polymer remained in the mold to cure for 24 hours and was then placed into a beaker containing 500 mL of Milli-Q water to soak and remove unreacted monomer and other components. The polymer film was then punched into circular discs 6.35 mm (1/4") in diameter and stored in a 37 °C oven until use.

3.6. Part B: Surface Grafting of Anti-Fouling pBIBEM-g-pMPC Polymer from Lens

3.6.1. Step 1- Grafting of ATRP Initiating Sites from Lens Surface (Intermediate-1)

For the creation of the first ATRP-initiating sites (Intermediate-1) based on a method previously described (Jin et al., 2009), approximately 28 samples of model silicone hydrogels (unmodified) were placed in a 100 mL round bottom flask equipped with a magnetic stir bar. Then, 40 mL of anhydrous toluene was added and the flask was de-aerated under a stream of nitrogen for 45 minutes while simultaneously cooling to -15 °C using an NaCl ice bath. 2.1 mL of anhydrous pyridine (26 mmol) was then added to the reaction flask with a nitrogen-purged glass syringe. To this cooled flask, 2.72 mL of BIBB (22 mmol), dissolved in 10 mL of anhydrous toluene was added in a dropwise manner over a period of 1 hr. The reaction was stirred at 0°C for 5 hours, followed by room temperature for a period of 24 hours. The lenses

were then rinsed with DMF to remove the pyridinium salts, extracted in Milli-Q water overnight, followed by drying in a vacuum oven for a period of 24 hours (Scheme 4).

3.6.2. Step 2- Primary ATRP of polyHEMA Brush from Lens (pHEMA-50)

In the creation of the pHEMA-50 discs, in a 25 mL round bottom flask, 650.7 mg (5 mmol) of HEMA, 3 mL of MeOH, as well as 25.7 mg (0.1 mmol) of the sacrificial BBIB initiator were added. The molar ratio of monomer: ATRP initiator was chosen to be 50:1 to yield a 50 chain length polymer. The flask was sealed with parafilm and degassed by bubbling with nitrogen on an ice bath for a period of 45 minutes. A 25 mL schlenk flask equipped with a magnetic stir bar was charged with 31.8 mg (0.2 mmol) of bpy ligand, 14.3 g (0.1 mmol) of CuBr catalyst and approximately 25 Intermediate-1 modified lenses for surface modification. The flask was degassed under vacuum and backfilled with nitrogen three times. A 10 mL nitrogen purged syringe was then used to transfer the liquid contents from the 25 mL round bottom flask into the 25 mL schlenk flask and stirred upon addition. The polymerization reaction was allowed to proceed for 24 hours at room temperature to ensure complete conversion. The reaction was stopped by exposure to air, where the dark brown solution turned blue to indicate the oxidation of Cu(I) to Cu(II). Residual Cu(II) and other impurities were removed by soxhlet extraction of the discs using a 70:30 ethanol: water solvent system overnight followed by drying in a vacuum oven for 24 hours (Scheme 4).

3.6.3. Step 3- Secondary ATRP Initiating Sites (Intermediate-2)

To create the Intermediate-2 lenses, the pHEMA-50 discs were again modified to create a second ATRP-initiating bromine site by reaction with the pHEMA terminal hydroxyl groups to create pBIBEM macroinitiating sites. The reaction conditions were identical to those seen in 3.6.1 with approximately 20 samples used for this portion of the synthesis (Scheme 4).

3.6.4. Step 4- Sequential ATRP of polyMPC (pMPC) from Lens (pMPC-50/pMPC-100)

The target modification consisted of the SI-ATRP of MPC from the pBIBEM macroinitiating sites, exploring the effects of two grafting densities (pMPC-50 or pMPC-100), performed similar to step 3.6.2. In a 25 mL round bottom flask, 6 mL of MeOH, 25.7 mg (0.1 mmol) of the sacrificial BBIB initiator, and either 3.0 g (10.2 mmol) or 1.5 g (5.1 mmol) of MPC was added. These molar ratios of MPC were chosen to be either 50:1 or 100:1 to give either a 50 or 100 chain length polymer respectively. The flask was sealed with parafilm and degassed by bubbling with nitrogen on an ice bath for a period of 45 minutes. A 25 mL schlenk flask equipped with a magnetic stir bar was charged with 31.8 mg (0.2 mmol) of bpy ligand, 14.3 g (0.1 mmol) of CuBr catalyst, and approximately 16 Intermediate-2 modified lenses for the final surface modification step. The flask was degassed under vacuum and backfilled with nitrogen three times. A 10 mL nitrogen purged syringe was then used to transfer the liquid contents from the 25 mL round bottom flask into the 25 mL schlenk flask and the mixture stirred upon addition. The polymerization reaction occurred for 24 hours at room temperature to ensure complete conversion. The reaction was stopped by exposure to air, where the dark red/brown solution turned blue to indicate the oxidation of Cu(I) to Cu(II). Residual Cu(II) and other impurities were removed by soxhlet extraction of the discs in a 70:30 ethanol: water solvent system overnight followed by drying in a vacuum oven for 24 hours (Scheme 4).

Step 1- Grafting of ATRP Initiating Sites from Lens Surface (Unmodified → Intermediate-1)

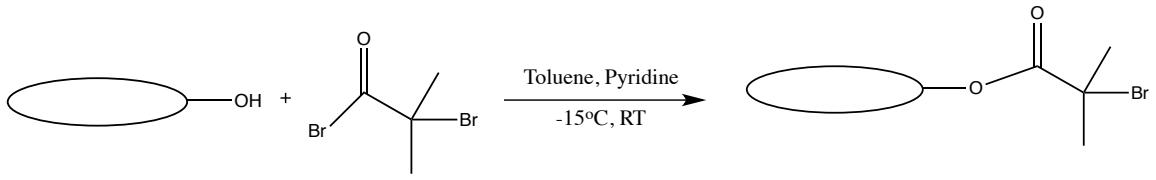

Step 2- Primary ATRP of polyHEMA50 (pHEMA-50) from Lens Surface (Intermediate 1 → pHEMA-50)

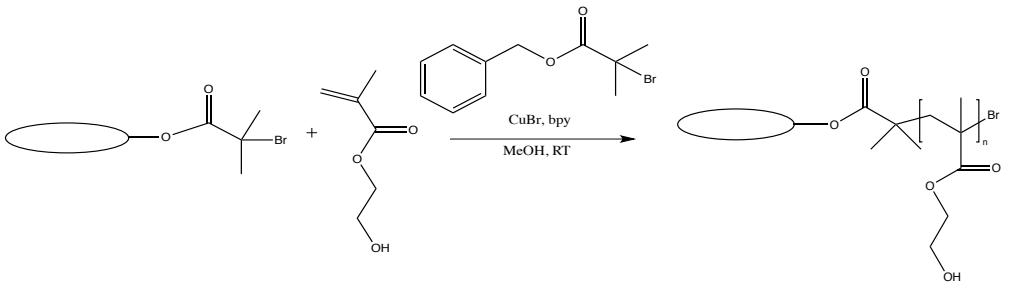

Step 3- Secondary ATRP Initiating Sites from Lens Surface (pHEMA-50 → Intermediate-2)

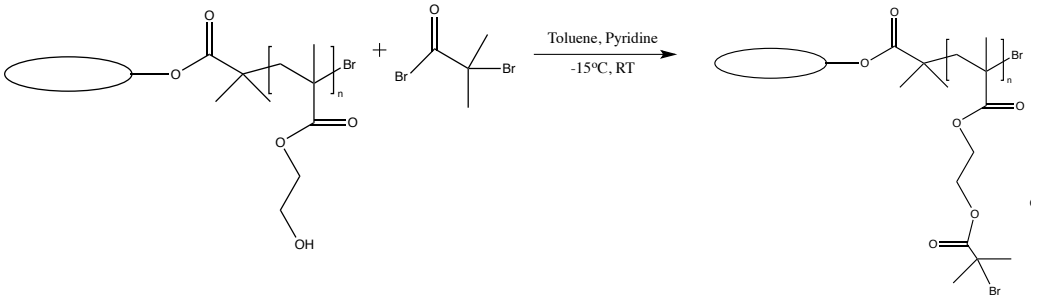

Step 4- Sequential ATRP of polyMPC (pMPC) from Lens Surface (Intermediate-2 → pMPC-50 or pMPC-100).

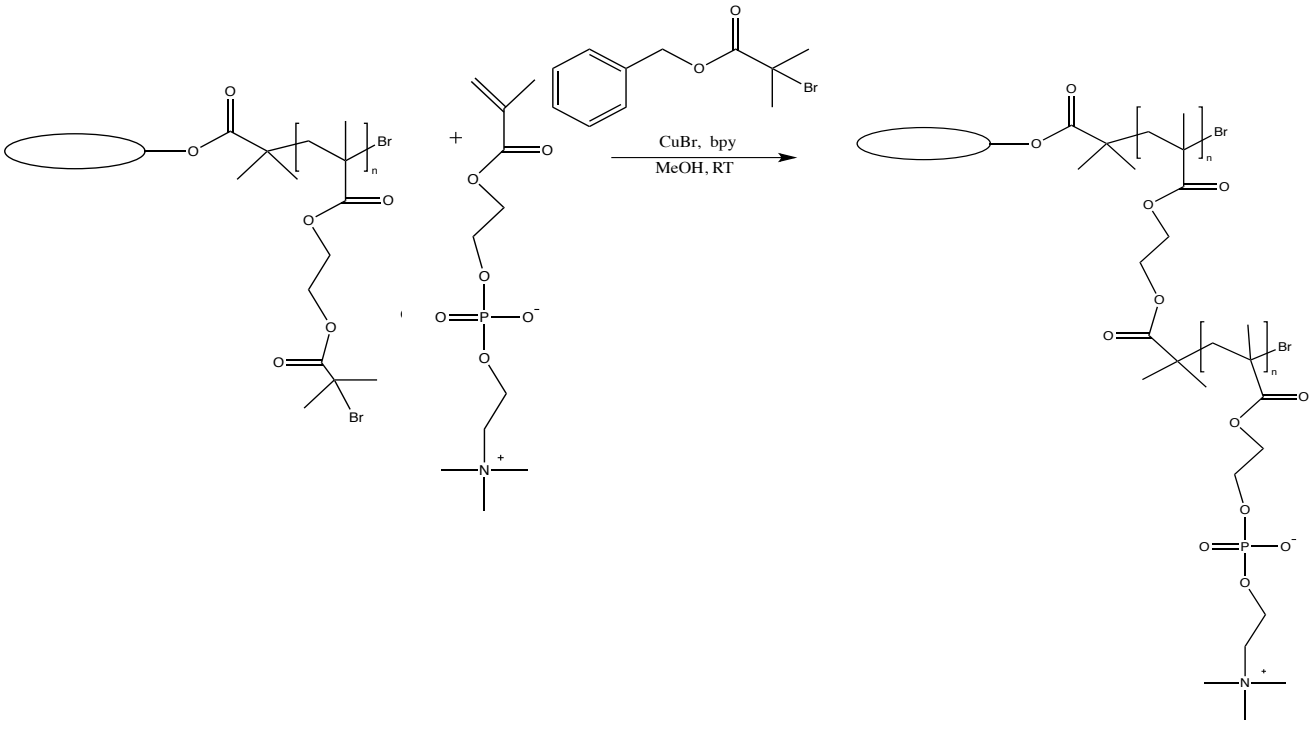

Scheme 4. Overall 4-step silicone hydrogel surface modification.

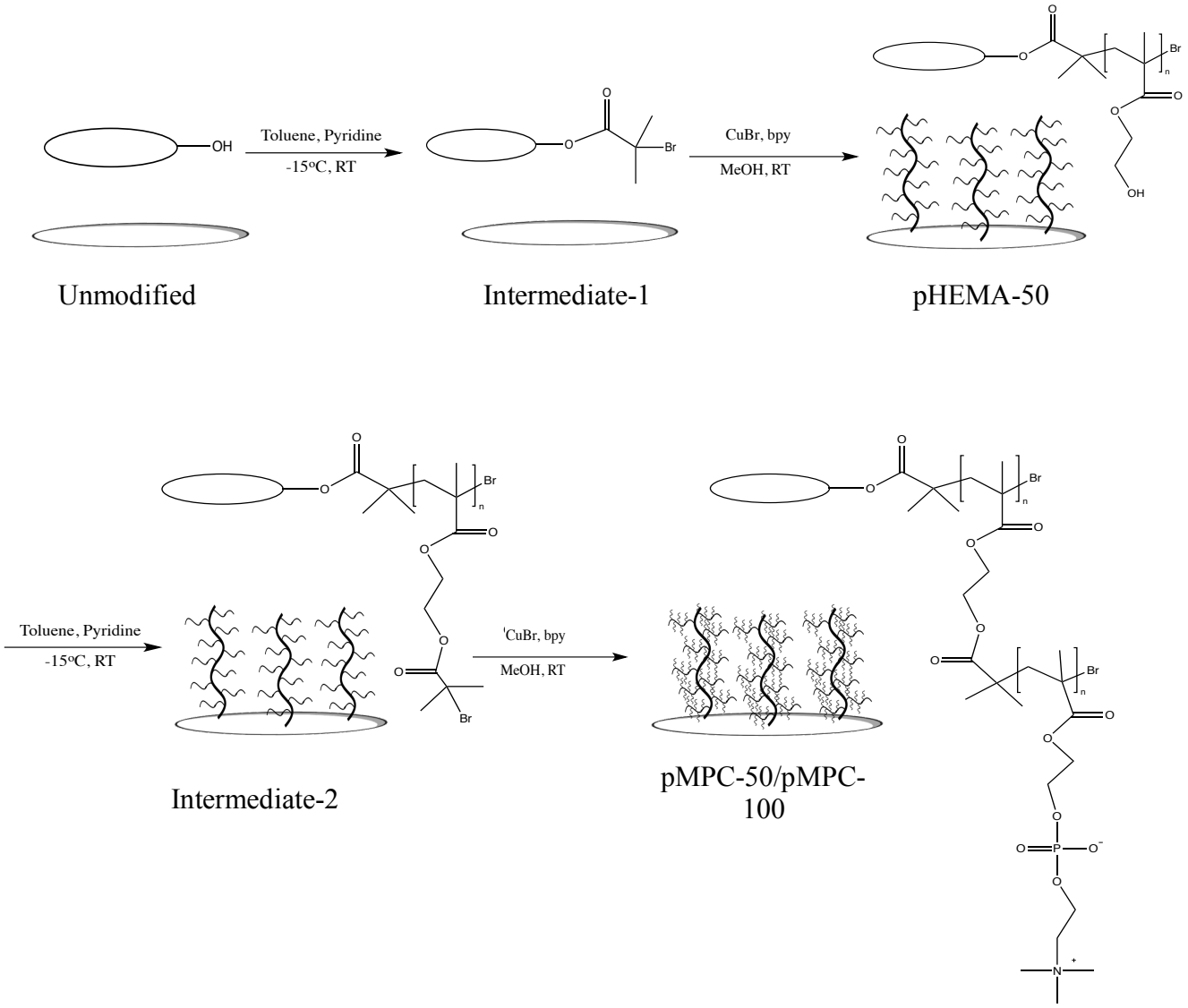

Figure 9. Graphic depiction of the overall 4-step sequential SI-ATRP graphing to produce target pMPC graft-on-graft brush materials with a high surface density of pMPC chains interacting with the surrounding surface.

3.7. Lens Characterization

3.7.1. Polymer Molecular Weight

3.7.1.1. Nuclear Magnetic Resonance

The theoretical MW (Mn) and conversion of the SI-ATRP grafted pHEMA and pMPC polymers was determined by ^{1}H-NMR spectroscopy (Bruker AV 600, methanol-d_4) using the terminal benzyl protons of the BBIB sacrificial initiator for end-group Mn determination of grafted polymers.

3.7.1.2. Gel Permeation Chromatography

Gel-Permeation Chromatography (GPC) was used to measure the MW and polydispersity index (PDI) of grafted pHEMA and pMPC polymers. For the pHEMA polymers, a Waters GPC was used consisting of a 590 HPLC pump and 441 absorbance detector. The mobile phase consisted of DMF as a solvent containing 50 mM lithium bromine with a flow rate of 0.5 mL/min at 30°C. For the pMPC polymers, a Waters GPC with a 717plus autosampler was used, with a 515 HPLC pump and 2414 refractive index detector. The mobile phase consisted of a 0.5 sodium nitrate buffer (pH 10.04) with 10 ppm sodium azide and 25 mM N-Cyclohexyl-2-aminoethanesulfonic acid with a flow rate of 0.8 mL/min at 30°C. Both systems were calibrated using poly(ethylene glycol) (PEG) standards (Waters Inc.) with molecular weights ranging from 106 Da to 881 kDa.

3.7.2. Surface Chemical Composition

The surface chemical composition was analyzed by Attenuated Total Reflectance-Fourier Transform Infrared Spectroscopy (ATR-FTIR) using a Bruker Hyperion 3000 Microscope and Vertex 70 Bench and HTS Plate Reader. The surface composition was also analyzed by X-ray Photoelectron Spectroscopy (XPS). Spectra were generated using a Physical Electronics (PHI)

Quantera II spectrometer equipped with an Al anode source for X-ray generation and a quartz crystal monochromator for focusing the generated X-rays. Survey scans and low resolution spectra were obtained at 30˚/90˚ take off angles, using a dual beam charge compensation system for neutralization of all samples. For XPS sample preparation, the discs were rinsed in a 1:1 ethanol: Milli-Q water solution and dried in a nitrogen purged glass vial (Karlgard, Sarkar, Jones, Moresoli, & Leung, 2004).

3.7.3. Surface Wettability

The surface wettability of the lenses was assessed by measuring the contact angle using the sessile drop technique. The lenses were hydrated in Milli-Q water for 48 hours at room temperature prior to measurement to ensure complete hydration (n=4). The lenses were gently blotted with a Kimwipe to remove excess water on the surface of the materials. The static contact angle of a dispensed 10 µL water droplet was then measured using an Optical Contact Angle (OCA 35) high speed instrument.

3.7.4. Lens Equilibrium Water Content (EWC)

Lens swelling was assessed by measuring the lens equilibrium water content (EWC). The samples were soaked in 10 mL of Milli-Q water for 48 hours at room temperature to ensure complete hydration (n=3). The discs were blotted with a Kimwipe to remove excess water and then weighed to determine the hydrated mass (M_H) of the discs. The lenses were then allowed to dry for a period of 48 hours at 37 ˚C to determine the dry mass (M_D). The EWC was calculated using the equation below:

$$EWC(\%) = \frac{M_H - M_D}{M_H} \, x \, 100 \qquad (1)$$

3.8. Protein Adsorption

Bovine serum albumin and lysozyme from chicken egg white were both radiolabelled with $Na^{125}I$ using the iodine monochloride method (Ceska, Sjodin, & Grossmuller, 1971). Unbound ^{125}I was removed by passing the solution through AG 1-X4 resin (100-200 dry mesh in chloride form, Bio-Rad, Hercules, CA) packed in two 3 mL syringes. Trichloroacetic acid precipitation of protein was used to measure the amount of free iodide present and for both radiolabelled BSA and lysozyme this amount was ensured to be <3% of total radioactivity. With respect to the sample preparation for the protein assay, the unmodified and pMPC modified discs were soaked in 1x PBS solution for 48 hours to ensure complete hydration. The discs were then gently blotted with a KimWipe to remove residual surface hydration and placed vertically into a 96-well plate. 250 µL of BSA (0.2 mg/mL) and lysozyme (1.9 mg/mL) containing 10% (w/w) radiolabeled protein was added to each well containing a disc (n=4). The concentration of the proteins were chosen to mimic that of lysozyme (Fullard & Tucker, 1991; King-Smith et al., 2000; Sack, Tan, & Tan, 1992) and BSA (Fullard & Snyder, 1990; Ng, Cho, Wong, & Chan, 2001) found within the tear film. Discs were then incubated in the radiolabelled protein solutions for a period of 24 hours at room temperature. After the incubation period, the discs were rinsed with fresh 1x PBS to remove loosely bound protein (3 cycles x 5 minutes each within the well plate). The discs were then counted for the amount of adsorbed radioactivity using an Automatic Gamma Counter Wizard 3 1480 (PerkinElmer). This adsorbed amount was calculated by surface counts that were background-corrected relative to the solution count for each individual protein solution.

4. RESULTS AND DISCUSSION

4.1. Part A: Characterization of Anti-Fouling Polymer

4.1.1. Benzyl-Bromo Isobutyrate Initiator (BBIB)

The identity of the ATRP initiator described in 3.2 was verified by ^{1}H-NMR spectroscopy (Figure 10). After purification by column chromatography using a 9:1 hexanes: ethyl acetate solvent system, ^{1}H-NMR (600 MHz, $CDCl_3$) verified the structure δ_H (ppm): 1.967 (s, 6H, 2xCH_3), 5.226 (s, 2H, CH_2), 7.385 (m, 5H, Aromatic H). Before column purification, the ATRP-initiator was a pale yellow oil, which turned to a clear oil following purification, giving a final yield of 86%.

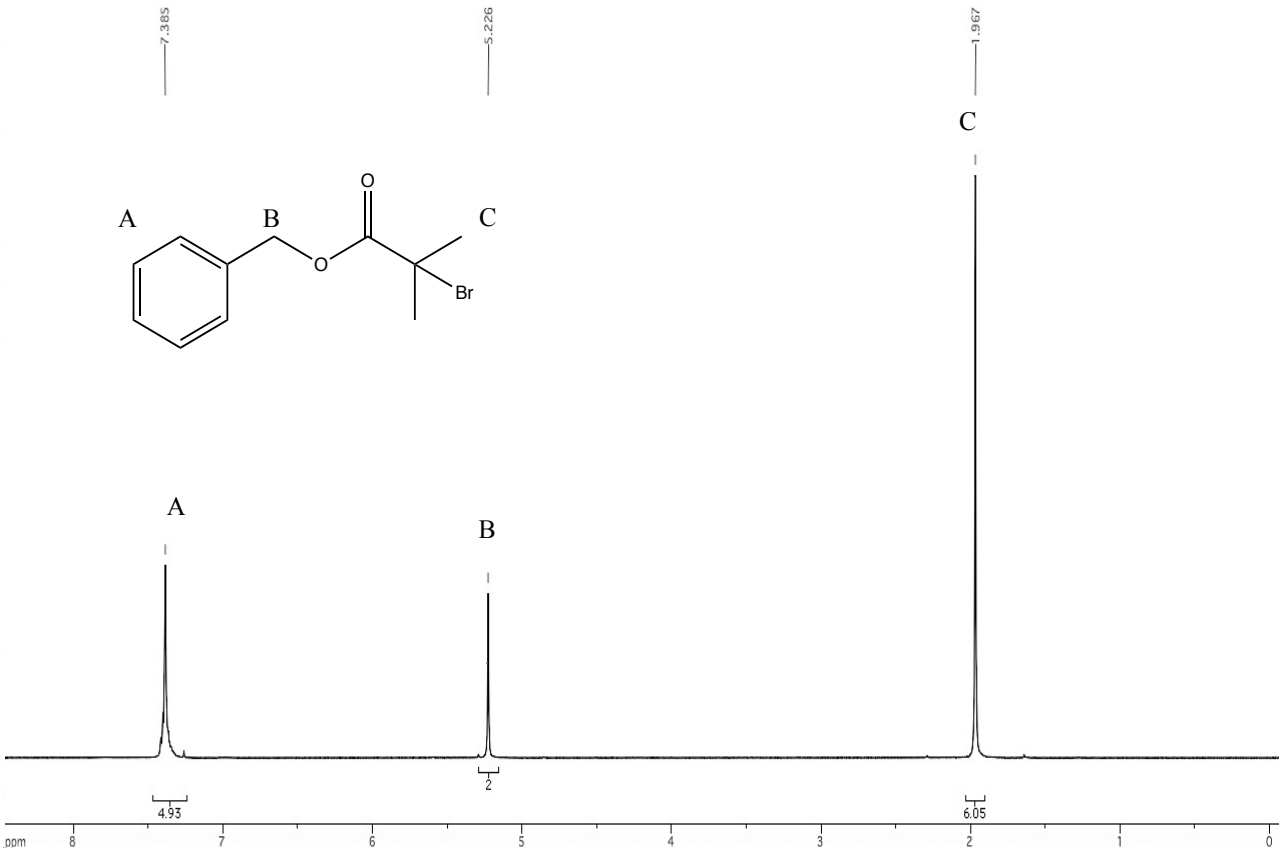

Figure 10. ^{1}H-NMR spectroscopy (600 MHz, $CDCl_3$) of BBIB ATRP initiator after column chromatography purification. Integrations represent the anticipated proton values, indicating a pure product.

For further polymer analysis, the aromatic benzyl proton peak at 7.385 ppm was used for end-group analysis to estimate Mn of the synthesized polymers. However, it is important to note that the use of ^{1}H-NMR spectroscopy for end-group analysis of polymer peaks is generally only accurate when the polymer Mn <~30 000 g/mol (Ghosh, 2006). This was therefore noted and taken into account for situations where the Mn of the synthesized polymers exceeded this value.

4.1.2. ATRP of polyHEMA

The pHEMA polymer described in 3.3.1 was analyzed by ^{1}H-NMR spectroscopy and GPC for the molecular weight determination. The process of ATRP of HEMA has proven to be quite challenging and easily affected by numerous factors, with one main factor being the solvent of choice (Hou et al., 2014; Robinson, Khan, De Paz Báñez, Wang, & Armes, 2001). In this work, the homopolymerization of polyHEMA was investigated using a variety of solvents and combination of solvent systems, with the synthesis parameters listed in Table 3. Buback and Kurz have demonstrated that compared to other methacrylates, HEMA has a faster rate of polymerization (k_p) (Buback & Kurz, 1998). In fact, in solvents with a high relative polarity such as aqueous media, the homopolymerization of HEMA can run into an "auto-acceleration" phenomena, increasing the Mn and PDI beyond the expected limits, leading to an uncontrolled polymerization (Billaud, Sarakha, & Bolte, 2000). This effect was seen when the solvent was a combination of methanol and water, causing the polymerization to demonstrate poor living character, reflected in a large PDI and Mn greater than the theoretical value. Using methanol and ethanol, the polymerization was more controlled and generated a lower PDI and Mn value, however due to the extended reaction time for ethanol, the formulation using pure methanol was chosen for the remainder of the work.

The ^{1}H-NMR spectrum for pHEMA-50 using MeOH as an ATRP solvent is shown in Figure 11. A calibration of the benzyl proton peak located at 7.373 ppm was used for end-group analysis in combination with the peaks at 4.029 ppm and 3.768 ppm to determine the Mn of the polymer (Table 3). The absence of remaining monomer vinyl proton peaks indicated that the polymer went to >99% conversion, as all of the HEMA monomer was polymerized.

The GPC chromatogram for pHEMA-50 can be seen in Figure 12. In GPC, lower molecular weight molecules/polymers appear at a longer elution time, as their movement is retarded on the column. Also, the more narrow the chromatogram peak, the lower the PDI of the polymer, indicative of a more monodisperse and controlled polymerization. For a controlled and successful polymerization by ATRP, the PDI typically ranges from 1-1.4, yielding polymers with living character (Matyjaszewski, 2012). As shown in Table 3, the PDI of the pHEMA-50 synthesized using EtOH and MeOH as ATRP solvents was well within this acceptable range, verifying the control of this homopolymerization reaction.

Table 3. Molecular weight data and synthesis parameters for the ATRP of the polyHEMA homopolymer. Note the bolded sample displays the conditions that were selected for the remainder of the work. The ^{1}H-NMR spectrum and GPC chromatogram for this formulation can be viewed below.

ID	Solvent	Reaction time (hrs)	Theoretical Mn (g/mol)	^{1}H-NMR Composition[a]	Mn by GPC (g/mol)[b]	PDI (Mw/Mn)
pHEMA-50	**MeOH**	**4**	**6507**	**pHEMA-52**	**6767**	**1.24**
pHEMA-50	EtOH	24	6507	pHEMA-48	5468	1.17
pHEMA-50	MeOH:H_2O 70:30	4	6507	pHEMA-68	8525	1.66

[a] ^{1}H-NMR composition determined by end-group analysis
[b] PEG standards were used for calibration purposes

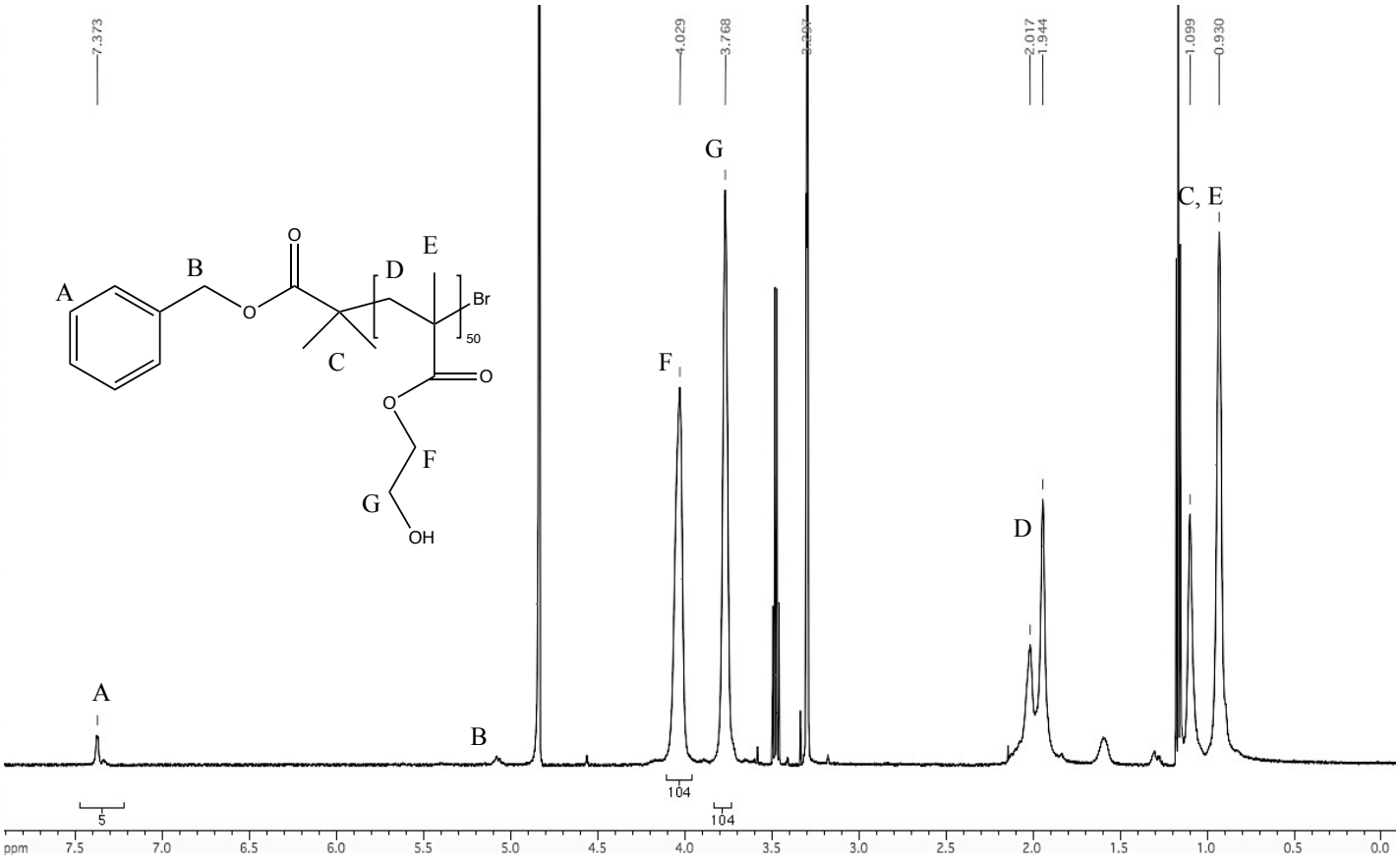

Figure 11. ^{1}H NMR spectrum (600 MHz, MeOD) of pHEMA-50 polymer using MeOH as an ATRP solvent. Conversion was determined based on the calibration of the aromatic benzyl peak at 7.373 ppm to represent 5 protons for end-group analysis.

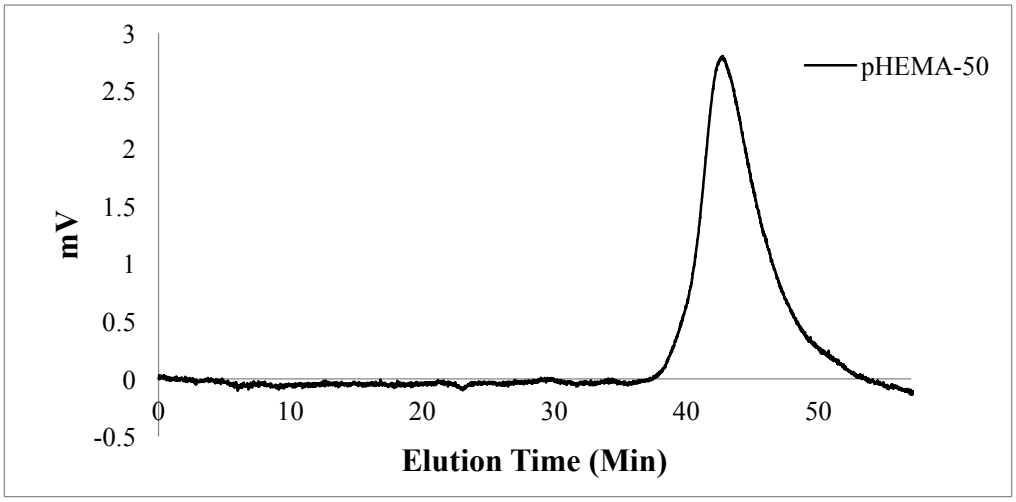

Figure 12. GPC chromatogram of pHEMA-50 polymer using MeOH as an ATRP solvent. The narrow peak presented is an indication of a low PDI and controlled polymerization.

4.1.3. PolyBIBEM Macroinitiator

In order to yield the target graft-on-graft anti-fouling polymer, the HEMA hydroxyl groups underwent an esterification reaction to form bromine macroinitiating sites. These sites were used to further graft off of with the corresponding MPC monomer. The identity of the macroinitiator was verified by ^{1}H-NMR spectroscopy (Figure 13). After purification using a toluene plug column, ^{1}H NMR (600 MHz, DMSO-d_6) verified the structure. δ_H (ppm) 3.968, 3.707 (s, 2H, -CH_2-) in pHEMA-50 shifted to 4.324, 4.138 (-CH_2-OCO) in pBIBEM-50 to confirm this successful esterification.

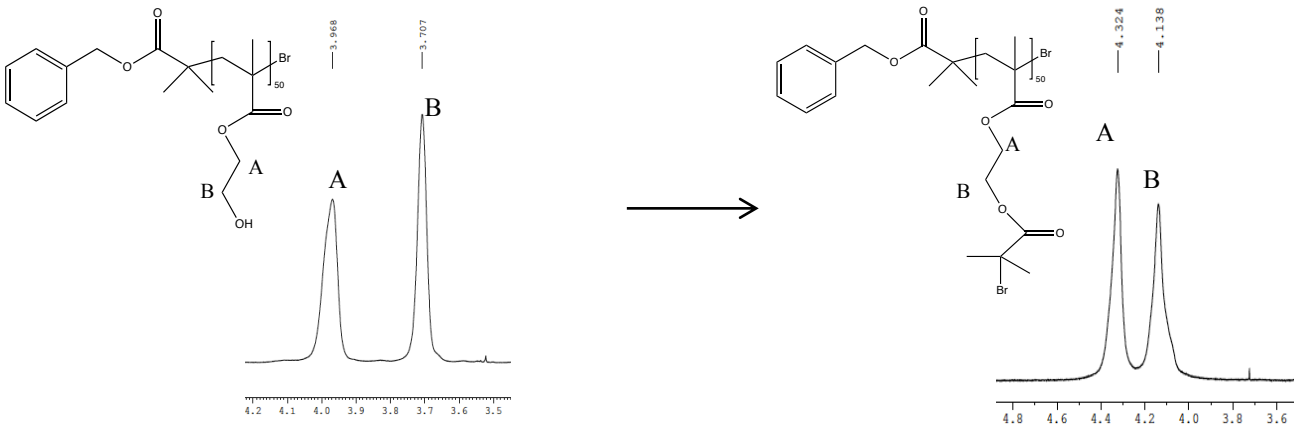

Figure 13. ^{1}H-NMR spectroscopy (600 MHz, DMSO-d_6) of the conversion of pHEMA-50 (left spectrum) to create the ATRP macroinitiator of pBIBEM-50 (right spectrum). A shift of the two broad peaks (A and B) in pHEMA-50 to a more downfield position indicated successful esterification to ATRP macroinitiating sites.

4.1.4. ATRP of pBIBEM-g-pMPC

Using the pBIBEM-50 macroinitiator, the graft-on-graft polymer of pBIBEM-g-pMPC was synthesized in three different variations of chain length. These variations were achieved based on the alteration of the MPC monomer and ATRP macroinitiator molar ratios, yielding pBIBEM-g-pMPC25, pBIBEM-g-pMPC50, and pBIBEM-g-pMPC100 polymers shown in Table

4. To determine the molecular weight characteristics of the polymer, ^{1}H-NMR spectroscopy and GPC were used. For the pHEMA and pBIBEM polymers, end-group analysis was used for Mn determination. However, as mentioned previously, for polymers with a molecular weight greater than approximately 30,000 g/mol, the sensitivity of ^{1}H-NMR becomes less precise and dependable, and therefore end-group analysis was not a dependable method for Mn determination (Ghosh, 2006). This was relevant when considering the pBIBEM-g-pMPC polymer, as by looking at Table 4, one can note that the polymer Mn largely exceeds the upper limit for end-group analysis by ^{1}H-NMR. In fact, when analyzing the ^{1}H-NMR spectra for all graft-on-graft polymers (Figure 14), the aromatic benzyl peak was hardly visible to allow for integration. ^{1}H-NMR was therefore unreliable for Mn approximation.

Due to the limitation of ^{1}H-NMR with respect to polymer analysis, GPC was used for the reminder of the Mn determination. In GPC analysis, all samples are required to be filtered through a 0.2 μm filter before entering the column. For the pBIBEM-g-pMPC100 formulation, the MW was so large that the polymer failed to pass through the filter, and therefore it was not possible to perform the analysis. The GPC Mn for the pBIBEM-g-pMPC25 and pBIBEM-g-pMPC50 formulations are summarized in Table 4. The theoretical Mn of both formulations was significantly greater than that determined by GPC. This is presumably due to the fact that the GPC operates based on PEG standards for calibration of the MW, and therefore does not provide a reliable method for exact Mn determination due to the varying hydrodynamic volumes of PEG compared to the graft-on-graft polymers. However, the theoretical Mn of the pBIBEM-g-pMPC25 was half that of the pBIBEM-g-pMPC50 formulation, which was also reflected in the Mn results by GPC. In Figure 15, the peak of the higher degree of polymerization (DP) formulation was eluted at a shorter elution time (min), as expected. Interestingly, despite the

large Mn and branching architecture of the graft-on-graft polymers, the polymerization was still controlled and within the range of living character, as indicated by the narrow peaks on the chromatogram and the low PDI values.

Table 4. Molecular weight data and synthesis parameters for the pBIBEM-g-pMPC graft-on-graft copolymers. The ^{1}H-NMR spectra of all formulations and GPC chromatogram for pBIBEM-g-pMPC25 and pBIBEM-g-pMPC50 can be viewed below.

ID	Theoretical Mn (g/mol)	Mn by GPC (g/mol)[a]	PDI (Mw/Mn)
pBIBEM50-g-pMPC25	383303	133692	1.25
pBIBEM50-g-pMPC50	752393	258980	1.27
pBIBEM50-g-pMPC100	1490572	-	-

[a] PEG standards were used for calibration purposes
Note- ^{1}H-NMR was no longer reliable for Mn determination due to decreased sensitivity and loss of end-group analysis >~30,000 (Ghosh, 2006).

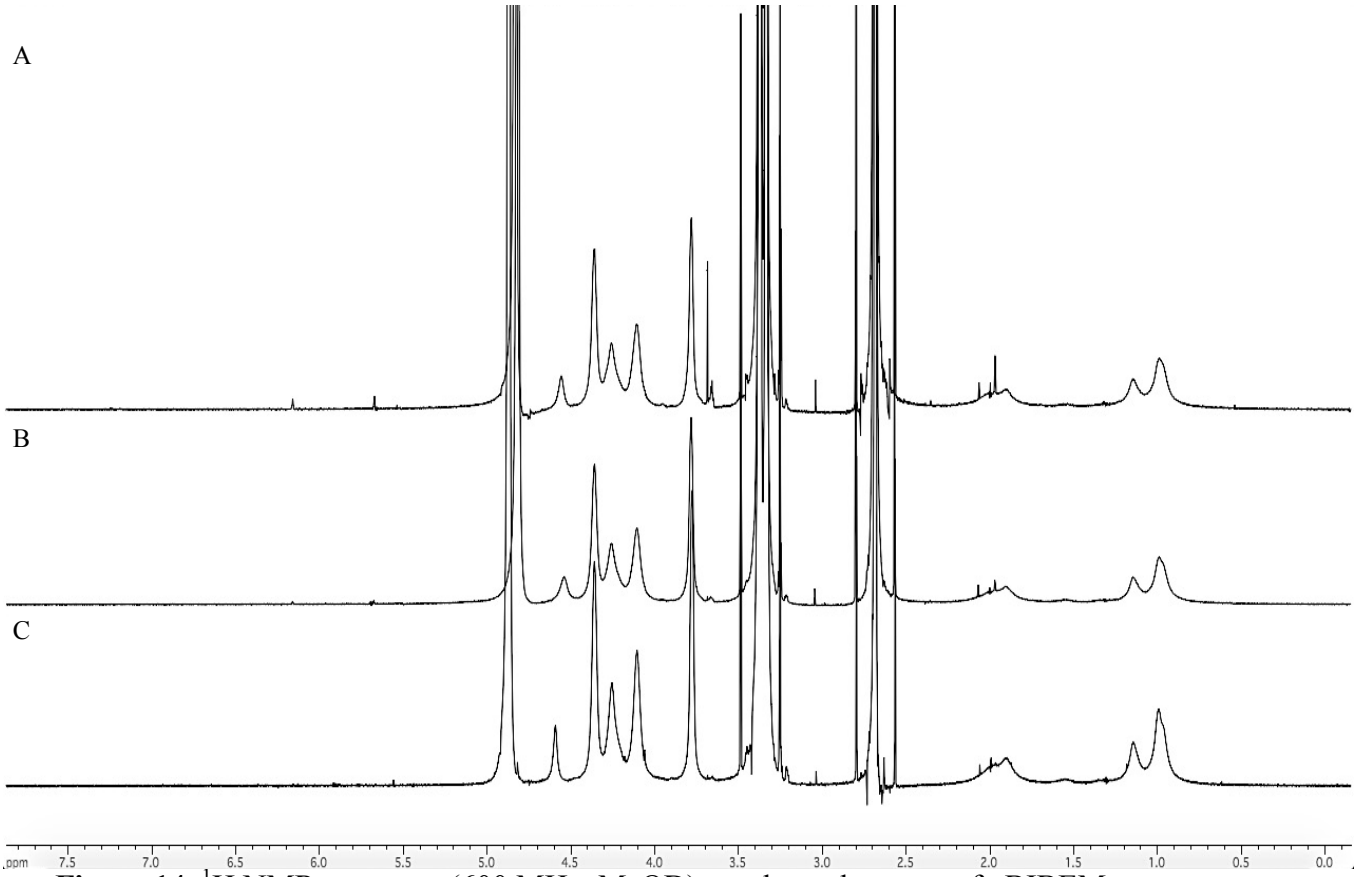

Figure 14. ^{1}H NMR spectrum (600 MHz, MeOD) overlapped spectra of pBIBEM-g-pMPC25(A), pBIBEM-g-pMPC50(B), and pBIBEM-g-pMPC100(C) polymers. Note end-group analysis could not be used to assess conversion due to loss of sensitivity with polymers >~30,000 g/mol.

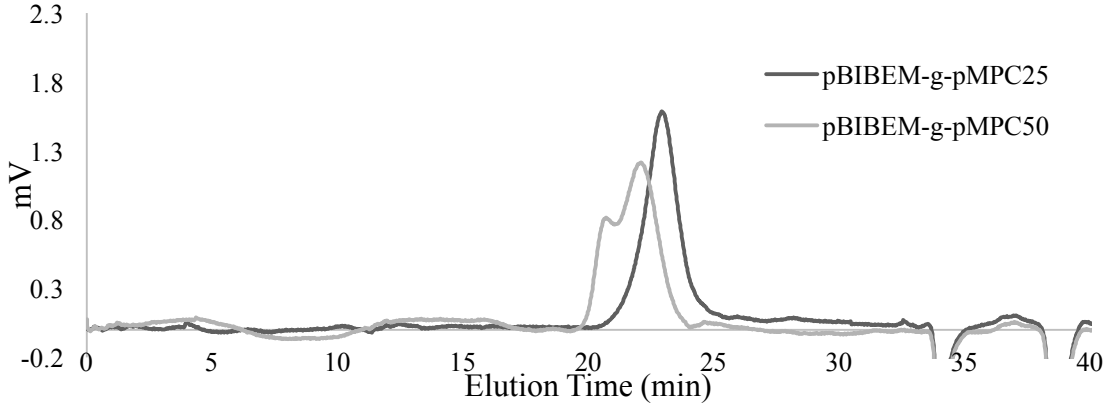

Figure 15. GPC chromatogram for the pBIBEM-g-pMPC25 and pBIBEM-g-pMPC50 formulations. The narrow peaks presented are an indication of a low PDI and controlled polymerization. The lower molecular weight polymers eluted at a longer elution time (min) as expected.

4.2. Part B: Lens Characterization

4.2.1. Creation of Model p(HEMA-co-TRIS) Silicone Hydrogels

The model silicone hydrogels in this work were prepared using monomers that are commonly incorporated into commercially available silicone hydrogel contact lenses. Due to the surface characteristics of commercially available silicone hydrogels, surface pre-treatment is necessary. A common type of surface pre-treatment typically used is referred to as oxygen plasma resurfacing (Keir & Jones, 2013).

In order to perform SI-ATRP on commonly used biomaterials, this type of gas plasma treatment is often required to create available hydroxyl (OH) groups on the surface for ATRP initiator immobilization. It is well known in literature that this modification is not permanent over extended periods of time (Roth et al., 2008). The ability for the oxidized silicone to remain in its hydrophilic state is temporary due to the ease with which the silicone chains migrate to the surface, recovering the native hydrophobic surface of the silicone material (Hillborg et al., 2004; Oláh, Hillborg, & Vancso, 2005; Xia & Whitesides, 1998).

Due to the fact that silicone hydrogels are CW lenses, surface modification by SI-ATRP was achieved in such a way to a provide a more permanent, cost effective, and lower maintenance alternative. The HEMA monomer, shown in Figure 16 was incorporated at 90 wt% within the cross-linked hydrogel network in the model CL formulation. This allowed for the presence of a large number of OH groups which are readily available on the model lens surface useful for direct "grafting-from". The surface modification was therefore covalently bound on the surface, decreasing the risk of exfoliation, while simultaneously eliminating the need for plasma treatment.

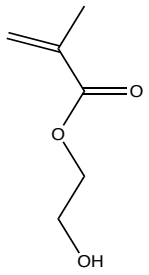

Figure 16. The structure of the HEMA monomer with a readily available terminal hydroxyl (OH) group.

4.2.2. Polymer Molecular Weight Characteristics

In this work, sequential SI-ATRP was performed from the unmodified silicone hydrogels in a four step synthesis depicted within Figure 9, to yield the target graft-on-graft pMPC surface modification. In step one, the unmodified discs were reacted with BIBB to create primary ATRP initiating sites, yielding Intermediate-1, in a protocol similar to that used by Jin et al., (Jin et al., 2009). Then, polyHEMA was grafted from the initiating bromine groups by the initial SI-ATRP to create the pHEMA-50 polymer brush. The BBIB initiator mentioned in 3.2 was added as a sacrificial initiator in order to create pHEMA-50 free polymer in solution, as well as from the surface under the same conditions. As described previously, it is assumed that the polymer brushes on the surface can be equated to those formed as free polymer in solution, and therefore can be characterized as having similar characteristics such as Mn and PDI (Pyun, Kowalewski, &

Matyjaszewski, 2003). As demonstrated in Table 5 and Figure 17, ^{1}H-NMR revealed that pHEMA-50 almost went to full conversion (98%), yielding a narrow peak on the GPC chromatogram (Figure 20), and low PDI of 1.17. The Mn determined by GPC was lower than the theoretical Mn of pHEMA-50. This could be attributed to the fact that the GPC was calibrated with PEG standards, which possess a lower hydrodynamic volume than pHEMA with the same Mn in DMF, underestimating the overall Mn.

From the pHEMA hydroxyl groups of the surface brush polymer, BIBB was reacted a second time to create Intermediate-2, a secondary SI-ATRP initiating site in an identical manner to Intermediate-1. The idea of sequential SI-ATRP was previously explored in order maximize the surface density of target polymer units (Jin, Feng, Zhu, Sheardown, & Brash, 2010b). In this study, polyMPC was sequentially grafted from the Intermediate-2 initiating bromine sites to maximize the surface density polyMPC chains in the graft-on-graft polymer. Two different chain lengths were chosen, pMPC-50 and pMPC-100, achieved through variation of the MPC: BBIB molar ratio as described previously.

^{1}H-NMR spectroscopy, displayed in Figure 18 and Figure 19, suggested complete conversion (>99%) for both pMPC-50 and pMPC-100, indicated by the complete disappearance of the MPC monomer vinyl proton peaks. The Mn was estimated by aqueous GPC using PEG standards, and is summarized in Table 5. For pMPC-50 and pMPC-100, the low PDI indicated control over the SI-ATRP process, increasing as the DP increased, as expected. Also, the GPC chromatogram (Figure 20) indicated a lower elution time (min) for the higher MW grafted polymer, also as expected. In both cases, the Mn measured by GPC was lower than the theoretical Mn, again presumably due to the difference in the hydrodynamic volume of PEG

compared to MPC; a trend also seen in the group of Ma et al., who used PEG standards with pMPC polymers of similar chain lengths (Ma et al., 2002).

Table 5. Molecular weight data and synthesis parameters for the SI-ATRP of HEMA and MPC from model silicone hydrogel surfaces using a sacrificial BBIB initiator. The ^{1}H-NMR spectra and GPC chromatogram for all formulations can be viewed below.

ID	Conversion (%)[a]	Theoretical Mn (g/mol)	Mn by NMR (g/mol)	Mn by GPC (g/mol)[b]	PDI (Mw/Mn)
pHEMA-50	98%	6507	6377	5468	1.17
pMPC-50	>99%	14764	14764	12299	1.19
pMPC-100	>99%	29527	29527	19636	1.34

[a] Conversion determine based on left over monomer vinyl proton peaks in ^{1}H-NMR spectrum (>99% indicated complete disappearance of the monomer vinyl protons)
[b] PEG standards were used for calibration purposes

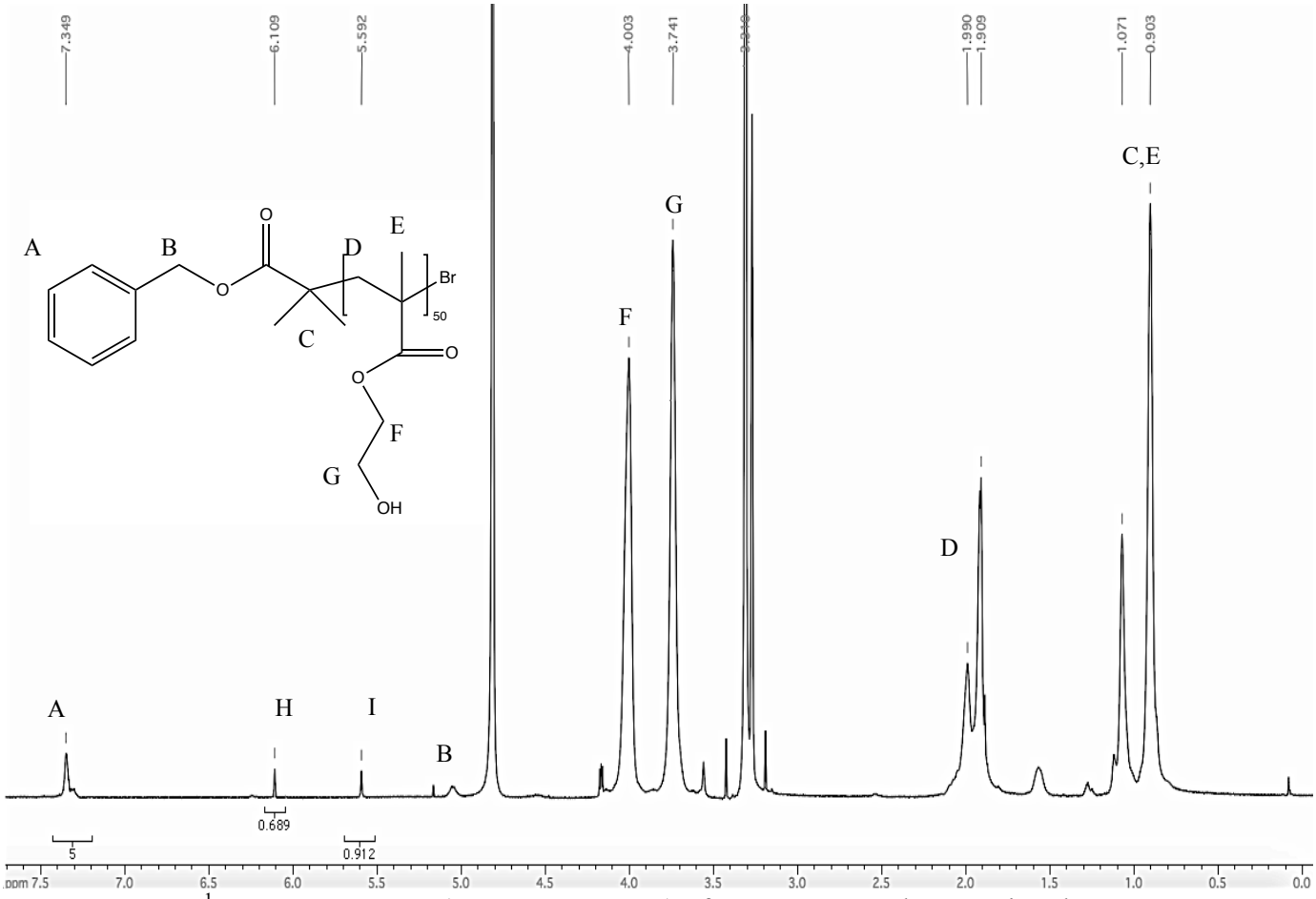

Figure 17. ^{1}H NMR spectrum (600 MHz, MeOD) of pHEMA-50 polymer using the BBIB sacrificial initiator. Conversion was determined to be 98% determined by end-group analysis based on the residual vinyl monomer peaks (H, I).

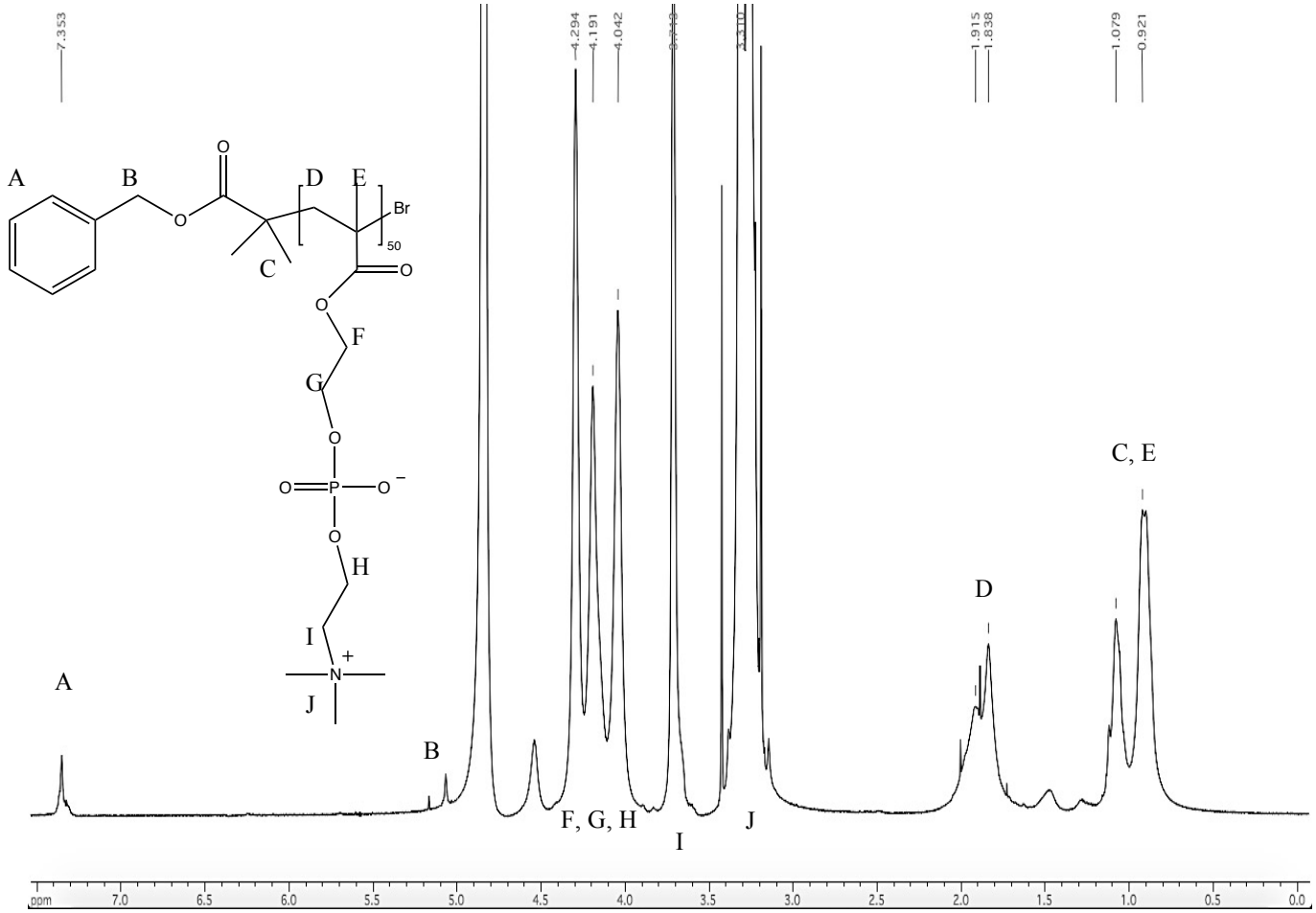

Figure 18. ^{1}H NMR spectrum (600 MHz, MeOD) of pMPC-50 polymer using the BBIB sacrificial SI-ATRP initiator. Conversion was determined to be >99% due to the disappearance of the monomer vinyl peaks.

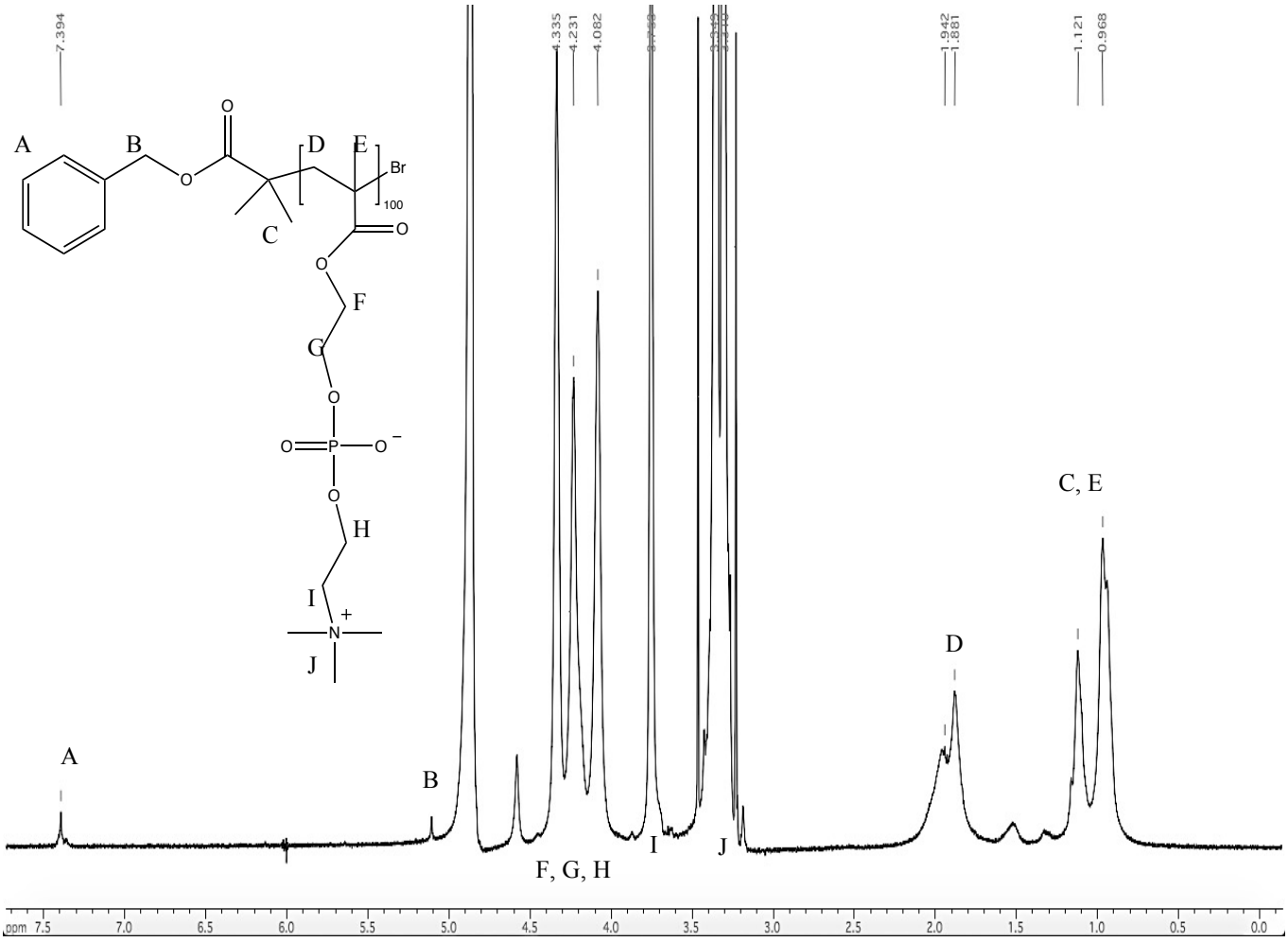

Figure 19. ^{1}H NMR spectrum (600 MHz, MeOD) of pMPC-100 polymer using the BBIB sacrificial SI-ATRP initiator. Conversion was determined to be >99% due to the disappearance of the monomer vinyl peaks.

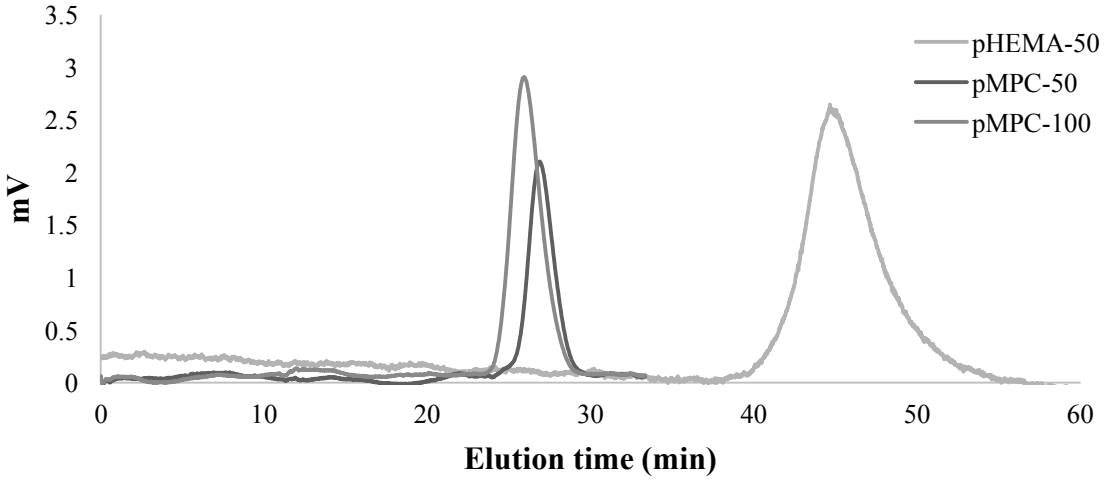

Figure 20. GPC chromatogram for pHEMA-50, pMPC-50, and pMPC-100 formulations using the BBIB sacrificial initiator. The narrow peaks presented are an indication of a low PDI and controlled polymerization. The lower molecular weight polymers eluted at a longer elution time (min) as expected.

4.2.3. Surface Chemical Composition

4.2.3.1. Attenuated Total Reflectance-Fourier Transform Infrared Spectroscopy (ATR-FTIR)

The surface composition of the silicone hydrogel discs was first examined by ATR-FTIR spectroscopy (Figure 21). The spectrum displays all 4-steps of the surface modification previously discussed in 3.6, including both chain lengths of the final target pMPC modification. A full view of the entire spectrum is seen in Figure 21 spectrum A, and two characteristic peaks within Figure 21 spectrum B/C.

In spectrum B, there was small broad a peak around 650 cm^{-1} for both Intermediate surfaces that was not present within the remaining samples. In literature, a C-Br stretch is estimated to be located around 515-690 cm^{-1} and it was therefore assumed that the peak in spectrum B was characteristic of a C-Br functional group (Urbaniak-domagala, 2012). The

presence of this peak confirmed the successful creation of the brominated ATRP-initiating groups.

In spectrum C, there was a large broad peak around 3100-3600 cm^{-1} that was present for the control, pHEMA-50, pMPC-50, and pMPC-100 surfaces, but not present in either of the intermediate surfaces. In the literature, an alcohol (OH) stretch appears around 3200-3600 cm^{-1} and therefore this peak in spectrum C was assumed to be indicative of a hydroxyl (OH) group (Ferreira et al., 2013). From Scheme 4, one can note the presence of a hydroxyl (OH) functional group for the control, pHEMA-50, pMPC-50, and pMPC-100 surfaces, and its absence in both of the intermediate surfaces due to the esterification of the OH group to the bromine initiating sites. The disappearance of the peak for both intermediate surfaces in spectrum C further confirmed the successful grafting of the bromine ATRP-initiating sites.

It is important to note that the absence of the OH stretch for the Intermediate-1 surfaces was more prominent than for the Intermediate-2 surfaces. This trend is also observed in the XPS spectra at both 30° and 90°, where the % bromine was greater for the Intermediate-1 surfaces compared to the Intermediate-2 surfaces. This could have occurred if the reaction for the esterification of the Intermediate-1 bromine sites was successful for the majority of the readily available control OH groups. With the ATRP-grafting of the pHEMA-50 brush, this created a larger number of OH groups and it is probable that they did not all completely react in the esterification reaction, yielding less bromine sites for the creation of Intermediate-2.

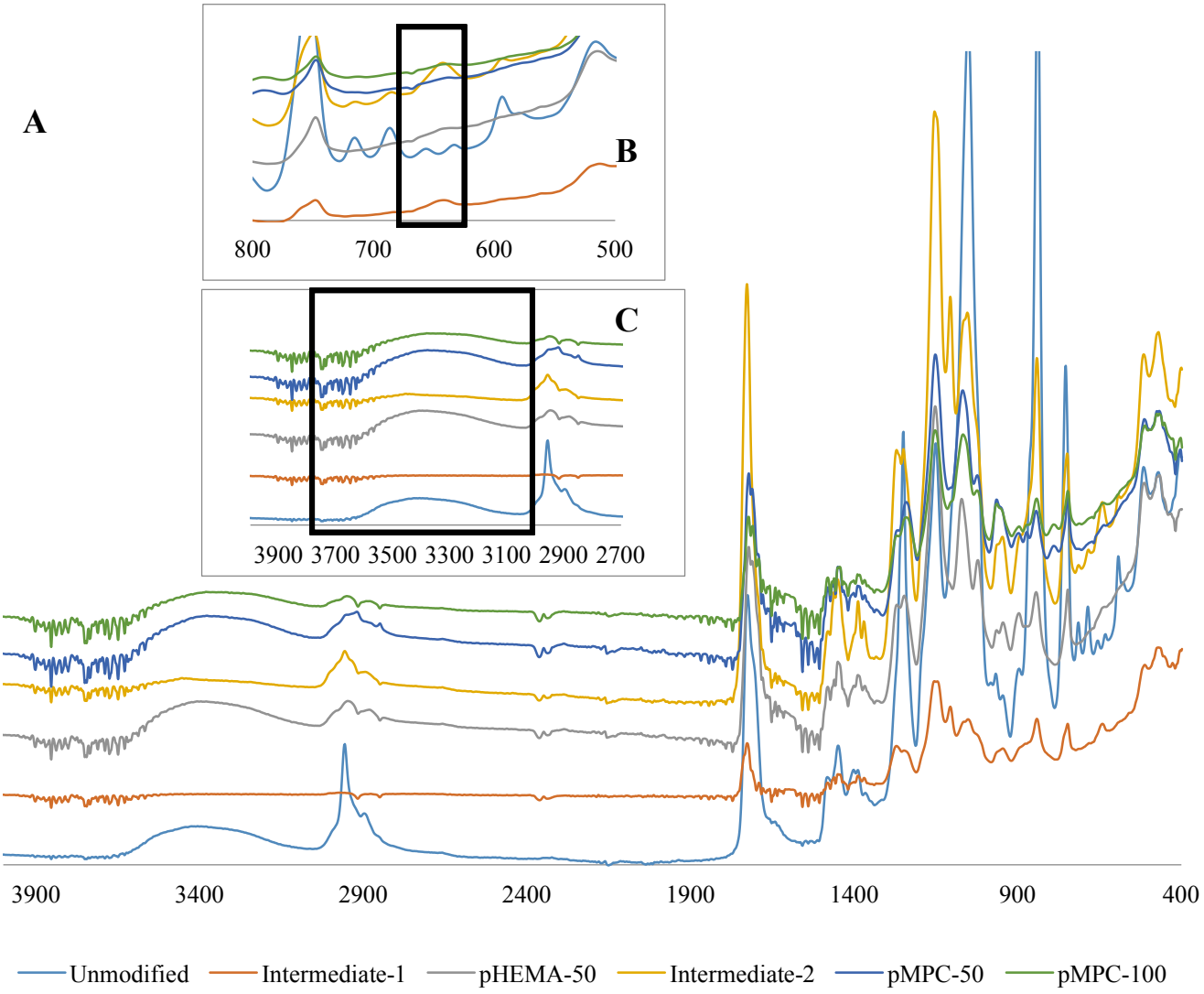

Figure 21. ATR-FTIR spectrum of all steps of the 4-part surface modification. (A) shows the full view of all discs for the 4-surface modification, (B) zoomed in view showing evidence of a C-Br stretch around 650 cm^{-1}, and (C) zoomed in view showing evidence of a hydroxyl (OH) peak from around 3100-3600 cm^{-1}.

4.2.3.2. X-ray Photoelectron Spectroscopy (XPS)

For a more precise surface chemical analysis, low resolution XPS was used to determine the elemental surface composition, displayed in Table 6 and Table 7. When comparing the unmodified to the Intermedate-1 and Intermedate-2 discs, there was no bromine detected in the unmodified discs, with the presence of bromine detected in both Intermediate modifications at

both recorded angles. The presence of bromine indicated the successful creation of ATRP initiating sites on the surface of the discs. In fact, the % of bromine for both Intermediate modifications was quite high compared to previous work (Jin et al., 2009, Jin, Feng, Zhu, Sheardown, & Brash 2010a; Yan & Ishihara, 2008). This suggests that the hydroxyl groups could have been more densely available on the surface, which upon the esterification into bromine initiating sites, would account for the greater surface bromine fraction. As well, the Si/C ratio for the unmodified discs decreased significantly upon Intermediate-1 and Intermediate-2 grafting. This further indicated successful Intermediate grafting by masking the highly mobile silicone domains and decreasing of the silicon %.

Upon the SI-ATRP of pHEMA-50 from the lens surface, the % bromine decreased, indicating that the polymer was successfully grafted from the bromine initiating sites, a trend similar to that found by Jin et al., (Jin, Feng, Zhu, Sheardown, & Brash, 2010a). There was also a further decrease in silicon % (decrease in Si/C ratio) from Intermediate-1 upon pHEMA-50 grafting at take off angles of both 30° and 90°, which indicated further surface coverage of the silicone domains by the polymer brush deposition.

The successful grafting of the pMPC in the final step of the modification was indicated by the obvious presence of phosphorous and nitrogen upon grafting both pMPC-50 and pMPC-100. Upon comparison of the pMPC-50 and pMPC-100 surfaces, it was hypothesized that the % of P and N would increase with increasing chain length the MPC; the results were however not indicative of this trend. The values for P and N were slightly greater for the pMPC-50 lower chain length, especially at 90°. XPS is a technique that operates under high vacuum conditions, which is known to dominate the more hydrophobic elements on the outermost surface of the material, while burying the more hydrophilic groups inside (Feng, Zhu, Ishihara, & Brash, 2005).

It is apparent that the pMPC-100 modified discs had a greater amount of carbon than that of the pMPC-50 discs, as more methacryl groups were present due to the longer polymer chain. It is therefore possible that under the high vacuum XPS conditions, the hydrophobic methacryl groups of the polymer chain could have been more present on the surface, while the hydrophilic PC groups could have been more buried within the polymer matrix away from the surface. This could conceivably be the reason for a greater carbon % and lower P and N % for the pMPC-100 discs compared to the pMPC-50 discs. Similar trends within the data were seen in the work of Feng et al., (Feng, Zhu, Ishihara, & Brash, 2006).

Another hypothesis for this phenomena is that the pMPC-50 shorter chains could actually have more surface mobility and flexibility than the longer pMPC-100 chains, covering more of the disc surface and increasing the P and N %. Due to the fact SI-ATRP is solely a surface modification technique, the longer pMPC-100 chains could possibly have been more tangled or sterically hindered than the more mobile short pMPC-50 chains, especially under XPS vacuum conditions. This hypothesis coincides with the lower Si/C ratio and Si % seen on the pMPC-50 surfaces compared to the pMPC-100 discs at both angles. The pMPC-50 discs could have been masking more of the underlying mobile silicone domains and have more surface coverage possibly by their greater mobility.

It is however important to note that theoretically, the P/N ratio should be 1:1 for this work for both pMPC-50 and pMPC-100 at both angles. Looking at Table 6 and Table 7, the P/N ratio was very close to 1 at both angles, validating the reproducibility and control of the SI-ATRP surface modification.

Table 6. XPS data at takeoff angle 30° recorded for all 4-steps of surface modification. Change (%) in expected surface elements indicated successful grafting for each modification. Sample preparation of the materials is listed in 3.7.2.

	Takeoff angle of 30° Elemental Composition (as atom %)							
	C (1s)	**O (1s)**	**Si (2p)**	**Br (3d)**	**N (1s)**	**P (2p)**	**Si/C**	**P/N**
Unmodified	66.03	21.43	12.64	-	-	-	0.19	-
Intermediate-1	68.08	23.98	6.06	1.89	-	-	0.089	-
pHEMA-50 Modified	71.26	23.16	5.06	0.067	-	-	0.071	-
Intermediate-2	70.50	21.32	6.66	1.3	-	-	0.094	-
pMPC-50 Modified	65.26	28.16	0.37	-	2.74	2.83	0.0057	**1.03**
pMPC-100 Modified	68.38	24.79	1.08	-	2.46	2.93	0.016	**1.19**

Table 7. XPS data at takeoff angle 90° recorded for all 4-steps of surface modification. Change (%) in expected surface elements indicated successful grafting for each modification. Sample preparation of the materials is listed in 3.7.2.

	Takeoff angle of 90° Elemental Composition (as atom %)							
	C (1s)	**O (1s)**	**Si (2p)**	**Br (3d)**	**N (1s)**	**P (2p)**	**Si/C**	**P/N**
Unmodified	66.17	22.18	11.65	-	-	-	0.18	-
Intermediate-1	67.95	23.45	6.38	2.19	-	-	0.094	-
pHEMA-50 Modified	70.16	24.06	5.84	0.11	-	-	0.083	-
Intermediate-2	70.38	22.22	4.93	2.02	-	-	0.070	-
pMPC-50 Modified	65.36	28.26	0.45	-	2.65	2.83	0.0070	**1.07**
pMPC-100 Modified	69.09	24.66	0.87	-	2.44	2.60	0.013	**1.07**

4.2.4. Surface Wettability by Advancing Water Contact Angle

In this work, advancing water contact angle measurements were determined by the sessile drop technique which measures the contact angle between a solid surface (disc) and the liquid phase (water). The lower the contact angle between the disc and water droplet, the more wettable the surface. Advancing water contact angles can be see in Figure 22.

Compared to the unmodified p(HEMA-co-TRIS) discs, the Intermediate-1 surfaces demonstrated a significant increase ($p<1.34x10^{-7}$) in the contact angle upon the creation of ATRP initiating sites, demonstrating that material modification clearly resulted in a change in

hydrophilicity. The hydrophilic HEMA hydroxyl groups of the pHEMA-co-TRIS unmodified discs were grafted from with more hydrophobic isobutyl bromide initiating sites, thus increasing the contact angle and decreasing surface wettability.

After the ATRP grafting of the pHEMA-50 brush from the Intermediate-1 discs, the contact angle decreased significantly ($p<1.93x10^{-18}$). As demonstrated in the XPS results, the increase in % bromine seen in the Intermediate-1 discs validated the existence of multiple initiating sites for the polyHEMA-50 polymer to theoretically graft from. The polyHEMA polymer contained many readily available hydroxyl groups, and therefore a decrease in the contact angle was observed as expected.

In the creation of Intermediate-2, the hydroxyl groups of the polyHEMA brush underwent a second esterification in an identical manner to Intermediate-1, thereby creating a secondary ATRP initiating site. There was a significant increase in the contact angle from the pHEMA-50 modification in the creation of Intermediate-2 ($p<5.06x10^{-19}$), again due to the change in hydrophilicity as described previously. As well, the Intermediate-1 and 2 discs generated contact angles that were not statistically significantly different from one another ($p=0.62$), thus further validating the repetition of the SI-ATRP surface grafting.

PolyMPC is a hydrophilic zwitterionic polymer that possesses a large free water fraction and has been used to increase surface wettability of materials (Goda & Ishihara, 2006). It was therefore hypothesized that not only would the contact angle decrease with the grafting of polyMPC, the angle should also be lower and more wettable with increasing polyMPC chain length. Following grafting from the Intermedate-2 surfaces, the advancing water contact angle decreased significantly upon pMPC modification, as anticipated based on the properties of MPC.

Specifically, as hypothesized, the greater the chain length of polyMPC, the lower the contact angle, decreasing from 16.04 ± 2.37º with pMPC-50, to complete wetting (~0º) for pMPC-100 materials. This is hypothesized because as the chain length of MPC increases, there is a greater surface density of hydrophilic MPC chains to electrostatically bind the surrounding water, thus making a more wettable surface. In fact, in the case of the pMPC-100 modified discs, when the water droplet hit the surface of the disc, it instantly spread over the entire surface, which is described in literature as a situation of "complete wetting" (Yuan & Lee, 2013).

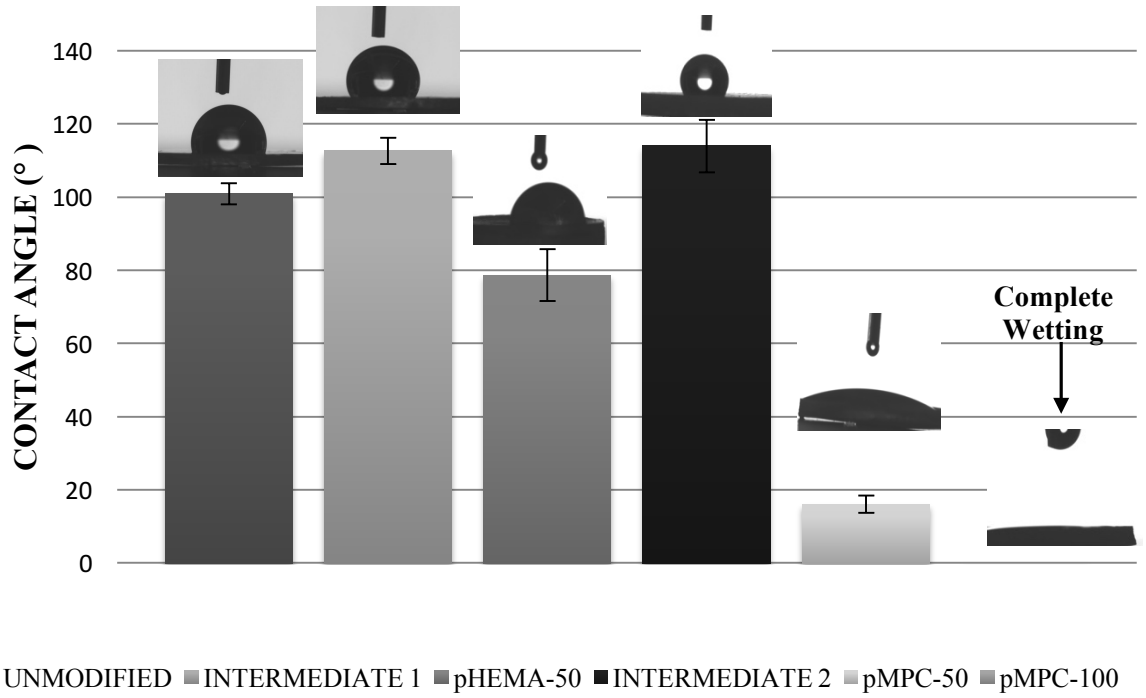

Figure 22. Advancing water contact angle changes for 4-step modification, including two different grafting densities of the target pMPC modification. A pictorial representation of the contact angle for each surface modification step is also shown above. Data shown represents mean ± SD (n=4).

4.2.5. Lens Equilibrium Water Content (EWC)

The level of swelling (EWC) of a contact lens is an important measure when considering comfort. Greater lens swelling indicates more water within the matrix of the lens, thought to be correlated with increasing overall comfort for the wearer. In terms of contact lens

wear, acceptable EWC values for overnight wear typically fall within the range of 24-38%, which is important to consider when comparing the modified lenses within this work (Austin & Hills, 2009), although it is important to note that the materials used in this work were model.

The EWC, calculated using Equation (1), for all steps of the surface modification can be seen in Table 8. Overall, the pMPC modified discs displayed the greatest EWC of all modification steps. Specifically, compared to the unmodified model silicone hydrogels, the pMPC-50 and pMPC-100 displayed a significantly greater EWC ($p<0.0009$ and $p<0.0009$ respectively). This result was as expected because of the nature of the pMPC material and its proposed mechanism which involves the electrostatic binding of large amounts of water, further described in 2.4.1. This water binding would presumably increase the hydrated mass (M_H) of the materials, contributing to the overall EWC increase. Theoretically, surface grafting by SI-ATRP should occur solely on the surface of the material and therefore it was not expected that the EWC would increase drastically upon surface modification, which the data demonstrated. This was also reflected in the work of Xu et al., who studied the surface modification of CL with an MPC-based polymer in a "grafting to" procedure, where the EWC increased to a similar degree (Xu et al., 2014).

When comparing the different chain lengths of the pMPC surfaces, the pMPC-100 modified lenses displayed a significantly greater EWC than the pMPC-50 lenses ($p<0.002$). This was as expected because the greater the chain length of pMPC, the greater the expected surface density of pMPC units and likely the greater the thickness of the surface layer, theoretically further increasing the EWC. This result also coincides with the advancing water contact angle results, with the pMPC-100 materials having a lower water contact angle than pMPC-50 modified lenses.

Table 8. EWC of materials for all 4-steps of the surface modification, including both grafting densities of pMPC, determined using Equation (1). Data shown represents mean ± SD (n=3).

	EWC %
Unmodified	24.7 ± 0.3
Intermedate-1	25.6 ± 0.04
pHEMA-50	26.6 ± 0.9
Intermediate-2	26.2 ± 0.6
pMPC-50	27.0 ± 0.2
pMPC-100	27.8 ± 0.1

4.3. Protein Adsorption

To test the anti-fouling characteristics of the pMPC modified lenses, lysozyme and bovine serum albumin (BSA) were chosen as model proteins to investigate protein adsorption based on a single protein solution. As explained in 2.3.1, there are specific proteins that have been identified to adsorb more readily to the surface of silicone hydrogel contact lenses; two of these well studied proteins being lysozyme and albumin (Green-Church & Nichols, 2008; Zhou et al., 2006). These proteins were chosen not only due to their preference for surface adsorption, but also due to their opposite overall charge, having the potential to demonstrate analogous adsorption behavior (Luensmann, Heynen, Liu, Sheardown, & Jones, 2010). The radiolabelled protein solutions were chosen to mimic that of the environment experienced within silicone hydrogel CL wear, incubated for a period of 24 hours at a concentration simulating that of their upper limit within the tear film.

Figure 23 and Figure 24 display the protein adsorption of lysozyme (1.9 mg/mL) and BSA (0.2 mg/mL) to the unmodified and pMPC50/pMPC100 modified surfaces respectively. In all cases, protein adsorption of the unmodified silicone hydrogel materials was significantly greater than that of the modified pMPC materials. This trend also coincides with that of the contact angle results. As expected, the pMPC-50/pMPC-100 materials both yielded extremely

low water contact angles due to their proposed mechanism of water binding and hydrophilic nature, which in turn was reflected in their ability to repel large amounts of protein.

In comparison to the unmodified discs, the protein adsorption to the pMPC-50 surfaces significantly decreased up to ~83% with respect to lysozyme ($p<0.00036$) and ~73% with respect to BSA ($p<0.0076$) single protein solutions. This trend was similar for the pMPC-100 surfaces, decreasing ~80% with respect to lysozyme ($p<0.0066$) and ~73% with respect to BSA ($p<0.0076$). The differences between the unmodified and pMPC modified materials were not significant despite the alteration in chain length of the target pMPC modification. This was a trend also seen within the work of Feng et al., who studied the adsorption of single protein solutions of lysozyme and fibrinogen on surface grafted pMPC layers (Feng, Zhu, Ishihara, & Brash, 2005). They reported no significant decrease in either fibrinogen or lysozyme in chain lengths of 50 units or greater for the grafted pMPC layers.

In a similar work to the mentioned, Jin et al., they also reported that the least adsorbed amount of fibrinogen and lysozyme occurred on surfaces grafted with single polyMPC-50 layers from surfaces of polyurethane, catheter, silicone hydrogel, and polydimethyl siloxane (PDMS) materials (Jin, Feng, Zhu, Sheardown, & Brash, 2010a). As described in 2.4.1, the protein resistance of these MPC-based materials is thought to be due to the water-barrier that forms as a response to the interaction with the surface PC units. It is possible that there was no significant difference seen with increasing chain length because of the surface density of the interacting PC units acting as a maximum at a 50 chain length polymer, binding a great amount of water and repelling corresponding protein. In fact, in the current work, the pMPC units were sequentially grafted by SI-ATRP, yielding an increased surface density of these sterically demanding MPC units beyond a singly grafted pMPC layer, which could further amplify this anti-fouling effect.

The amount of protein adsorbed to the unmodified materials was in the range of 0.5-0.85 $\mu g/cm^2$ for lysozyme and 0.3-0.35 $\mu g/cm^2$ for BSA. These values were well within the range of the formation of a closed-packed monolayer. Specifically for BSA, the amount to form a monolayer on most surfaces is ~0.15 $\mu g/cm^2$ and therefore in this work, a monolayer of BSA was expected to be formed on the surface of the unmodified discs (Mura-Galelli, Voegel, Behr, Bres, & Schaaf, 1991). As well, in terms of lysozyme, a close-packed monolayer typically forms at a surface density of 0.2-0.3 $\mu g/cm^2$, which was well exceeded by the unmodified discs in this work. This was expected based on previous studies of Jadi and colleagues as well as Luensmann et al., who demonstrated a much greater lysozyme adsorption in comparison to any other protein on the surface of unmodified silicone hydrogel lenses (Jadi, Heynen, Luensmann, & Jones, 2012; Luensmann, Heynen, Liu, Sheardown, & Jones, 2010). Based on the work of Kim & Somorjai, at high surface concentrations, lysozyme also can form a tight multilayer instead of a singular monolayer (Kim & Somorjai, 2003). It was therefore quite probable that upon adsorption, lysozyme could have had the potential to form a tightly packed multilayer on the surface of the unmodified discs.

Upon pMPC modification, protein adsorption decreased to a level as low as ~0.11 $\mu g/cm^2$ for lysozyme and 0.09 $\mu g/cm^2$ for BSA, and likely represented only a fraction of the monolayer remaining on the material surface, as the values were well below the range of specific monolayer formation. Jin and colleagues studied the lysozyme protein adsorption to model silicone hydrogel CL modified by a linear polymer brush of polyMPC by SI-ATRP (Jin, Feng, Zhu, Sheardown, & Brash, 2010a). The lysozyme decrease in this work was less significant than this current study, despite using a significantly lower lysozyme concentration and incubation time. This finding could support the hypothesis that materials surface modified by densely grafted and sterically

demanding polymer brushes may induce the capability to repel more protein than linear brushes, as described in 2.6.2 (Gunkel, Weinhart, Becherer, Haag, & Huck, 2011).

For BSA, the decrease in adsorption compared to the unmodified materials was not as significant as was observed with lysozyme. The concentration of BSA used for radiolabelling studies was much lower than that of lysozyme, so a less significant decrease was expected. One of the major differences amoungst BSA and lysozyme, other than their charge is their size, with BSA much larger of a protein than lysozyme (66 kDa vs.14.3 kDa). It is possible that the anti-fouling mechanism induced by the PC units in this densely grafted architecture was most effective at preventing adsorption from smaller protein molecules such as lysozyme, in comparison to larger proteins such as albumin. Halperin proposed a model for protein adsorption to polymer brush surfaces using a scaling law approach, predicting different responses of adsorption for small and large proteins (Halperin, 1999). The work concluded that primary adsorption occurs directly close to or at the substrate and is most significant for smaller proteins that can penetrate the brush layer. The secondary mechanism of adsorption is proposed to occur solely on the outer portion of the polymer brush layer and is most significant for larger proteins approaching the surface by compressing the brush layer. Feng and colleagues proposed that, based on this model, it is likely that secondary adsorption may be the main mechanism of protein adsorption to poly(MPC) surfaces (Feng, Zhu, Ishihara, & Brash, 2005). This could explain why BSA, a larger protein, did not decrease adsorption to the degree that was achieved with lysozyme, a smaller protein.

All in all, the ability to repel large amounts of lysozyme was especially important due to the proven abundance of lysozyme adsorption to the surface of silicone hydrogel contact lenses,

mentioned previously. The substantial decrease in lysozyme adsorption to the surface of the pMPC modified lenses compared to the unmodified discs was therefore a very promising result.

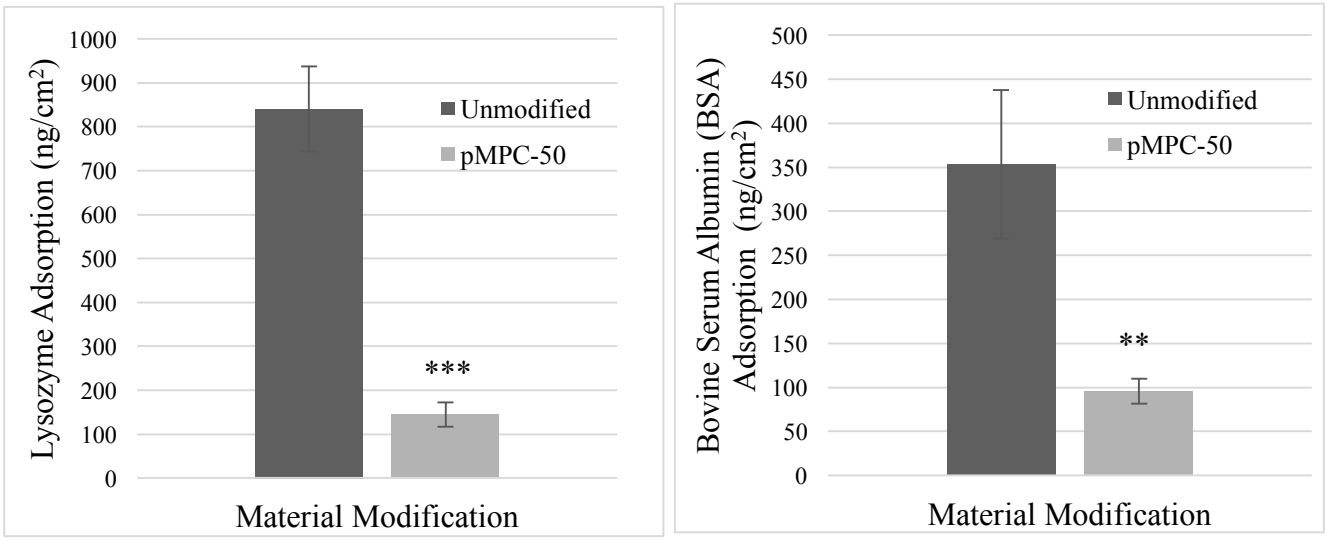

Figure 23. The amount of lysozyme (1.9 mg/mL) and BSA (0.2 mg/mL) adsorbed to unmodified vs. pMPC-50 modified model silicone hydrogel lenses after a 24-hour incubation period. Data shown represents mean ± SD (n=4). P value <0.0025 (**) and <0.005 (***).

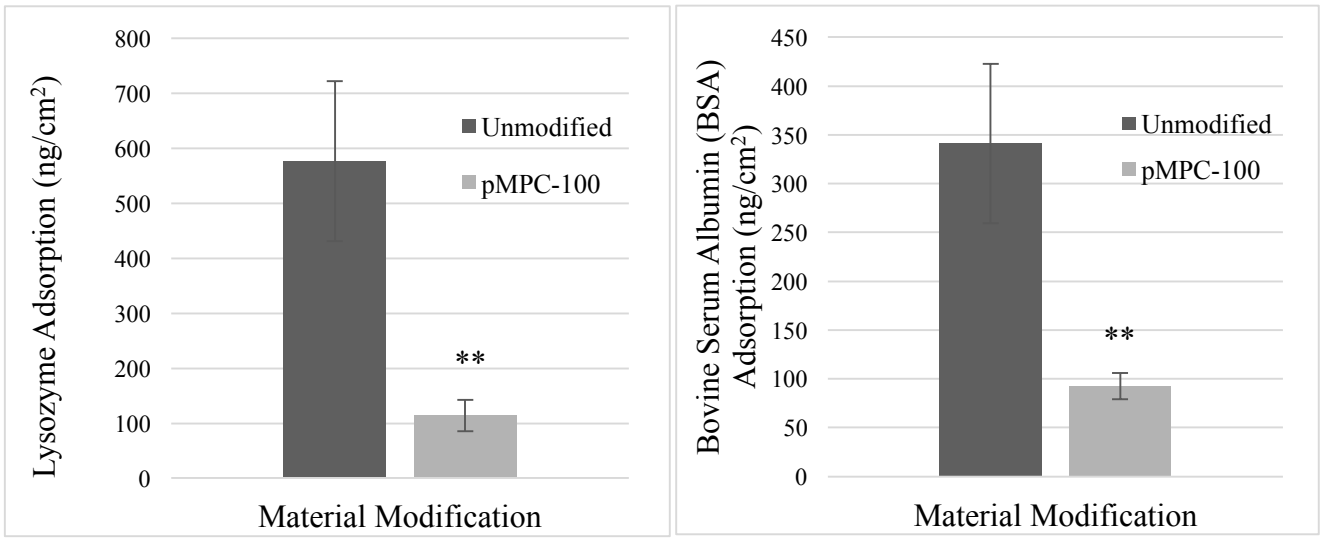

Figure 24. The amount of lysozyme (1.9 mg/mL) and BSA (0.2 mg/mL) adsorbed to unmodified vs. pMPC-100 modified model silicone hydrogel lenses after a 24-hour incubation period. Data shown represents mean ± SD (n=4). P value <0.0025 (**) and <0.005 (***).

5. CONCLUSIONS

The novel poly(MPC)-based polymer in this work demonstrates significant potential for improving the surface characteristics of model silicone hydrogel CL materials. The free pBIBEM-g-pMPC polymers of varying poly(MPC) chain lengths demonstrated living character as shown by the ^{1}H-NMR and GPC results. When applied to the surface of the model lenses, the polymer was grafted by SI-ATRP in a more permanent and cost effective method without the need for traditional O_2-plasma treatment. Using the synthesized BBIB sacrificial initiator, the pHEMA-50 and pMPC-50/pMPC-100 polymers were shown to be well-controlled, reflected in the predictable molecular weight by ^{1}H-NMR and low PDI values by GPC. The surface chemical grafting of the polymer was confirmed by ATR-FTIR and XPS. ATR-FTIR was able to determine the successful Intermediate-1/2 grafting by the appearance of the unique C-Br peak and disappearance of the hydroxyl (OH) peak. Low resolution XPS demonstrated that the surface modification was successful at each of the 4-steps of the SI-ATRP by an increase and decrease in the percentage of expected surface elements. Of particular importance was the decrease in the percentage of Si from the unmodified to the target pMPC-50 and pMPC-100 surfaces. This signified the potential of the novel polymer to mask the underlying highly hydrophobic silicone domains even under hydrophobic conditions, as desired. Advancing water contact angle and EWC measurements indicated an improvement in surface wettability and water content from the unmodified to the pMPC-50/100 modified materials. The contact angle decreased as low as $16.04 \pm 2.37^{\circ}$ for pMPC-50 and showed complete wetting on the pMPC-100 surfaces. The EWC increased from $24.7 \pm 0.3\%$ for unmodified discs to $27.0 \pm 0.2\%$ ($p<0.0009$) for pMPC-50 and $27.8 \pm 0.1\%$ ($p<0.0009$) for pMPC-100 discs. Therefore, the contact angle and EWC demonstrated improvement with increasing chain length for the pMPC-50 to pMPC-100

surfaces. For single protein adsorption, in comparison to the unmodified discs, lysozyme decreased ~83% ($p<0.00036$), followed by a decrease in BSA of ~73% ($p<0.0076$) for pMPC-50 modification. With respect to the pMPC-100 discs, similar results were seen with a decrease in ~80% ($p<0.00036$) for lysozyme and ~73% ($p<0.0076$) for BSA. Interestingly, unlike the trend of surface wettability and EWC, there was no significant difference in the single protein adsorption data for both BSA and lysozyme upon increasing chain length of pMPC.

All in all, these results suggest that the novel phosphorylcholine-based polymer has potential in providing a surface that is extremely wettable as well as anti-fouling. This polymer specifically showed great potential in improving the surface characteristics of model silicone hydrogel CL. Although it is expected that the surface modification will be relatively stable for extended periods of time, future experimentation should evaluate the stability of the polymer on the surface over a significant time period, specifically post-sterility. As well, future experimentation should focus on the evaluation of the adsorbed protein on the surface of the CL in order to quantify protein denaturation following exposure.

6. REFERENCES

Allansmith, M. R. (1985). Identification of Proteins in Contact-Lens Surface Deposits By Immunofluorescence Microscopy. *Archives of Ophthalmology*, *103*(9), 1270.

Allansmith, M. R., Korb, D. R., Greiner, J. V., Henriquez, A.S., Simon, M.A., & Finnemore, V. M. (1977). Giant papillary conjunctivitis in contact lens wearers. *American Journal of Ophthalmology*, *83*(5), 697–708.

Alvord, L., Court, J., Davis, T., Morgan, C., Schindhelm, K., Vogt, J., & Winterton, L. (1998). Oxygen Permeability of a New Type of High Dk Soft Contact Lenses. *Optometry and Vision Science*, *75*(1), 30–36.

ASM International. (2003). Overview of Biomaterials and Their Use in Medical Devices. *ASM International*, 1–11.

Austin, D. T. R., & Hills, B.P. (2009). Two-dimensional NMR relaxation study of the pore structure in silicone hydrogel contact lenses. *Applied Magnetic Resonance*, *35*(4), 581–591.

Banerjee, S., Paira, T. K., & Mandal, T. K. (2014). Surface confined atom transfer radical polymerization: access to custom library of polymer-based hybrid materials for speciality applications. *Polymer Chemistry*, *5*(14), 4153–4167.

Barbey, R., Lavanant, L., Paripovic, D., Schüwer, N., Sugnaux, C., Tugulu, S., & Klok, H.A. (2009). Polymer brushes via surface-initiated controlled radical polymerization: synthesis, characterization, properties, and applications. *Chemical Reviews*, *109*(11), 5437–5527.

Benjamin, W. (1993). Optimization of oxygenation: a water content "rule of thumb." *International Contact Lens Clinic*, *30*(3–4), 61–64.

Billaud, C., Sarakha, M., & Bolte, M. (2000). Polymerization of 2-hydroxyethyl methacrylate initiated by excitation of [Co(NH3)5N3]2+ at 365 and 546 nm. *European Polymer Journal*, *36*(7), 1401–1408.

Bruce, A. S., Golding, T. R., Au, S. W. M., & Rowhani, H. (1995). Mechanisms of dryness in soft lens wear— role of BUT and deposits. *Clinical and Experimental Optometry*, *78*(5), 168–175.

Buback, M., & Kurz, C. H. (1998). Free-radical propagation rate coefficients for cyclohexyl. *Macromolecular Chemistry and Physics*, *199*(1998), 2301–2310.

Canfield, R. E. (1963). The amino acid sequence of egg white lysozyme. *Journal of Biological Chemistry*, *238*(8), 2698–2707.

Carrot, G., Rutot-Houzé, D., Pottier, A., Degée, P., Hilborn, J., & Dubois, P. (2002). Surface-initiated ring-opening polymerization: A versatile method for nanoparticle ordering. *Macromolecules*, *35*(22), 8400–8404.

Castillo, E. J., Koenig, J. L., Anderson, J. M., & Lo, J. (1985). Protein adsorption on hydrogels. II. Reversible and irreversible interactions between lysozyme and soft contact lens surfaces. *Biomaterials*, *6*(5), 338–345.

Ceska, M., Sjodin, A., & Grossmuller, F. (1971). Some quantitative aspects of the labelling of proteins with 125I by the iodine monochloride method. *Biochem J*, *121*(1), 139–143.

Chen, S., Li, L., Boozer, C. L., & Jiang, S. (2000). Controlled chemical and structural properties of mixed self-assembled monolayers of alkanethiols on Au(111). *Langmuir*, *16*(24), 9287–9293.

Chen, S., Li, L., Zhao, C., & Zheng, J. (2010). Surface hydration: Principles and applications toward low-fouling/nonfouling biomaterials. *Polymer*, *51*(23), 5283–5293.

Choy, C. K. M., Cho, P., Benzie, I. F. F., & Ng, V. (2004). Effect of one overnight wear of orthokeratology lenses on tear composition. *Optometry and Vision Science:Official Publication of the American Academy of Optometry*, *81*(6), 414–420.

Currie, E. P. K., Norde, W., & Cohen Stuart, M. A. C. (2003). Tethered polymer chains: Surface chemistry and their impact on colloidal and surface properties. *Advances in Colloid and Interface Science*, *100-102,* 205-265.

Davidson, H. J., & Kuonen, V. J. (2004). The tear film and ocular mucins. *Veterinary Ophthalmology*, *7*(2), 71-77.

de Souza, G. A., Godoy, L. M. F., & Mann, M. (2006). Identification of 491 proteins in the tear fluid proteome reveals a large number of proteases and protease inhibitors. *Genome Biology*, *7*(8), R72.

De Vos, W. M., Leermakers, F. A. M., Lindhoud, S., & Prescott, S. W. (2011). Modeling the structure and antifouling properties of a polymer brush of grafted comb-polymers. *Macromolecules*, *44*(7), 2334–2342.

Dee, K. C., Puleo, D. A., & Bizios, R. (2002). *An Introduction to Tissue-Biomaterial Interactions Protein-Surface Interactions,* Hoboken, New Jersey: Wiley & Sons Ltd.

Driver, P. J., & Lemp, M. A. (1996). Meibomian gland dysfunction. *Survey of Ophthalmology*. *40*(5), 343-367.

Dumbleton, K. (2003). Noninflammatory silicone hydrogel contact lens complications. *Eye & Contact Lens*, *29*(1 Suppl), S186-9–1, S190-1, S192-4.

Edmondson, S., Osborne, V. L., & Huck, W. T. S. (2004). Polymer brushes via surface-initiated polymerizations. *Chemical Society Reviews*, *33*(1),14.

Efron, N., Morgan, P. B., Cameron, I. D., Brennan, N. A, & Goodwin, M. (2007). Oxygen permeability and water content of silicone hydrogel contact lens materials. *Optometry and Vision Science : Official Publication of the American Academy of Optometry*, *84*(4), 328–337.

Ejaz, M., Yamamoto, S., Ohno, K., Tsujii, Y., & Fukuda, T. (1998). Controlled Graft Polymerization of Methyl Methacrylate on Silicon Substrate by the Combined Use of the Langmuir−Blodgett and Atom Transfer Radical Polymerization Techniques. *Macromolecules*, *31*, 5934–5936.

Eltis, M. (2011). Contact-lens-related microbial keratitis: case report and review. *Journal of Optometry, 4*(4), 122-127.

Feng, W., Brash, J. L., & Zhu, S. (2006). Non-biofouling materials prepared by atom transfer radical polymerization grafting of 2-methacryloloxyethyl phosphorylcholine: Separate effects of graft density and chain length on protein repulsion. *Biomaterials*, *27*(6), 847–855.

Feng, W., Brash, J., & Zhu, S. (2004). Atom-transfer radical grafting polymerization of 2-methacryloyloxyethyl phosphorylcholine from silicon wafer surfaces. *Journal of Polymer Science, Part A: Polymer Chemistry*, *42*(12), 2931–2942.

Feng, W., Zhu, S., Ishihara, K., & Brash, J. L. (2005). Adsorption of fibrinogen and lysozyme on silicon grafted with poly(2-methacryloyloxyethyl phosphorylcholine) via surface-initiated atom transfer radical polymerization. *Langmuir*, *21*(13), 5980–5987.

Feng, W., Zhu, S., Ishihara, K., & Brash, J. L. (2006). Protein resistant surfaces: Comparison of acrylate graft polymers bearing oligo-ethylene oxide and phosphorylcholine side chains. *Biointerphases*, *1*(1), 50–60.

Ferreira, P., Carvalho, Á., Correia, T. R., Antunes, B. P., Correia, I. J., & Alves, P. (2013). Functionalization of polydimethylsiloxane membranes to be used in the production of voice prostheses. *Science and Technology of Advanced Materials*, *14*(5), 55006.

Fonn, D., & Holden, B. A. (1988). Rigid gas-permeable vs. hydrogel contact lenses for extended wear. *American Journal of Optometry and Physiological Optics*, *65*(7), 536–544.

Fullard, R. J., & Snyder, C. (1990). Protein levels in nonstimulated and stimulated tears of normal human subjects. *Investigative Ophthalmology and Visual Science*, *31*(6), 1119–1126.

Fullard, R. J., & Tucker, D. L. (1991). Changes in human tear protein levels with progressively increasing stimulus. *Investigative Ophthalmology and Visual Science*, *32*(8), 2290–2301.

Garrett, Q., Garrett, R. W., & Milthorpe, B. K. (1999). Lysozyme sorption in hydrogel contact lenses. *Investigative Ophthalmology and Visual Science*, *40*(5), 897–903.

Garrett, Q., & Milthorpe, B. K. (1996). Human serum albumin adsorption on hydrogel contact lenses in vitro. *Investigative Ophthalmology & Visual Science*, *37*(13), 2594–2602.

Ghosh, P. (2006). *Fundamentals of Polymer Science.* Retrieved from http://nsdl.niscair.res.in/jspui/bitstream/123456789/404/2/Basic%20concepts.pdf

Goda, T., & Ishihara, K. (2006). Soft contact lens biomaterials from bioinspired phospholipid polymers. *Expert Review of Medical Devices*, *3*(2), 167–174.

Goda, T., Ishihara, K., & Miyahara, Y. (2015). Critical update on 2-methacryloyloxyethyl phosphorylcholine (MPC) polymer science. *Journal of Applied Polymer Science*, *132*(16).

Goddard, J. M., & Hotchkiss, J. H. (2007). Polymer surface modification for the attachment of bioactive compounds. *Progress in Polymer Science (Oxford)*, *32*(7), 698-725.

González-Méijome, J.M., Lira, M., López-Alemany, A., Almeida, J. B., Parafita, M. A., & Refojo, M. F. (2006). Refractive index and equilibrium water content of conventional and silicone hydrogel contact lenses. *Ophthalmic & Physiological Optics : The Journal of the British College of Ophthalmic Opticians (Optometrists)*, *26*(1), 57–64.

Green-Church, K. B., & Nichols, J. J. (2008). Mass spectrometry-based proteomic analyses of contact lens deposition. *Molecular Vision*, *14*, 291–297.

Guillon, M., Optom, F. C., & Maissa, C. (2008). Contact Lens Wear Affects Tear Film Evaporation. *Eye & Contact Lens*, *34*(6), 326–330.

Gunkel, G., Weinhart, M., Becherer, T., Haag, R., & Huck, W.T.S. (2011). Effect of polymer brush architecture on antibiofouling properties. *Biomacromolecules*, *12*(11), 4169–4172.

Halperin, A. (1999). Polymer Brushes that Resist Adsorption of Model Proteins: Design Parameters, *Langmuir, 15*(7), 2525–2533.

Halperin, A., & Leckband, D. E. (2000). From ship hulls to contact lenses: repression of protein adsorption and the puzzle of PEO. *Comptes Rendus De L Academie Des Sciences Serie Iv Physique Astrophysique*, *1*(9), 1171–1178.

Harrington, S. (2011). Omafilcon A (K110099), 1–8.

Heiting, G. (2016). *Silicone Hydrogel Contact Lenses.* Retrieved from http://www.allaboutvision.com/contacts/silicone-hydrogel.htm

Herrwerth, S., Eck, W., Reinhardt, S., & Grunze, M. (2003). Factors that determine the protein resistance of oligoether self-assembled monolayers - Internal hydrophilicity, terminal hydrophilicity, and lateral packing density. *Journal of the American Chemical Society*, *125*(31), 9359–9366.

Hillborg, H., Tomczak, N., Olàh, A., Schönherr, H., Vancso, G. J., Ola, A., Scho, H., & Vancso, G. J. (2004). Nanoscale Hydrophobic Recovery:A Chemical Force Microscopy Study of UV/Ozone-Treated Cross-Linked Poly (dimethylsiloxane). *Symposium A Quarterly Journal In Modern Foreign Literatures*, *20*(3), 785–794.

Holden, B. A., & Mertz, G. W. (1984). Critical oxygen levels to avoid corneal edema for daily and extended wear contact lenses. *Investigative Ophthalmology and Visual Science*, *25*(10), 1161–1167.

Holland, E. J., Mannis, M. J., & Lee, W. B. (2013). *Ocular Surface Disease: Cornea, Conjunctiva and Tear Film*. Philadelphia, Pennsylvania: Elsevier.

Holly, F. J. (1981). Tear film physiology and contact lens wear. II. Contact lens-tear film interaction. *American Journal of Optometry and Physiological Optics*, *58*(4), 331–341.

Hou, C., Lin, S., Liu, F., Hu, J., Zhang, G., Liu, G., Tu, Y., Zhu, H., Luo, H. (2014). Synthesis of poly(2-hydroxyethyl methacrylate) end-capped with asymmetric functional groups via atom transfer radical polymerization. *New Journal of Chemistry*, *38*(6), 2538.

Hu, X., Hao, L., Wang, H., Yang, X., Zhang, G., Wang, G., & Zhang, X. (2011). Hydrogel contact lens for extended delivery of ophthalmic drugs. *International Journal of Polymer Science*, 2011, 1-9.

Hui, A., Sheardown, H., & Jones, L. (2012). Acetic and Acrylic Acid Molecular Imprinted Model Silicone Hydrogel Materials for Ciprofloxacin-hcl Delivery. *Materials*, *5*(1), 85–107.

Ishihara, K., & Takai, M. (2009). Bioinspired interface for nanobiodevices based on phospholipid polymer chemistry. *Journal of The Royal Society Interface*, *6*(Suppl3), S279–S291.

Iwasaki, Y., & Ishihara, K. (2005). Phosphorylcholine-containing polymers for biomedical applications. *Analytical and Bioanalytical Chemistry*, *381*(3), 534-546.

Iwasaki, Y., & Ishihara, K. (2012). Cell membrane-inspired phospholipid polymers for developing medical devices with excellent biointerfaces. *Science and Technology of Advanced Materials*, *13*(6), 64101.

Iwata, R., Suk-In, P., Hoven, V. P., Takahara, A., Akiyoshi, K., & Iwasaki, Y. (2004). Control of nanobiointerfaces generated from well-defined biomimetic polymer brushes for protein and cell manipulations. *Biomacromolecules*, *5*(6), 2308–2314.

Iwata, S. (1983). Chemical composition of the aqueoous phase. *International Ophthalmology Clinics*, *13*, 29–46.

Jadi, S., Heynen, M., Luensmann, D., & Jones, L. W. (2012). Composition of incubation solution impacts in vitro protein uptake to silicone hydrogel contact lenses. *Molecular Vision*, *18*, 337–347.

Jin, Z., Feng, W., Beisser, K., Zhu, S., Sheardown, H., & Brash, J. L. (2009). Protein-resistant polyurethane prepared by surface-initiated atom transfer radical graft polymerization (ATRgP) of water-soluble polymers: Effects of main chain and side chain lengths of grafts. *Colloids and Surfaces B: Biointerfaces*, *70*(1), 53–59.

Jin, Z., Feng, W., Zhu, S., Sheardown, H., & Brash, J. L. (2010a). Protein-Resistant Materials via Surface-Initiated Atom Transfer Radical Polymerization of 2-Methacryloyloxyethyl Phosphorylcholine. *Journal of Biomaterials Science, Polymer Edition*, *21*(10), 1331–1344.

Jin, Z., Feng, W., Zhu, S., Sheardown, H., & Brash, J. L. (2010b). Protein-resistant polyurethane by sequential grafting of poly(2-hydroxyethyl methacrylate) and poly(oligo(ethylene glycol) methacrylate) via surface-initiated ATRP. *Journal of Biomedical Materials Research - Part A*, *95*(4), 1223–1232.

Jones, L. (2007). Comfilcon A: a new silicone hydrogel material. *Contact Lens Spectrum*, *22*(8), 15.

Jones, L., Mann, A., Evans, K., Franklin, V., & Tighe, B. (2000). An in vivo comparison of the kinetics of protein and lipid deposition on group II and group IV frequent-replacement contact lenses. *Optom Vis Sci*, *77*(10), 503–510.

Jones, L., Senchyna, M., Glasier, M.A., Schickler, J., Forbes, I., Louie, D., & May, C. (2003). Lysozyme and lipid deposition on silicone hydrogel contact lens materials. *Eye & Contact Lens*, *29*(1), S75-S84, S83-S84, S192–S194.

Jones, R. A. L., Lehnert, R. J., Schonherr, H., & Vancso, J. (1999). Factors affecting the preparation of permanently end-grafted polystyrene layers. *Polymer*, *40*(2), 525–530.

Jordan, R., & Ulman, A. (1998). Surface initiated living cationic polymerization of 2-oxazolines. *Journal of the American Chemical Society*, *120*(2), 243–247.

Jordan, R., Ulman, A., Kang, J. F., Rafailovich, M. H., & Sokolov, J. (1999). Surface-Initiated Anionic Polymerization of Styrene by Means of Self-Assembled Monolayers. *Journal of the American Chemical Society*, *121*(5), 1016–1022.

Kamigaito, M., Ando, T., & Sawamoto, M. (2001). Metal-catalyzed living radical polymerization. *Chemical reviews*, *101*, 3689-3746.

Karlgard, C. C. S., Sarkar, D. K., Jones, L. W., Moresoli, C., & Leung, K. T. (2004). Drying methods for XPS analysis of PureVision, Focus Night & Day and conventional hydrogel contact lenses. *Applied Surface Science*, *230*(1–4), 106–114.

Keir, N., & Jones, L. (2013). Wettability and Silicone Hydrogel Lenses. *Eye & Contact Lens: Science & Clinical Practice*, *39*(1), 99–107.

Khabibullin, A., Mastan, E., Matyjaszewski, K., & Zhu, S. (2016). Surface-Initiated Atom Transfer Radical Polymerization. *Adv. Polym. Sci*, *270*, 29–76.

Kiel, J. (2010). *The Ocular Circulation*. San Rafael, California: Morgan & Claypool Life Sciences.

Kim, J., & Somorjai, G. A. (2003). Molecular packing of lysozyme, fibrinogen, and bovine serum albumin on hydrophilic and hydrophobic surfaces studied by infrared-visible sum frequency generation and fluorescence microscopy. *Journal of the American Chemical Society*, *125*(10), 3150–3158.

King-Smith, P. E., Fink, B. A., Fogt, N., Nichols, K. K., Hill, R. M., & Wilson, G. S. (2000). The thickness of the human precorneal tear film: Evidence from reflection spectra. *Investigative Ophthalmology and Visual Science*, *41*(11), 3348–3359.

Kitano, H., Mori, T., Takeuchi, Y., Tada, S., Gemmei-Ide, M., Yokoyama, Y., & Tanaka, M. (2005). Structure of water incorporated in sulfobetaine polymer films as studied by ATR-FTIR. *Macromolecular Bioscience*, *5*(4), 314–321.

Korb, D. R., Allansmith, M. R., Greiner, J. V, Henriquez, A. S., Richmond, P. P., & Finnemore, V. M. (1980). Prevalence of conjunctival changes in wearers of hard contact lenses. *American Journal of Ophthalmology*, *90*(3), 336–341.

Korogiannaki, M., Guidi, G., Jones, L., & Sheardown, H. (2015). Timolol maleate release from hyaluronic acid-containing model silicone hydrogel contact lens materials. *Journal of Biomaterials Applications*, *30*(3), 361–76.

Lamberts, D. (1994). *Physiology of the tear film. In: The Cornea*. New York: Little Brown & Co.

Latour, R. (2005). Biomaterials: protein-surface interactions. *Biomaterials and Biomedical Engineering*, 1–15.

Lee, J., Li, T., & Park, K. (2001). *Solvation interactions for protein adsorption to biomaterial surfaces. In: Morra M, Ed. Water in Biomaterials Surface Science.* Chichester, UK: Wiley & Sons Ltd.

Lemp, M. A., & Blackman, H. J. (1981). Ocular surface defense mechanisms. *Annals of Ophthalmology*, *13*(1), 61–63.

Lewis, A. L. (2000). Phosphorylcholine-based polymers and their use in the prevention of biofouling. *Colloids and Surfaces B: Biointerfaces*, *18*(3-4), 261-275.

Li, L., Chen, S., Zheng, J., Ratner, B. D., & Jiang, S. (2005). Protein Adsorption on Oligo (ethylene glycol) -Terminated Alkanethiolate Self-Assembled Monolayers: The Molecular Basis for Nonfouling Behavior. *Surface Science*, 2934–2941.

Lindgren, M., Sörgjerd, K., & Hammarström, P. (2005). Detection and Characterization of Aggregates, Prefibrillar Amyloidogenic Oligomers, and Protofibrils Using Fluorescence Spectroscopy. *Biophysical Journal*, *88*(6), 4200–4212.

López-Alemany, A., Compañ, V., & Refojo, M. F. (2002). Porous structure of Purevision™ versus Focus® Night&Day™ and conventional hydrogel contact lenses. *Journal of Biomedical Materials Research*, *63*(3), 319–325.

Lorentz, H., & Jones, L. (2007). Lipid deposition on hydrogel contact lenses: how history can help us today. *Optometry and Vision Science: Official Publication of the American Academy of Optometry*, *84*(4), 286–295.

Luensmann, D., Heynen, M., Liu, L., Sheardown, H., & Jones, L. (2010). The efficiency of contact lens care regimens on protein removal from hydrogel and silicone hydrogel lenses. *Molecular Vision*, *16*, 79–92.

Luensmann, D., & Jones, L. (2012). Protein deposition on contact lenses: The past, the present, and the future. *Contact Lens and Anterior Eye*, *35*(2), 53-64.

Ma, I. Y., Lobb, E. J., Billingham, N. C., Armes, S. P., Lewis, A. L., Lloyd, A. W., & Salvage, J. (2002). Synthesis of biocompatible polymers. 1. Homopolymerization of 2-methacryloyloxyethyl phosphorylcholine via ATRP in protic solvents: An optimization study. *Macromolecules*, *35*(25), 9306–9314.

Matyjaszewski, K. (2012). Atom Transfer Radical Polymerization (ATRP): Current Status and Future Perspectives. *Macromolecules*, *45*(10), 4015–4039.

Matyjaszewski, K., Miller, P. J., Shukla, N., Immaraporn, B., Gelman, A., Luokala, B.B., Siclovan, T.M., Kickelbick, G., Vallant, T., Hoffmann, H., & Pakula, T. (1999). Polymers at Interfaces: Using Atom Transfer Radical Polymerization in the Controlled Growth of Homopolymers and Block Copolymers from Silicon Surfaces in the Absence of Untethered Sacrificial Initiator. *Macromolecules*, *32*(26), 8716–8724.

Matyjaszewski, K., & Tsarevsky, N. V. (2009). Nanostructured functional materials prepared by atom transfer radical polymerization. *Nature Chemistry*, *1*(4), 276–288.

Matyjaszewski, K., & Xia, J. (2001). Atom transfer radical polymerization. *Chemical Reviews*, *101*(9), 2921–2990.

McCaa, C. S. (1982). The eye and visual nervous system: anatomy, physiology and toxicology. *Environmental Health Perspectives*, *44*, 1-8.

Mura-Galelli, M. J., Voegel, J. C., Behr, S., Bres, E. F., & Schaaf, P. (1991). Adsorption/desorption of human serum albumin on hydroxyapatite: a critical analysis of the Langmuir model. *Proceedings of the National Academy of Sciences of the United States of America*, *88*(13), 5557–5561.

Ng, V., Cho, P., Wong, F., & Chan, Y. (2001). Variability of tear protein levels in normal young adults: diurnal (daytime) variation. *Graefe's Archive for Clinical and Experimental Ophthalmology*, *239*(4), 257–263.

Nichols, B. A., Chiappino, M. L., & Dawson, C. R. (1985). Demonstration of the mucous layer of the tear film by electron microscopy. *Investigative Ophthalmology and Visual Science*, *26*(4), 464–473.

Nichols, J. J., & King-Smith, P. E. (2004). The impact of hydrogel lens settling on the thickness of the tears and contact lens. *Investigative Ophthalmology and Visual Science*, *45*(8), 2549–2554.

Nichols, J. J., Mitchell, G. L., & King-Smith, P. E. (2005). Thinning rate of the precorneal and prelens tear films. *Investigative Ophthalmology and Visual Science*, *46*(7), 2353–2361.

Nicolson, P. C. (2003). Continuous Wear Contact Lens Surface Chemistry and Wearability. *Eye & Contact Lens*, *29*(1), S30–S32.

Nicolson, P. C., & Vogt, J. (2001). Soft contact lens polymers: An evolution. *Biomaterials*, *22*(24), 3273-3283.

Norde, W. (1986). Adsorption of proteins from solution at the solid-liquid interface. *Advances in Colloid and Interface Science*, *25*, 267-340.

Norde, W. (1992). Energy and Entropy of Protein Adsorption. *Journal of Dispersion Science and Technology*, *13*(4), 363–377.

Norde, W., & Anusiem, A. C. I. (1992). Adsorption, desorption and re-adsorption of proteins on solid surfaces. *Colloids and Surfaces*, *66*(1), 73–80.

Norde, W., & Lyklema, J. (1991). Why proteins prefer interfaces. *Journal of Biomaterials Science. Polymer Edition*, *2*(3), 183–202.

Oláh, A., Hillborg, H., & Vancso, G. J. (2005). Hydrophobic recovery of UV/ozone treated poly(dimethylsiloxane): Adhesion studies by contact mechanics and mechanism of surface modification. *Applied Surface Science*, *239*(3–4), 410–423.

Omali, N. B., Subbaraman, L. N., Coles-Brennan, C., Fadli, Z., & Jones, L. W. (2015). Biological and Clinical Implications of Lysozyme Deposition on Soft Contact Lenses. *Optometry and Vision Science : Official Publication of the American Academy of Optometry*, *92*(7), 750–757.

Ostuni, E., Chapman, R. G., Holmlin, R. E., Takayama, S., & Whitesides, G. M. (2001). A survey of structure-property relationships of surfaces that resist the adsorption of protein. *Langmuir*, *17*(18), 5605-5620.

Patten, T. E., Xia, J., Abernathy, T., & Matyjaszewski, K. (1996). Polymers with Very Low Polydispersities from Atom Transfer Radical Polymerization. *Science*, *272*(5263), 866–868.

Prydal, J. I., Artal, P., Woon, H., & Campbell, F. W. (1992). Study of human precorneal tear film thickness and structure using laser interferometry. *Invest Ophthalmol Vis Sci*, *33*(6), 2006–2011.

Prydal, J. I., & Campbell, F. W. (1992). Study of precorneal tear film thickness and structure by interferometry and confocal microscopy. *Investigative Ophthalmology and Visual Science*, *33*(6), 1996–2005.

Pyun, J., Kowalewski, T., & Matyjaszewski, K. (2003). Synthesis of Polymer Brushes Using Atom Transfer Radical Polymerization. *Macromolecular Rapid Communications*, *24*(18), 1043–1059.

R.N. Keller, & Wycoff, H. D. (1946). Purification of CuBr. *Inorganic Synthesis*, *2*, 1–4.

Roach, P., Farrar, D., & Perry, C. C. (2005). Interpretation of protein adsorption: Surface-induced conformational changes. *Journal of the American Chemical Society*, *127*(22), 8168–8173.

Robinson, K. L., Khan, M. A., De Paz Báñez, M. V., Wang, X. S., & Armes, S. P. (2001). Controlled polymerization of 2-hydroxyethyl methacrylate by ATRP at ambient temperature. *Macromolecules*, *34*(10), 3155–3158.

Rossner, C., & Vana, P. (2016). Controlled Radical Polymerization at and from Solid Surfaces. *Advances in Polymer Science, 270,* 193-220.

Roth, J., Albrecht, V., Nitschke, M., Bellmann, C., Simons, F., Zschoche, S., Michel, S., Luhmann, C., Grundke, K., & Voit, B. (2008). Surface functionalization of silicone rubber for permanent adhesion improvement. *Langmuir*, *24*(21), 12603–12611.

Sack, R.A., Tan, K.O., & Tan, A. (1992). Diurnal tear cycle: Evidence for a nocturnal inflammatory constitutive tear fluid. *Investigative Ophthalmology and Visual Science, 33*(3), 626–640.

Sankaridurg, P. R., de la Jara, P. L., & Holden, B. A. (2013). The future of silicone hydrogels. *Eye & Contact Lens*, *39*(1), 125–129.

Senaratne, W., Andruzzi, L., & Ober, C. K. (2005). Self-assembled monolayers and polymer brushes in biotechnology: current applications and future perspectives. *Biomacromolecules*, *6*(5), 2427–2448.

Senchyna, M., Jones, L., Louie, D., May, C., Forbes, I., & Glasier, M.A. (2004). Quantitative and conformational characterization of lysozyme deposited on balafilcon and etafilcon contact lens materials. *Current Eye Research*, *28*(1), 25–36.

Seo, J. H., Matsuno, R., Konno, T., Takai, M., & Ishihara, K. (2008). Surface tethering of phosphorylcholine groups onto poly(dimethylsiloxane) through swelling-deswelling methods with phospholipids moiety containing ABA-type block copolymers. *Biomaterials*, *29*(10), 1367–1376.

Shimizu, T., Goda, T., Minoura, N., Takai, M., & Ishihara, K. (2010). Super-hydrophilic silicone hydrogels with interpenetrating poly(2-methacryloyloxyethyl phosphorylcholine) networks. *Biomaterials*, *31*(12), 3274–3280.

Spring, T. (1974). Reaction to hydrophillic lenses. *Med J Aust*, *1,* 449–450.

Stamm, M. (2008). *Polymer Surfaces and Interfaces*. Dresden, Germany: Springer Berlin Heidelberg.

Stapleton, F., Stretton, S., Papas, E., Skotnitsky, C., & Sweeney, D. F. (2006). Silicone Hydrogel Contact Lenses and the Ocular Surface. *The Ocular Surface*, *4*(1), 24–43.

Subbaraman, L., Glasier, M.A., Senchyna, M., & Jones, L. (2005). Stabilization of Lysozyme Mass Extracted From Lotrafilcon Silicone Hydrogel Contact Lenses. *Optometry and Vision Science*, *82*(3), 209–214.

Suwala, M., Glasier, M.A., Subbaraman, L. N., & Jones, L. (2007). Quantity and conformation of lysozyme deposited on conventional and silicone hydrogel contact lens materials using an in vitro model. *Eye & Contact Lens*, *33*(3), 138–143.

Sweeney, D. (2000). *Silicone Hydrogels: The Rebirth of Continuous Wear Contact Lenses* (1st ed.). London, United Kingdom: Butterworth-Heinemann.

Sweeney, D. F., Millar, T. J., & Raju, S. R. (2013). Tear film stability: A review. *Experimental Eye Research*.

Tan, K. O., Sack, R. A., Holden, B. A., & Swarbrick, H. A. (1993). Temporal sequence of changes in tear film composition during sleep. *Current Eye Research*, *12*(11), 1001–1007.

Tang, L., Thevenot, P., & Hu, W. (2008). Surface Chemistry Influences Implant Biocompatibility. *Current Topics in Medicinal Chemistry*, *8*(4), 270–280.

Thissen, H., Gengenbach, T., du Toit, R., Sweeney, D. F., Kingshott, P., Griesser, H. J., & Meagher, L. (2010). Clinical observations of biofouling on PEO coated silicone hydrogel contact lenses. *Biomaterials*, *31*(21), 5510–5519.

Tighe, B., Jones, L., Evans, K., & Franklin, K. (1998). Patient-dependent and material dependent factors in contact lens deposition processes. *Adv Exp Med Biol*, *438*, 745–751.

Tighe, B. (2004). *Silicone hydrogels: Structure, properties and behaviour. Silicone Hydrogels: Continuous Wear Contact Lenses.* Oxford: Butterworth-Heinemann.

Tomlinson, A. (1992). Tear film changes with contact lens wear. In *Complications of Contact Lens Wear (A.Tomlinson, ed.)*. Mosby Year Book.

Trocme, S. D., Kephart, G. M., Allansmith, M. R., Bourne, W. M., & Gleich, G. J. (1989). Conjunctival deposition of eosinophil granule major basic protein in vernal keratoconjunctivitis and contact lens-associated giant papillary conjunctivitis. *Am J Ophthalmol*, *108*(1), 57–63.

Tsujii, Y., Ohno, K., Yamamoto, S., Goto, A., & Fukuda, T. (2006). Structure and Properties of High-Density Polymer Brushes Prepared by Surface-Initiated Living Radical Polymerization. *Advances in Polymer Science, 197*, 1–45.

Urbaniak-domagala, W. (2012). The Use of the Spectrometric Technique FTIR-ATR to Examine the Polymers Surface. *Advanced Apects of Spectroscopy*, 86–104.

Van Buskirk, E. M. (1989). The anatomy of the limbus. *Eye (London, England)*, *3(Pt 2)*, 101–108.

Voet, D., Voet, J. G. (2004). *Three-dimensional structures of proteins. Biochemistry* (3rd ed.). Hoboken, New Jersey: Wiley.

Wang, J. S., & Matyjaszewski, K. (1995). Controlled/"living" radical polymerization. Atom transfer radical polymerization in the presence of transition-metal complexes. *Journal of the American Chemical Society*, *117*(6), 5614–5615.

Willis, S. L., Court, J. L., Redman, R. P., Wang, J. H., Leppard, S. W., O'Byrne, V. J., & Stratford, P. W. (2001). A novel phosphorylcholine-coated contact lens for extended wear use. *Biomaterials*, *22*(24), 3261–3272.

Wolff, E. (1951). *The Anatomy of the Eye and Orbit.* Philadelphia, Pennsylvania: Blakiston Co.

Xia, Y. N., & Whitesides, G. M. (1998). Soft lithography. *Annual Review Of Materials Science*, *37*(5), 551–575.

Xu, F. J., Neoh, K. G., & Kang, E. T. (2009). Bioactive surfaces and biomaterials via atom transfer radical polymerization. *Progress in Polymer Science (Oxford), 34*(8), 719-761.

Xu, L., Yuan, B., Chen, Q., Lin, S., Chen, X., Hua, Z., & Shen, J. (2014). Immobilized layers of zwitterionic polymer by one-step modification. *RSC Adv*, *4*, 15030–15035.

Yamada, M., Mochizuki, H., Kawai, M., Yoshino, M., & Mashima, Y. (1997). Fluorophotometric measurement of pH of human tears in vivo. *Current Eye Research*, *16*(5), 482–486.

Yan, L., & Ishihara, K. (2008). Graft copolymerization of 2-methacryloyloxyethyl phosphorylcholine to cellulose in homogeneous media using atom transfer radical polymerization for providing new hemocompatible coating materials. *Journal of Polymer Science, Part A: Polymer Chemistry*, *46*(10), 3306–3313.

Yuan, Y., & Lee, T. R. (2013). Contact angle and wetting properties. *Springer Series in Surface Sciences*, *51*(1), 3–34.

Zdyrko, B., & Luzinov, I. (2011). Polymer brushes by the "grafting to" method. *Macromolecular Rapid Communications*, *32*(12), 859-869.

Zhao, B., & Brittain, W. J. (2000). Polymer brushes: Surface-immobilized macromolecules. *Progress in Polymer Science (Oxford)*, *25*(5), 677–710.

Zhao, H., Jumblatt, J. E., Wood, T. O., & Jumblatt, M. M. (2001). Quantification of MUC5AC protein in human tears. *Cornea*, *20*(8), 873–877.

Zheng, J., Li, L., Tsao, H.K., Sheng, Y.J., Chen, S., & Jiang, S. (2005). Strong Repulsive Forces between Protein and Oligo (Ethylene Glycol) Self-Assembled Monolayers: A Molecular Simulation Study. *Biophysical Journal*, *89*(1), 158–166.

Zhou, L., Beuerman, R. W., Foo, Y., Liu, S., Ang, L. P. K., & Tan, D. T. H. (2006). Characterisation of human tear proteins using high-resolution mass spectrometry. *Annals of the Academy of Medicine Singapore*, *35*(6), 400–407.